

Helicopter Flight Simulation Motion Platform Requirements

Jeffery Allyn Schroeder

The NASA STI Program Office . . . in Profile

Since its founding, NASA has been dedicated to the advancement of aeronautics and space science. The NASA Scientific and Technical Information (STI) Program Office plays a key part in helping NASA maintain this important role.

The NASA STI Program Office is operated by Langley Research Center, the Lead Center for NASA's scientific and technical information. The NASA STI Program Office provides access to the NASA STI Database, the largest collection of aeronautical and space science STI in the world. The Program Office is also NASA's institutional mechanism for disseminating the results of its research and development activities. These results are published by NASA in the NASA STI Report Series, which includes the following report types:

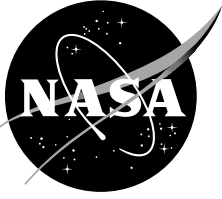
- **TECHNICAL PUBLICATION.** Reports of completed research or a major significant phase of research that present the results of NASA programs and include extensive data or theoretical analysis. Includes compilations of significant scientific and technical data and information deemed to be of continuing reference value. NASA's counterpart of peer-reviewed formal professional papers but has less stringent limitations on manuscript length and extent of graphic presentations.
- **TECHNICAL MEMORANDUM.** Scientific and technical findings that are preliminary or of specialized interest, e.g., quick release reports, working papers, and bibliographies that contain minimal annotation. Does not contain extensive analysis.
- **CONTRACTOR REPORT.** Scientific and technical findings by NASA-sponsored contractors and grantees.

- **CONFERENCE PUBLICATION.** Collected papers from scientific and technical conferences, symposia, seminars, or other meetings sponsored or cosponsored by NASA.
- **SPECIAL PUBLICATION.** Scientific, technical, or historical information from NASA programs, projects, and missions, often concerned with subjects having substantial public interest.
- **TECHNICAL TRANSLATION.** English-language translations of foreign scientific and technical material pertinent to NASA's mission.

Specialized services that complement the STI Program Office's diverse offerings include creating custom thesauri, building customized databases, organizing and publishing research results . . . even providing videos.

For more information about the NASA STI Program Office, see the following:

- Access the NASA STI Program Home Page at <http://www.sti.nasa.gov>
- E-mail your question via the Internet to help@sti.nasa.gov
- Fax your question to the NASA Access Help Desk at (301) 621-0134
- Telephone the NASA Access Help Desk at (301) 621-0390
- Write to:
NASA Access Help Desk
NASA Center for AeroSpace Information
7121 Standard Drive
Hanover, MD 21076-1320



Helicopter Flight Simulation Motion Platform Requirements

*Jeffery Allyn Schroeder
Ames Research Center, Moffett Field, California*

National Aeronautics and
Space Administration

Ames Research Center
Moffett Field, California 94035-1000

Available from:

NASA Center for AeroSpace Information
7121 Standard Drive
Hanover, MD 21076-1320
(301) 621-0390

National Technical Information Service
5285 Port Royal Road
Springfield, VA 22161
(703) 487-4650

Contents

Summary	1
1. Introduction	3
Background.....	3
Purpose of This Report.....	10
Approach.....	10
Contributions.....	10
Outline	11
2. The Vertical Motion Simulator.....	13
General Description.....	13
Performance Characteristics.....	13
3. Yaw Experiment.....	15
Background.....	15
Experimental Setup.....	15
Results	19
4. Vertical Experiment I: Attitude Control.....	31
Background.....	31
Experimental Setup.....	31
Results	34
5. Vertical Experiment II: Compensatory Tracking.....	41
Background.....	41
Experimental Setup.....	41
Results	42
6. Vertical Experiment III: Altitude and Altitude-Rate Estimation	49
Background.....	40
Experimental Setup.....	49
Results: Objective Performance Data	51
7. Roll-Lateral Experiment.....	55
Background.....	55
Experimental Setup.....	55
Results	57
8. Discussion of Overall Results	63
General Discussion.....	63
Proposed Fidelity Criteria versus Results of Previous Research.....	63
A General Method for Configuring Motion Systems.....	66

9. Conclusions.....	69
Summary	69
Recommendations for Future Work	69
Appendix A—Human Motion Sensing Characteristics.....	71
Appendix B—Height Regulation Analysis with Previous Model.....	75
Appendix C—Example of Repeated-Measures Analysis.....	81
Appendix D—Review of Cooper-Harper Handling Qualities Rating Scale.....	83
References	85

Helicopter Flight Simulation Motion Platform Requirements

JEFFERY ALLYN SCHROEDER

Ames Research Center

Summary

Flight simulators attempt to reproduce actual flight pilot-vehicle behavior on the ground reasonably and safely. This reproduction is especially challenging for helicopter flight simulators, which is the subject of this work, for the pilot is often inextricably dependent on external cues for pilot-vehicle stabilization. One of the important simulator cues is platform motion; however, its required fidelity is not known. Cockpit motion effects on pilot-vehicle performance, on pilot workload, and on pilot motion perception were examined in several experiments in order to determine the required motion fidelity for helicopter flight simulation. In each experiment, a large-displacement motion platform was used that, for some configurations, allowed pilots to fly tasks with a one-to-one correspondence between the motion and visual cues. In all evaluations, representative helicopter math models were employed, and in two cases a specially developed model from AH-64 Apache flight test data was used. Platform motion characteristics were modified to give motion cues varying from full motion, relative to the visual scene, to no motion. Four of the six rigid-body degrees of freedom were explored: roll rotation, yaw rotation, lateral translation, and vertical translation. The pitch rotation and longitudinal translation degrees of freedom remain for future work; however, it was hypothesized that their requirements mirror those of roll rotation and lateral translation. Several key results were found from the evaluations. First, lateral and vertical translational motion platform cues had significant effects on simulation fidelity. Their presence improved pilot-vehicle

performance, reduced pilot physical and mental workload, and improved pilot opinion of how faithfully the simulations represented flight. Second, yaw and roll rotational motion platform cues were not as important as the lateral and the vertical translational platform cues. In particular, the yaw rotational motion platform cue did not appear at all useful in improving performance or reducing workload. Third, when the lateral translational motion platform cues were combined with visual yaw rotational cues, pilots believed they were physically rotating when the motion platform was not rotating. Thus, an overall efficiency in the use of motion cues can be obtained by combining only the lateral translational platform cues with satisfactory visual cues. Fourth, vertical and roll/lateral specifications were revised and validated that provide simulator users with a prediction of motion fidelity based on the frequency-response characteristics of their motion control laws. Fifth, vertical platform motion affected pilot estimates of steady-state altitude during altitude repositionings. This refutes the view that pilots estimate altitude and altitude rate in simulation solely from visual cues. Since these studies have shown that translational motion platform cues had more important effects on simulation fidelity than did rotational cues, an alternative to today's hexapod platform design is suggested which emphasizes the translational cues. And sixth, the combined results led to a general method for configuring helicopter motion systems as well as for developing simulator tasks that more likely represent actual flight. The overall results can serve as a guide to future simulator designers and to today's operators.

1. Introduction

Background

Purpose of Flight Simulation

Flight simulation had its origins near to those of powered flight itself (ref. 1). Since then, simulation has been used principally for two distinct disciplines in aviation: training and research and development. However, flight training is its most frequent application, in which it is used primarily to reduce cost and increase safety. Almost all of the major airlines use flight simulation today whenever they can receive a training credit for doing so. This is because an hour in the simulator is less expensive than an hour in the airplane. For example, a B-747 aircraft costs about \$12,500 per hour to operate versus about \$750 per hour for a 747 simulator (ref. 2).

These cost reductions are put to both training and retraining uses. The Federal Aviation Administration (FAA) will certify certain simulators such that, with only simulator training, a new pilot may fly the actual aircraft for the first time carrying passengers (ref. 3). Once a pilot is qualified in a particular aircraft, mandatory periodic proficiency checks are then conducted in the simulator. Some of these latter checks may also include recovery from failures or unusual attitudes (ref. 4). This training is considered too hazardous to perform in the actual aircraft.

Although the previous discussion relates to fixed-wing transport training, a similar use for flight simulation is under way for helicopter training. For helicopters, however, less is known about what level of fidelity is needed for these simulators. The FAA has released an Advisory Circular suggesting fidelity requirements for helicopter simulators (ref. 5), but little data exist to support the requirements. Its development started with the fixed-wing Advisory Circular (ref. 3), and the specifications in most areas were made more stringent owing to the greater dependency a pilot places on external cues in helicopter flight than in fixed-wing flight.

The other principal use of flight simulation is for research and development. When an aircraft system, or component, reaches a mature level of development, it is often evaluated by a pilot in simulation. These simulations may be used to evaluate a new vehicle's handling qualities or the functionality of a new system component in a more realistic and safer environment prior to flight testing. Flight simulation results may also yield a final product, such as data for a handling-qualities specification. Finally, flight simulation may be used to determine the causal factors in an accident. An accident scenario can be

duplicated in order to hypothesize crew action in response to events.

In the above instances, flight simulation attempts to imitate flight. Figure 1 illustrates the key components of simulation and flight. In flight, a pilot receives cues that indicate vehicle motion in three main ways. First, motion is perceived from visual cues with the eyes. Second, the pilot perceives motion from the vehicle's acceleration. Third, the pilot can infer, or predict motion, via the kinesthetic force and position cues that the vehicle's force-feel system provides. The latter is an often neglected, but important, cueing source (refs. 6, 7).

In contrast, the pilot seldom receives any of these cues accurately in simulation. The aircraft is now represented by a mathematical aircraft model, which is likely to contain inaccuracies. The visual system, which is typically computer generated, does not provide the cueing richness of the real world. The simulator visual field of view is usually less than that of the vehicle, and the visual acuity provided today is incapable of rendering 20/20 vision. The vehicle's force-feel system is usually the easiest to replicate, although matching the nonlinear effects (friction, free-play, and hysteresis) and the inertia characteristics can be challenging. This challenge results both from a surprising lack of flight data and from simulator force-feel system limitations. And because the simulator displacements are constrained, the motion system can typically provide only a subset of the in-flight accelerations. It is the motion system that is the focus of this report.

Of the above cueing sources, only the motion platform has practical hard technological limits in its capability to reproduce the in-flight cues. Thus, in light of those hard limits and the associated costs of providing them, establishing reliable motion fidelity requirements is warranted. This is especially true for helicopters, since the pilot often stabilizes the pilot-vehicle system, and this stabilization is only possible via feedback from the simulator's cueing systems.

The Role of Platform Motion in Flight Simulation

The role of platform motion has been the subject of great debate. Some researchers and users believe in the extreme that no platform motion is necessary. Some believe in the exact opposite. As pointed out by Boldovici (ref. 8), "Debates about whether to buy motion bases often include anecdotes, misinterpretation of research results, and incomplete knowledge of the research issues that underlie the research results." Toward understanding the role of motion in flight simulation, the arguments for the support of each of these views are given below.

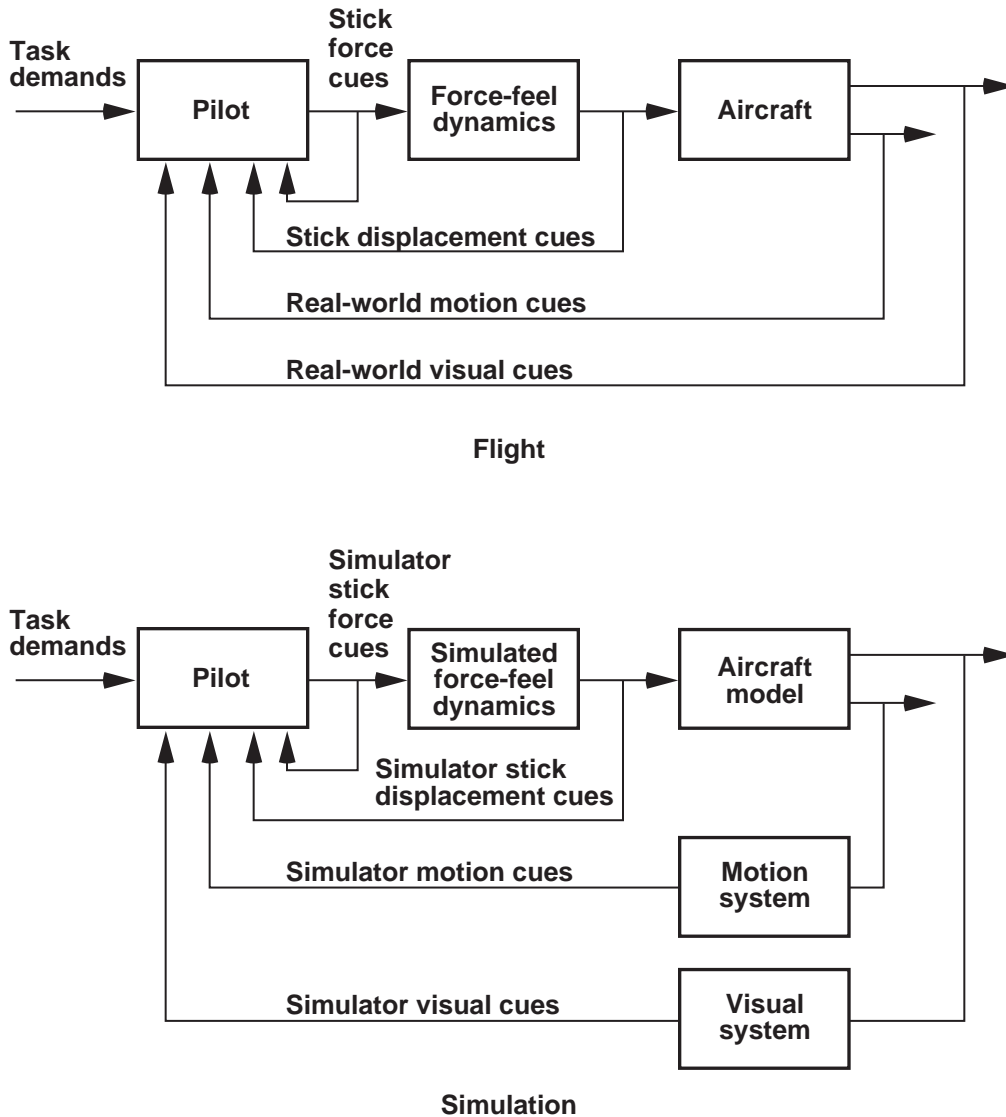


Figure 1. Flight versus simulation.

The Case Against Platform Motion. Cardullo cites many of the reasons users either do not employ motion or believe it is unnecessary (ref. 9). First, platform motion usually does not have the face validity that a simulation component such as the visual system does. Face validity is defined as a seamless one-to-one correspondence with the real world. Some subsequently argue that since the true motion environment cannot be duplicated faithfully, a subset of it should not be presented, for the cues are incorrect. It is also argued that providing platform motion is not cost effective. Finally, opponents of motion note that transfer-of-training studies have found no basis for a motion requirement. In particular, the U.S. Air Force's

standard view for training is that motion is not required in the simulation of any aircraft with centerline thrust.

Roscoe (ref. 10) states that "Complex cockpit motion, whether slightly beneficial or detrimental on balance . . . has so little effect on training transfer that its contribution is difficult to measure at all." The two studies most often cited showing that motion did not have a training benefit for several tasks are those by Waters et al. (ref. 11) and Gray and Fuller (ref. 12). However, Cardullo points out that these two studies have largely been discredited because of the poor experimental apparatus used in each study (ref. 9). In particular, the motion systems had large motion platform delays.

Boldovici (ref. 8), in an extensive review for the U.S. Army, presents several reasons for not using motion platforms: (1) the absence of supporting research results, (2) possible learning of unsafe behavior based on incorrect platform cueing, (3) achievement of greater training transfer by means other than motion cueing, (4) undesirable effects of poor motion synchronization, (5) direct, indirect, and hidden costs, (6) alternatives to motion bases for producing motion cueing (e.g., g-seats, pressure suits), and (7) benign force environments.

Poor motion synchronization, which does not have a precise definition, has caused some pilots to experience simulator sickness. This discomfort affects both the pilot's performance and his acceptance of a simulator. Surprisingly the discomfort can last, or even develop, hours after the simulator session. The U.S. Navy has recommended that motion bases be turned off if sickness develops; however, that recommendation notes that some crews also become sick in the actual vehicle (ref. 13). Some branches of the armed services require a waiting period between a simulator session and flight.

Finally, several researchers have defined tasks for which motion does not seem to add benefit. Hunter et al. (ref. 14) and Puig et al. (ref. 15) indicate that motion does not seem to be very beneficial for tasks in which the pilot creates his own motion. Such instances would be for tracking tasks in a disturbance-free environment.

The Case For Platform Motion. Hall attempts to determine when platform motion is and is not important (ref. 16). He contends that non-visual cues are of little importance for primarily open-loop, low pilot-vehicle gain, low workload maneuvers with strong visual cues. However, he also states that motion cues are more important when the pilot workload increases, when the pilot-vehicle gain rises, or when the vehicle stability degrades. The latter certainly occurs in helicopter simulation.

Showalter and Parris conducted a study in which pilots had to recover from an engine-out during takeoff in a KC-135 aircraft (ref. 17). They showed that the addition of motion significantly reduced the amount of yaw activity during an engine-out when compared to the no-motion case. In the same study, they also showed that the addition of motion affected inexperienced pilots' ability to perform precision rolling maneuvers, but that the addition of motion had no significant effect on experienced pilots for the same task.

Young showed that platform motion reduced the pilot's response time to a failure or disturbance while on a glide path compared to the no-motion case (ref. 18). In the same paper, results were presented showing that when helicopter pilots and highly trained non-pilots hovered an

unaugmented helicopter model, their performance significantly improved with the addition of motion. Performance did not improve for the moderately trained non-pilots.

Hosman and van der Vaart (ref. 19) found that performance improved with motion in roll for both disturbance rejection and tracking over that of the no-motion case. However, the roll motion in this case included the spurious lateral specific force cues owing to the lack of simulator translational motion available to account for coordination.

One of the few studies that has examined the performance effects of full motion versus no motion was performed for the roll axis by McMillan et al. (ref. 20). That study also showed significant improvement in tracking, but little improvement in a transfer-of-training metric when full motion was present over the no-motion case. Similar results were present by Levison et al. (ref. 21).

Boldovici (ref. 8), in his balanced presentation on both sides of the motion argument, gives a set of reasons for employing motion platforms: (1) to reduce the incidence of simulator sickness (note that this argument is used both for and against motion), (2) users' and buyers' acceptance of improved validity, (3) trainees' motivation, (4) to learn how to perform time-constrained dangerous tasks, and (5) to overcome the inability to perform some tasks without motion.

For difficult control tasks, early studies showed that motion allows a pilot to form the necessary lead compensation more readily with acceleration cues than with the visual displays alone (refs. 18, 22). For stabilization tasks a pilot will often use this lead compensation to reduce the open-loop system phase loss and thus allow an increase in the pilot-vehicle open-loop crossover frequency to a point higher than that achieved without motion (ref. 23). This increased crossover frequency, with the same or better phase margin, yields tracking performance more akin to that of flight.

Interestingly, the FAA has been a strong supporter of platform motion. Indeed, if a device is to be called a simulator by the FAA, it must have motion. If a device does not have motion, then the FAA terms it "a flight training device" (refs. 3, 5).

Developing Requirements for Motion

Since instances have clearly arisen in which the addition of platform motion shows significant benefits, the question remains "For those instances, what are the motion requirements?" Defining the necessary requirements for the quality, or fidelity, of that motion has been difficult. The fact that requirements are not known is

evident from the following quotes from the literature. “Unfortunately, explicit definitions of ‘valuable’ motion fidelity, for specific research or training objectives, remain for the most part undetermined” (ref. 24). “Formal experiments to determine acceptable attenuation and phase lag of the force vector are limited in scope . . .” (ref. 25). “Future research topics in the area of flight simulation techniques should encompass minimum essential visual and motion cueing requirements for a particular flying mission” (ref. 2).

Although definitive answers regarding necessary motion requirements do not exist, regulators still suggest which motion degrees of freedom may be useful. These suggestions depend on the level of simulator sophistication desired by the user. For instance, the FAA specifies two levels of motion sophistication for helicopter flight simulators: full six-degrees-of-freedom motion, and three-degrees-of-freedom motion (ref. 5). For the latter, the nominal three degrees of freedom are pitch, roll, and vertical. If degrees of freedom different from these are selected by a user, they must be qualified by the FAA on a case-by-case basis. Although the selection of the pitch, roll, and vertical degrees of freedom is reasonable, evidence to support the selection of these axes or any set of axes is lacking.

Even though existing motion criteria are incomplete, however, considerable research has been performed. To divide and conquer the problem, the six degrees of freedom are often broken into two categories: rotational motion and translational motion. But even at this high level, differences in opinion exist on the relative cueing importance of these two categories. For example Stapleford et al. (ref. 26) state, for tracking, “Translational motion cues appear to be generally less important than rotational ones, although linear motion can be significant in special situations.” Young states “For most applications, simulation of vehicle angular motions is more important than translational simulation” (ref. 18). In contrast, the concluding remarks of Bray (ref. 27) state, “For large aircraft, due to size and to the basic nature of their maneuvering dynamics, the cockpit lateral translational acceleration cues appear to be much more important than the roll acceleration cues. There was the indication that this observation might be extended to the generalization that, in each plane of motion, the linear cues are much more valuable than the rotational cues.”

Reasons for these differences of opinion at a high level are unclear and point to the need for additional research. But before the appropriate directions for the additional research can be determined, a careful review of past work is warranted. Those analytical and experimental efforts that have addressed motion requirements are discussed below.

Analytical Motion Research. Many decisions are made during both the design and development of a particular simulation. All of the components shown in figure 1 must be selected, and their characteristics must be specified. If an analytical model was available that accounted for the fidelity effects of these components, then one could inexpensively make performance trade-offs to optimize both the cost and utility of a simulator system. So, a good analytical model would have great use.

Although the dynamics of the non-piloted components of figure 1 are straightforward, the difficulty facing the modeler is the pilot block. Pilots are often adaptive, nonlinear, and inconsistent, and modeling their input/output characteristics is a challenge. A possible breakdown of the key processes carried out by a pilot is shown in figure 2. These key processes are sensation, perception, and compensation. The general characteristics of these processes are discussed next, because knowledge of them is relevant to the experimental designs presented in later sections.

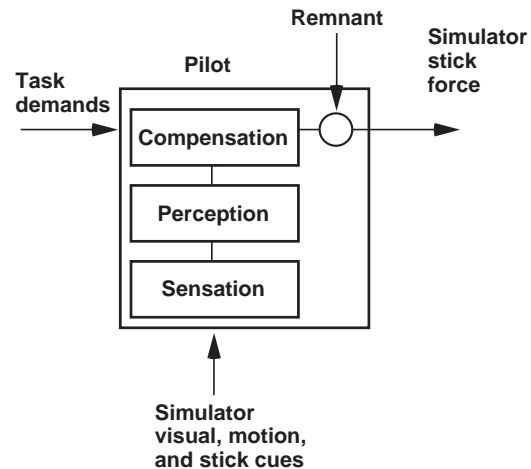


Figure 2. Top-level pilot model.

The sensation block in figure 2 is often used as the starting point when motion requirements are hypothesized, and a large database exists on human motion-sensing characteristics (refs. 28–36). The details of the human motion sensing systems are given in appendix A, but four key points are made here. First, the bandwidth of the total human motion sensory system encompasses the typical pilot-vehicle range of frequencies (0.1–10 rad/sec). Second, for the experiments that are subsequently described, the thresholds of human motion sensors were exceeded; however, the literature acknowledges that motion-sensing thresholds differ among individuals and that they depend on whether the subject is active or passive during the

motion stimulus (ref. 36). Third, previous incorporation of the motion dynamics and thresholds into models of a pilot-vehicle system has not resulted in an improved ability to model pilot-vehicle behavior (ref. 35). Finally, previous efforts to generate an integrated motion cueing model have concluded that additional experiments need to be conducted before that goal can be accomplished (ref. 31).

Once the cues are sensed, the perception block of figure 2 comes next. At this point, an integrated perceptual process likely occurs, but how it is accomplished is not known exactly. One has to know how all of the external cues (visual, kinesthetic, and tactile) are summed to develop the pilot's perception of motion. Unfortunately, little is known about how these cues affect motion perception, and further careful experiments are required to explore the perceptual interactions that occur among these cues.

After the pilot has developed an estimate of the vehicle state from the output of the perception block, compensation is then applied to this state vector. Fundamentally, it is known that the pilot applies compensation necessary to have "integrator-like" or "K/s-like" characteristics in the crossover region of the pilot-vehicle open-loop combination (ref. 37). To do this, a pilot will typically provide up to 1 sec of lead before his estimate of a task workload is degraded.

Application of the above concepts is presented in appendix B, which gives details of a structural pilot model for the vertical axis experiment described in section 4. It is shown that the model captures the general closed-loop performance trends. However, it underpredicts the magnitude of these trends to the point that it suggests no fidelity differences should exist when, in fact, they do exist. In addition, the model is incomplete, for it does not account for the gain on motion platform acceleration.

To summarize, a credible analytical model does not yet exist for flight simulation. More experimental data are needed to develop and refine the model further. The experiments that have been performed to date are discussed next.

Experimental Motion Research. Many previous experiments have contributed toward the development of motion-fidelity requirements. Although some of the data from these previous studies may be correlated, differences in visual and motion systems, tasks, and vehicle dynamics typically prevent the consistent understanding and development of motion-fidelity criteria. Below, key results of both rotational and translational experiments are presented.

Experimental Rotational Criteria. Stapleford et al. examined the effects of roll and roll-lateral motion on a pilot's ability to track a target during a disturbance

(ref. 26). Using both a tracking and a disturbance input, some key aspects of how the pilot closes the visual and motion feedback loops were presented. They suggested that angular cues be accurate in the 0.5–10 rad/sec range; however, "accurate" was not precisely defined.

Bergeron evaluated the effects of attenuating only the motion filter gain in the angular degrees of freedom (ref. 38). For the highly stabilized vehicle that was simulated, the results suggested that motion has no effect on the performance of single-axis stabilization tasks. Motion effects became evident only when simultaneous control of two angular axes was required. Presenting as little as 25% of the full motion produced results comparable to those for full motion.

In the Netherlands, van Gool suggested that second-order pitch and roll high-pass filters with break frequencies of 0.5 rad/sec appear adequate (ref. 39). This result was for stabilizing the pitch and roll attitude of a DC-9 on approach. Both the high-frequency gain and damping ratio of the motion filter were unity in all of van Gool's motion configurations.

Cooper and Howlett examined five tasks with a helicopter model in an attempt to determine motion fidelity requirements for a particular six-degrees-of-freedom hexapod motion platform (ref. 40). They made the point that to achieve maximum results from a simulator, the structure and values of the high-pass motion filters need to be tailored for the task while staying within the platform excursion limits. Although motion amplitude can be reduced by either reducing the motion filter gain or the time-constant, their experience had been that it was better to use the combination of both rather than reducing only the time-constant. Their tentative conclusion was that it was best to use a gain of 0.8 in pitch and roll with a time-constant of 4 sec.

Using a fixed-wing model, the effects of roll-only motion were examined by Jex et al. (ref. 41). Their recommendation was to provide the pilot with accurate roll-rate motion cues at frequencies above 0.5–1.0 rad/sec with a first-order high-pass filter. A filter time-constant of 2–3 sec was recommended. Here, the word "accurate" included the allowance of a 0.5–0.7 gain on the filter. Not providing the initial full roll-rate cue was deemed acceptable.

Shirachi and Shirley used a model of a Boeing 367 transport for a disturbance-rejection task in roll (ref. 42). The simulator motion platform had sufficient lateral translational displacement to coordinate the rolling maneuvers. The results suggested that if the high-frequency gain on the roll high-pass filter was lower than about 0.5 performance would approach that of no motion.

This gain limitation was deemed acceptable with a second-order high-pass filter break frequency of 0.7 rad/sec.

Bray found that for a large transport aircraft with full roll gain, motion filter break frequencies of 0.5 rad/sec caused slight contradictions in the visual and roll motions (ref. 27). Increasing the break frequency to 1.0 or 1.4 rad/sec resulted in a reduction of some pilots' ability to stabilize the Dutch roll motions.

Experimental Translational Criteria. Fewer experiments have examined translational motion than rotational motion. Cooper and Howlett (ref. 40) suggested a lateral translational-axis fidelity criterion, as shown in figure 3. Second-order filters were used with a hexapod platform capable of ± 5 ft of lateral translation. The specific points tested to arrive at the best compromise region were not given.

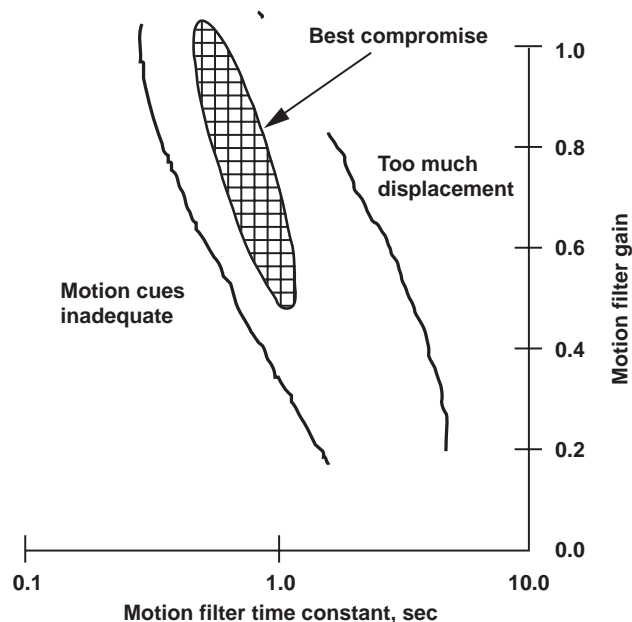


Figure 3. Suggested lateral translational axis criterion.

Jex et al. expanded their roll study (ref. 41) into the roll and sway axes (ref. 43), and the effects of the false lateral translational cue owing to roll attitude were investigated. A second-order high-pass filter with a damping ratio of 0.7 was inserted into the lateral translational drive path, and a suggested motion-fidelity criterion of the filter's gain versus frequency was proposed as shown in figure 4. A large region of uncertainty exists because of the limited range of points tested.

Bray focused on the vertical axis and determined the effects of motion filter natural frequency on tracking and stabilization tasks with an idealized helicopter model (ref. 24).

He suggested that the vertical acceleration phase-fidelity should be accurate down to 1.0–1.5 rad/sec. Fidelity was somewhat arbitrarily defined as the simulation motion cue not having a phase error of more than 20° relative to the model. Moderate decreases in pilot-vehicle crossover frequency and phase margin were noted if the vertical motion platform gain was lowered from 1.0 to 0.5. No other gains were examined.

Sinacori Criteria. Sinacori used a six-degrees-of-freedom helicopter model (ref. 44). Criteria relating the motion-drive dynamics to motion fidelity were postulated from a very limited set of data (four test points); they are shown in figure 5. The criteria suggest that motion fidelity can be predicted by examining the gain and phase shift between the math model and the commanded motion system accelerations at a particular frequency. The phase shift between these two accelerations is due to the high-pass motion filter placed between the two signals. The gain and phase of this filter at 1 rad/sec determine the x and y locations on figure 5, respectively. The amount by which the commanded motion-system acceleration phase angle differs from 0° is defined as its phase distortion. Apparently, a frequency of 1 rad/sec is used, since that is where the semicircular canals have the highest gain, as shown in appendix A. The resulting gain and phase distortions are then located on the appropriate criterion in figure 5, depending on whether the filter is a translational or rotational filter.

The criteria show three levels of motion fidelity: high, medium, and low. The definitions are given at the bottom of figure 5. As expected, high motion fidelity is associated with high-gain and low-phase distortion, and low motion fidelity is associated with low-gain and high-phase distortion. Sinacori notes that these criteria "... have little or no support other than 'intuition'" (ref. 44). Still, these are the most complete criteria proposed to date. The criteria are either unknown or unused in the simulator community today, perhaps because they still need to be validated.

Summary of Criteria. Summarizing the above criteria, there is apparent agreement that the rotational gain can be reduced to 0.5 without a fidelity loss, and that the phase distortion from the high-pass filter should be minimized at 0.5 rad/sec and above. These requirements come primarily from studies of roll and of limited pitch. However, many investigators, somewhat arbitrarily, place the same requirements on yaw, since they believe the yaw requirements are natural extensions of the pitch and roll requirements.

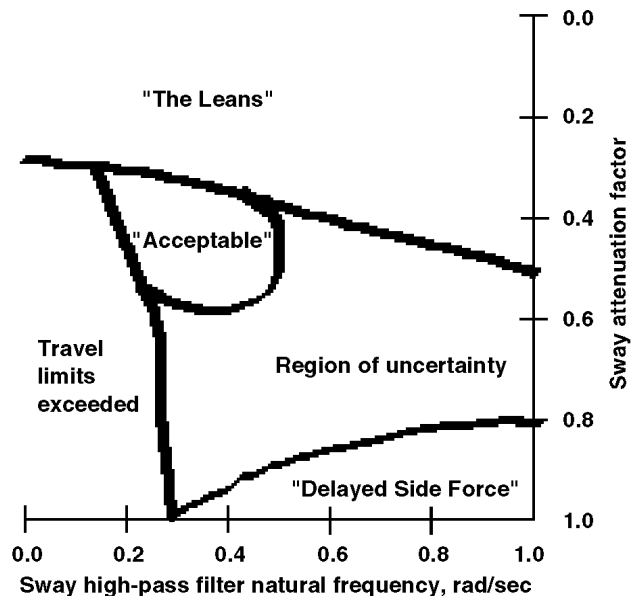


Figure 4. Sway motion fidelity criterion (ref. 43).

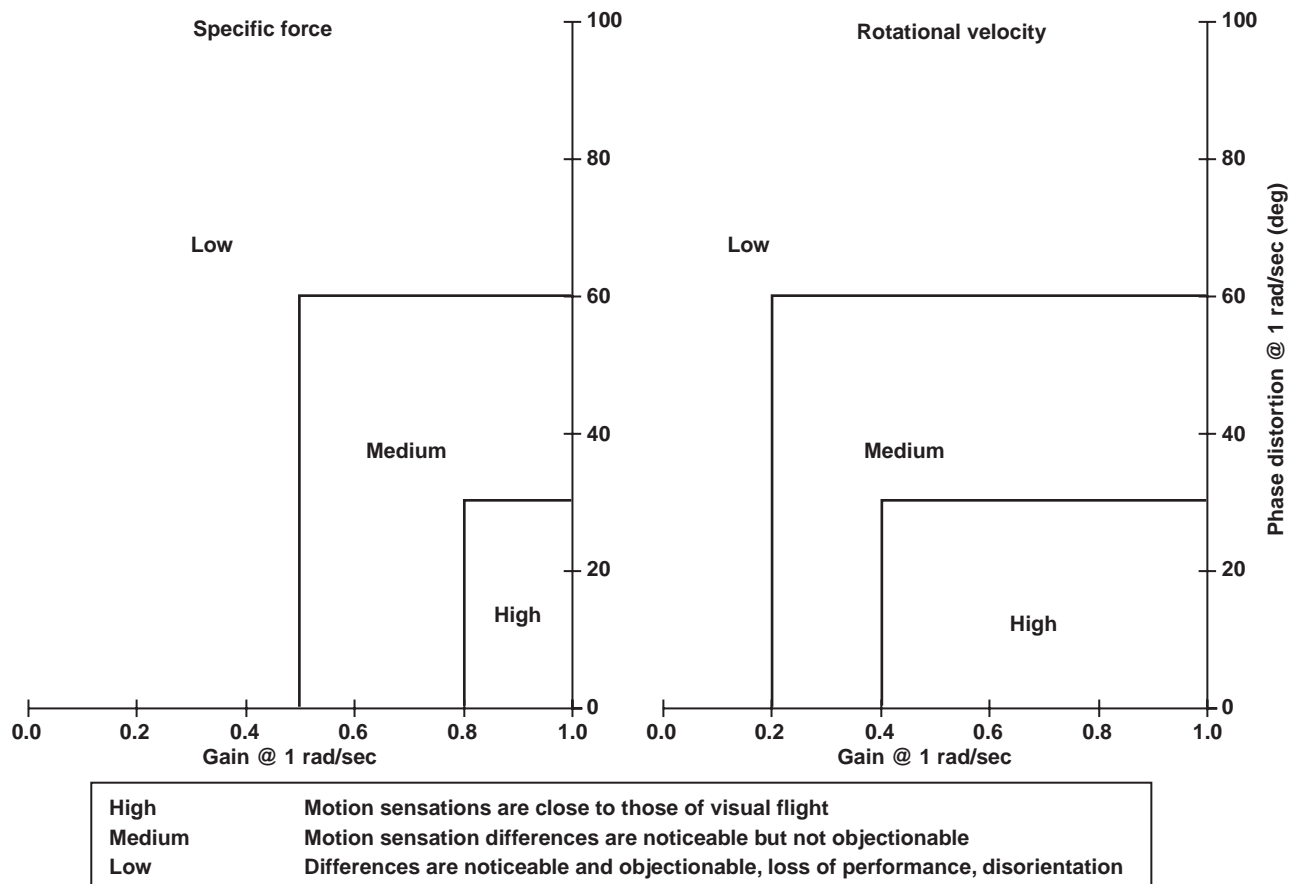


Figure 5. Sinacori motion-fidelity criteria (ref. 44).

For the translational motion fidelity, the agreement is less apparent. The data for the translational requirements are primarily from lateral translational-axis experiments, with some data from the vertical axis. There are also disagreements as to whether these translational cues are more important than the rotational cue, or vice versa.

Since motion fidelity has not been thoroughly examined in all axes, it is possible that some motion degrees of freedom are redundant with the other simulator cues that also allow motion perception. If a motion degree of freedom is unnecessary, then a savings might be realized as a result of the reduced complexity in the design, development, and operation of flight simulators. If a savings benefit is not chosen by a manufacturer, at least an operator would know not to concentrate on tuning the motion in an unnecessary degree of freedom.

An answer to “How much platform motion is enough?” is likely to be vehicle and task dependent. Vehicles that rely greatly on the pilot for stabilization, such as helicopters, will have more stringent platform-motion requirements than vehicles that do not depend on the pilot for stabilization. As such, this report focuses on the former, more stringent case.

Purpose of This Report

The purpose of this report is to develop reasonable guidelines for the use of motion in helicopter simulations. Areas in which weak guidance exists on how to employ key motion cues will be strengthened. Specifically, it will be first determined if yaw requirements are a natural extension of pitch and roll requirements. Second, the fidelity effects of vertical motion and their interaction with visual cues in altitude control will be determined. Finally, requirements for the relative magnitudes of roll and lateral translational motion will be investigated.

Approach

Although platform-motion research has been conducted previously, the approach used here is, perhaps, more valid. There are several reasons for this greater validity. First, the world’s largest displacement flight simulator was used in all of the experiments. Use of this experimental device allows selected flying tasks to be duplicated faithfully. That is, the math model, the visual cues, and the motion cues can be matched as a baseline, and then the effects of altering motion can be subsequently determined. Second, representative helicopter math models were used, with one model identified from flight test. This

approach allows helicopter-specific requirements to be determined. Third, highly experienced test pilots were used as subjects, and their insightful comments allow confident extrapolations from simulation to flight. Finally, the results were corroborated with both objective and subjective data. In most cases, enough data were collected to allow the measures to be quantified statistically, an advantage that limited facility-use time often does not allow.

These methods should provide a high degree of confidence in the results. They were applied in order to the yaw, vertical, roll, and lateral translational degrees of freedom. Motions in the yaw and vertical axes were examined first, because these motions are the simplest. That is, the gravity vector remains aligned relative to the cockpit for these motions. Next, the coupled roll and lateral axes were explored. These motions are coupled, since the gravity vector rotates relative to the cockpit. The coupled pitch and longitudinal axes have been left for future work; however, the requirements in pitch and longitudinal are not expected to differ substantially from those of roll and lateral.

Contributions

1. The results indicate that yaw rotational platform motion has no significant effect in hovering flight simulation. For three tasks that broadly represented hovering flight, the addition of yaw-rotational motion yielded insignificant changes in pilot-vehicle positioning performance, pilot control activity, pilots’ rating of required control compensation, and pilots’ opinion of motion fidelity.
2. Lateral translation of the motion platform has a significant effect on hovering flight simulation. For three tasks that broadly represent hovering flight, the addition of lateral translational motion improved pilot-vehicle positioning performance, reduced pilot control activity, lowered pilot ratings of required control compensation, and improved pilots’ opinions of motion fidelity.
3. Lateral translation of the motion platform, plus typical visual cues, made pilots believe that the motion platform was rotating when it was not. That is, pilots believed they were physically rotating when the yaw platform degree of freedom was stationary. A hypothesis is that the time delay for the onset of vection is reduced, thus making pilots believe they are rotating.

4. The three previous contributions may be combined to suggest that if lateral translational platform motion is presented, available simulator platform actuator displacement should not be used for yaw. Instead, the actuator displacement should be diverted to axes that can derive more benefit from motion.
5. Vertical platform motion has a significant effect on simulation fidelity. For target tracking and disturbance-rejection tasks, the following occurred as the platform motion neared visual scene motion: (a) improved tracking and disturbance-rejection performance, (b) reduced pilot control activity, (c) improved pilot opinion of motion fidelity, (d) improved pilot-vehicle target-tracking phase margin, (e) higher pilot-vehicle disturbance-rejection crossover frequencies that were correlated with vertical acceleration phasing rather than with vertical axis gain, and (f) additional pilot-vehicle disturbance-rejection phase margin that was correlated with vertical axis gain rather than with vertical acceleration phasing.
6. A previously developed and unvalidated motion-fidelity criterion for the vertical axis was revised and validated. The new criterion predicts the fidelity effects of changes in the gain and the break frequency of high-pass motion filters. The revised specification allows for more reduction in the vertical gain than previously specified. The revision also suggests that the combination of a reduction in gain and an increase in filter natural frequency is worse than either perturbation alone.
7. Vertical platform motion affected pilot estimates of steady-state altitude during altitude repositionings. This result refutes the generally accepted view that a pilot's altitude and altitude-rate feedbacks are derived from the visual cues alone. The implication is that the input and output cueing assumptions in existing pilot models are incorrect.
8. For coordination requirements in the coupled roll and lateral motion axes, a combination of previous and herein revised criteria resulted in a good prediction of motion fidelity. Also, substantial improvements in performance and opinion were demonstrated between the full-motion and no-motion configurations.
9. A procedure was developed that allows simulator users to configure their motion platforms to extract the most simulator fidelity they can from the device. The procedure uses the fidelity criteria validated herein. It suggests to users that if they are not satisfied with their predicted fidelity they should consider modifying the simulated task.

These results will provide guidance to simulator manufacturers, operators, and regulators on how to build better helicopter simulators and how to use them more effectively for training and research.

Outline

Because the Vertical Motion Simulator at NASA Ames Research Center was used in all the experiments discussed in this report, that facility is described first. Five experiments are then discussed: the Yaw Experiment; Vertical Experiments I, II, and III; and the Roll-Lateral Experiment. The experiments are presented in a common format in which each experiment addresses key questions that still remain regarding how pilots use platform-motion cues. The Yaw Experiment focused on the interaction between lateral translational platform motion and yaw rotational platform motion. Vertical Experiment I explored the ways in which the quality of vertical motion cues affects end-to-end pilot-vehicle performance and pilot opinion. Vertical Experiment II determined how key metrics in the pilot-vehicle control loops vary as the quality of vertical motion cues changes. Vertical Experiment III examined the interaction between the vertical platform-motion cue and the visual cues. And in the Roll-Lateral Experiment, the interaction between roll and lateral translational platform-motion cues was explored.

The results of these five experiments are then summarized and presented as a set of recommendations for the manufacturer and user communities. In the interest of consistency, the recommendations of this work are also discussed comparatively with the results of previous work in motion cueing. Finally, a procedure that makes the most effective use of the recommendations in configuring motion cues for any motion platform is suggested, principal conclusions are set forth, and areas requiring further research are identified.

2. The Vertical Motion Simulator

General Description

The Vertical Motion Simulator (VMS) (ref. 45) at NASA Ames Research Center was used in all of the experiments reported herein. It is the world's largest flight simulator. A cutaway view of the motion system and its position, velocity, and acceleration limits are shown in figure 6. It is an electrohydraulic servo system, with a payload of 140,000 lb. This payload is pneumatically counter-weighted with pressurized nitrogen. Both the vertical and lateral translational degrees of freedom are driven with separate electric motors in a rack-and-pinion arrangement. The remaining degrees of freedom are hydraulic.

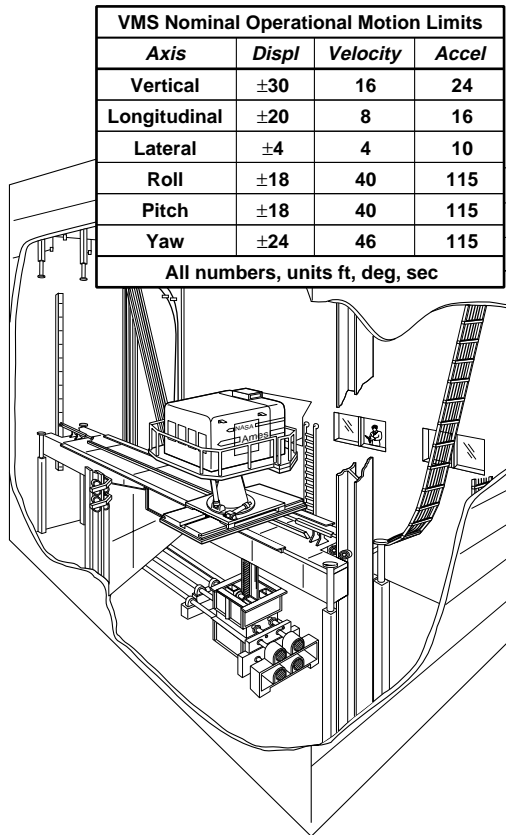


Figure 6. Vertical Motion Simulator.

Five interchangeable cockpits are available from which to choose for each experiment. Each cockpit has a different window layout and can have a different stick, instruments, and visual system image generators. Thus, these characteristics are described separately for each experiment.

Performance Characteristics

The dynamic performance of the VMS depends on the axis. Using frequency-response testing techniques (ref. 46), the dynamics of the yaw rotational, longitudinal, lateral, and vertical translational axes were fitted with equivalent time delays (that is, the phase response was approximated as a pure time delay) as shown below. Equations (2) and (3) are taken from previous work (ref. 47).

$$\frac{\ddot{\Psi}_{\text{sim}}}{\ddot{\Psi}_{\text{com}}}(s) \approx e^{-0.13s} \quad (1)$$

$$\frac{\ddot{x}_{\text{sim}}}{\ddot{x}_{\text{com}}}(s) \approx e^{-0.17s} \quad (2)$$

$$\frac{\ddot{y}_{\text{sim}}}{\ddot{y}_{\text{com}}}(s) \approx e^{-0.13s} \quad (3)$$

$$\frac{\ddot{h}_{\text{sim}}}{\ddot{h}_{\text{com}}}(s) \approx e^{-0.14s} \quad (4)$$

The subscript sim refers to the actual simulator acceleration, and the subscript com refers to the commanded simulator acceleration. Only these four degrees of freedom are listed because the other two degrees of freedom were not used in this work.

3. Yaw Experiment

Background

Research in the yaw axis has been sparse and inconclusive. Meiry, in the first detailed investigation into the effects of yaw rotational motion, found that adding the motion was beneficial (ref. 22). The study indicated a reduction in pilot time delay of 100 msec, with a concomitant improvement in performance. In contrast, two studies that examined a pilot's ability to perform hovering flight tasks with a representative vehicle model found little or no effect of yaw rotational platform motion on pilot-vehicle performance or on pilot opinion (refs. 48, 49).

In the latter studies, the variations in yaw rotational platform motion ranged from no-motion to full-motion, where full-motion refers to a platform that moves the same amount that the math model moves. Pilots were intentionally located at the vehicle's center of rotation and only experienced the rotational motion cues associated with the vehicle yaw motion. Thus, the translational accelerations typically produced by yaw motion, when the pilot is displaced from the center-of-rotation, were absent by design. The tasks were target tracking in the presence of an atmospheric disturbance and heading captures. These results suggested that the usefulness of the yaw degree of freedom be explored further.

The purpose of the study described in this section is to extend the previous research and, more specifically, to determine if yaw platform motion has a significant effect on pilot-vehicle performance and pilot opinion in situations more representative of flight. If yaw platform motion is unnecessary, then a savings might be realized from a reduced level of complexity in the design, development, and operation of flight simulators. In addition, the actuator displacement usurped by the yaw degree of freedom could be made available for more useful displacements in other degrees of freedom.

First, the experimental setup is described, which includes the three piloting tasks, the vehicle math model, the simulator cueing systems, and the motion system configurations that were evaluated. This description is followed by a presentation of both the objective and subjective results, which are summarized at the end.

Experimental Setup

There can be confusion when the words "yaw motion" are used to describe a motion situation. This confusion arises because the motion that occurs at the vehicle's center of

mass is different from the motion experienced at the pilot's location. For instance, for the purposes here, when a pilot sits forward of the yaw center of rotation, a vehicle yawing motion produces both yaw and lateral translation cues at the pilot's location. Since the motion at the pilot's location is what the simulator is trying to reproduce, all subsequent discussions of motion refer to pilot-station motion. In addition, in this section, the word "rotation" refers to orientation changes about the yaw axis, and the word "translation" refers to sway motion in the vehicle's y body-axis.

Tasks

Three tasks were developed to represent a broad class of situations in which both lateral-translational and yaw-rotational motion cues may be useful in flight simulation. Task 1 was a small-amplitude command task that allowed for full math-model motion to be provided by the motion system. Task 2 was a large-amplitude command task that did not allow full math-model motion to be presented, for the simulator cab rotational and longitudinal translational limits would have been exceeded; however, it was accompanied by strong rotational visual cues. Task 3 was a disturbance-rejection task, which also allowed full math-model motion to be provided by the motion system, but with the pilot also controlling vehicle altitude.

Task 1: 15° yaw rotational capture

In the first task, the pilot controlled the vehicle only about the yaw axis. The pilot was required to acquire rapidly a north heading from 15° yaw rotational offsets to either the east or west. This task allowed for full math-model motion to be represented by the motion system in all axes (rotational and translational). An aircraft plan view, with the pilot's simulated position relative to the inertially fixed center of mass (c.m.), is shown in figure 7.

The desired pilot-vehicle performance for the task was to rapidly capture and stay within $\pm 1^\circ$ about north with two overshoots or less. This 2° range was visually demarcated by the sides of a vertical pole, shown in the pilot's forward field of view in figure 8. The pilot's reference on the aircraft for positioning was a fixed vertical line centered on the head-up display. Pilots performed six captures with each motion configuration, alternating between initial west and east directions. The repositionings from north to the initial east or west initial positions were not part of the task.

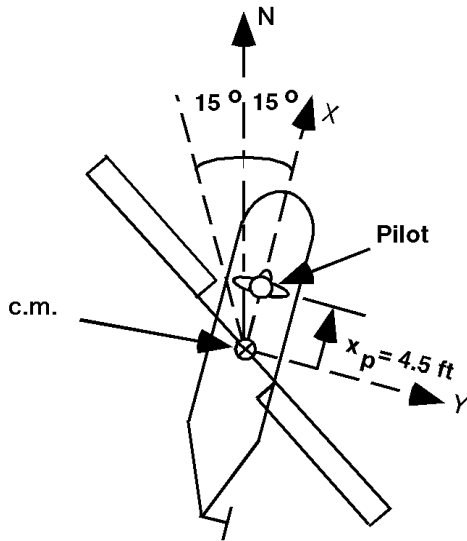


Figure 7. Pilot location in plan view.

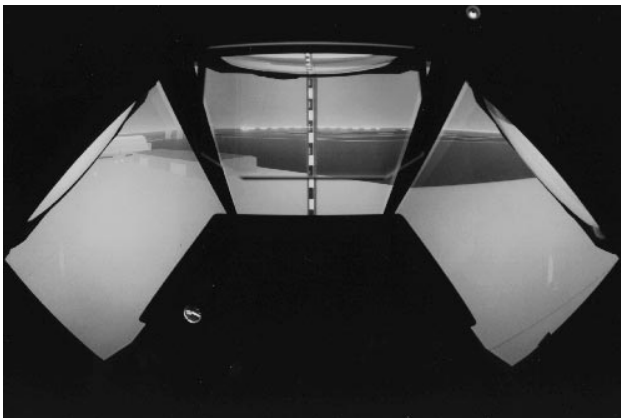


Figure 8. Pilot's visual scene in Tasks 1 and 3.

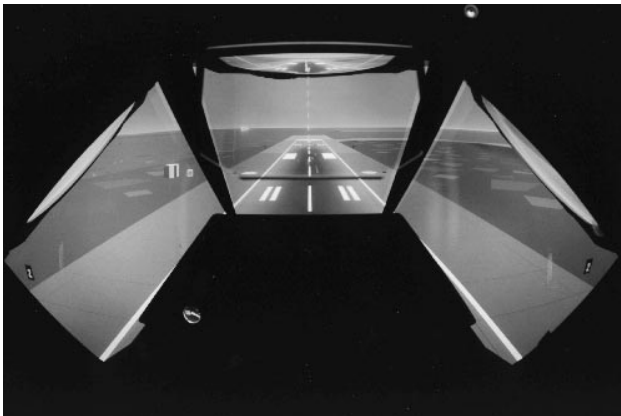


Figure 9. Pilot's visual scene in Task 2.

Task 2: 180° hover turn

The second task required a 180° pedal turn over a runway, which was to be performed in 10 sec. The pilot again controlled the aircraft with the pedals only, and the position of the c.m. remained fixed with respect to Earth. This maneuver was taken from the current U.S. Army rotary-wing design standard (ref. 50) and, with one proviso, is representative of a handling qualities maneuver performed for the acceptance of military helicopters. However, in the military acceptance maneuver, the pilot controls all six degrees of freedom rather than one.

This maneuver did not allow for full math-model motion, since the simulator cab cannot rotate 180°. As a result, attenuated motion was used, as described later. Desired performance was to stabilize at the end of the turn to within $\pm 3^\circ$ and within 10 sec. Pilots performed six 180° turns, always turning over the same side of the runway to keep the visual scene consistent for the set of turns. Figure 9 shows the visual scene from the starting position.

Task 3: Yaw rotational regulation

The third task required the pilot to perform a rapid 9-ft climb while attempting to maintain a constant heading. This disturbance-rejection task was challenging, because collective lever movement in the unaugmented AH-64 model results in a substantial yawing moment disturbance (because of engine torque) that must be countered (rejected) by the pilot with pedal inputs. This task allowed full vertical, yaw-rotational, and lateral-translational motion at the pilot's station. Desired performance was for the pilot to acquire the new height as quickly as possible while keeping the heading within $\pm 1^\circ$ of north. The same visual scene was presented as in Task 1 (fig. 8), but with the scene also indicating height variations as the vehicle model changed altitude.

Simulated Vehicle Math Model

The math model represented an unaugmented AH-64 Apache helicopter in hover, which had been identified from flight-test data and subsequently validated by several AH-64 pilots (ref. 51). Equation (5) describes the vehicle dynamics for the rotational ψ and vertical h degrees of freedom:

$$\begin{bmatrix} \ddot{\Psi} \\ \ddot{h} \\ \dot{z}_1 \end{bmatrix} = \begin{bmatrix} -0.270 & 0.000 & 0.000 \\ 0.000 & -0.122 & -118. \\ 0.000 & 0.000 & -12.9 \end{bmatrix} \begin{bmatrix} \dot{\Psi} \\ \dot{h} \\ z_1 \end{bmatrix} \quad (5)$$

$$+ \begin{bmatrix} 0.494 & 0.266 \\ 0.000 & 14.6 \\ 0.000 & 1.000 \end{bmatrix} \begin{bmatrix} \delta_r \\ \delta_c \end{bmatrix}$$

The collective position δ_c and pedal position δ_r are in inches. The variable z_1 was an additional state added to approximate the effects of dynamic inflow (ref. 51). All other vehicle states were kinematically related to the above dynamics. So, in effect, the vehicle c.m. was constrained to remain on a vertical axis fixed with respect to Earth for all tasks. Although the tail rotor in an actual helicopter produces both a side force and a moment about the c.m., only the moment was represented in this experiment, a result of the fixed c.m. These vehicle constraints were introduced to simplify the number of motion sensations that had to be interpreted by the pilot. In addition, no coordination of the gravity vector was required, for it remained fixed relative to the pilot. No atmospheric turbulence was present in any of the tasks. The collective lever was used for Task 3 only.

The pilot was located 4.5 ft forward of the c.m., which represents the AH-64 pilot location. Thus for this case, math model rotational accelerations were accompanied by lateral translational accelerations at the pilot's station, and rotational rates were accompanied by longitudinal accelerations at the pilot's station. Specifically, the accelerations at the pilot's station in this experiment were as follows:

$$a_{x_p} = -4.5\dot{\Psi}^2 \quad (6)$$

$$a_{y_p} = 4.5\ddot{\Psi} \quad (7)$$

$$\ddot{\Psi}_p = \ddot{\Psi} \quad (8)$$

where the subscript p refers to the pilot's station.

Simulator and Cockpit

The Vertical Motion Simulator, described in section 2, was used. The mainframe-computer cycle time was 25 msec. The Evans and Sutherland CT5A visual system provided the visual cues, and it had a math-model-to-visual-image-generation delay of 86 msec (ref. 52). This delay is typical of today's flight simulators. The visual field of view is shown in figure 10. The visual cues

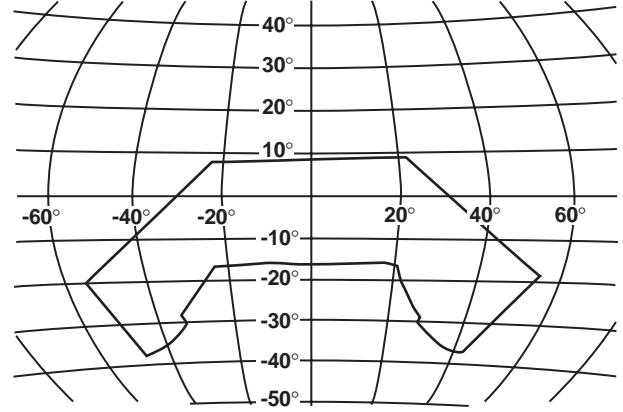


Figure 10. Cockpit visual field of view.

presented to the pilot did not vary and were always those of the math model. These cues represented the pilot's physical offset of 4.5 ft forward of the vehicle's c.m.

Conventional pedals and a left-hand collective lever were used. The pedals had a travel of ± 2.7 in, a breakout force of 3.0 lb, a force gradient of 3 lb/in, and a damping ratio of 0.5. The collective had a travel of ± 5 in, no force gradient, and the friction was adjustable by the pilot.

All cockpit instruments were disabled, which made the visual scene and motion system cues the only primary cues available to the pilot. Rotor and transmission noises were present to mask the motion-system noise. Six NASA Ames test pilots participated in Task 1, and five of the same six participated in Tasks 2 and 3. All pilots had extensive rotorcraft flight and simulation experience.

Motion System Configurations

Four motion-system configurations were examined for each of three tasks: (1) translational and rotational motion, (2) translational without rotational motion, (3) rotational without translational motion, and (4) no motion. Figure 11 illustrates, in a plan view, the simulator cab motion for these configurations for Task 1, which was the $\pm 15^\circ$ heading turns. In the Translation+Rotation case, the cab translates and rotates as if it were placed on the end of a 4.5-ft vector rotating in the horizontal plane. This case represented physical reality, or the truth case. In the Translational case, the pilot always points in the same direction, as the cab translates in x and y. In the Rotation case, the cab rotates but does not translate. Finally, in the Motionless case, the cab does not move.

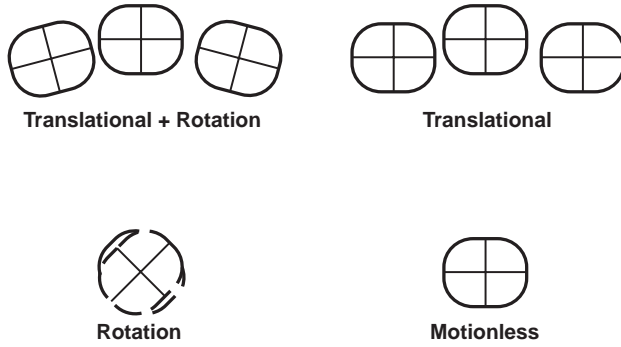


Figure 11. Simulator cockpit motion configurations in plan view.

When either translational motion or rotational motion was present for Tasks 1 and 3 (yaw rotational regulation), it was the full translational or rotational motion calculated by the vehicle math model. That is, the cockpit provided the full accelerations that the math model calculated and that the visual scene provided, along with the effective motion delays in equations (1)–(4). This statement was true, except for the longitudinal motion provided by the translational motion configuration; for yaw turns about a point, the longitudinal acceleration at the pilot's station is always negative (centripetal acceleration in eq. (6)). These accelerations, if integrated twice to motion-system position commands, would cause continual longitudinal cab movement aft for this motion configuration. Eventually, the simulator cab would exceed its available longitudinal displacement. Thus, a second order, high-pass filter was used in the longitudinal axis so that the cab would return to its initial position in the steady state. This type filter is typically used in flight simulation, and it had the form of

$$\frac{\ddot{x}_{com}}{a_{xp}}(s) = \frac{Ks^2}{s^2 + 2\zeta\omega_m s + \omega_m^2} \quad (9)$$

where \ddot{x}_{com} is the commanded longitudinal acceleration of the simulator cab, a_{xp} is the math model's longitudinal acceleration at the pilot's position, K is the motion gain, ζ is the damping ratio, and ω_m is the filter's natural frequency.

As described earlier, Task 2 (180° hover turn) did not allow full motion. Thus, a high-pass filter of the same form in equation (9) was used in all axes. The values of K and ω_m were empirically selected to use as much cockpit motion as available (fig. 6).

For Task 3, the vertical motion was always the full math model vertical motion, even in the Motionless condition.

That is, Motionless for Task 3 refers to the simulator cab being motionless in the horizontal plane. Table 1 lists K and ω_m for each tested configuration in each axis. A configuration with $K = 1$ and $\omega_m = 1.0E-5$ rad/sec effectively makes the filter in equation (9) unity for the tasks, considering the task time-scale. The filter damping ratio (ζ) was 0.7 for all configurations.

Each of these tasks could be performed on a typical hexapod motion system, except for the vertical translations required in Task 3. In particular, the amount of cab translation corresponding to the $\pm 15^\circ$ rotations in Task 1 is less than ± 1.2 ft. For Task 2, typical pilot aggressiveness levels resulted in maximum cab yaw orientations of less than $\pm 5^\circ$ and lateral travels of less than ± 0.5 ft. Finally, for Task 3, maximum cab yaw orientations were also less than $\pm 5^\circ$ and lateral travels were less than ± 0.5 ft. However, the vertical simulator cab translation for Task 3 was near 10 ft, which could not be accomplished by today's hexapods.

Procedure

Pilots were asked to rate the overall level of compensation required for a task using the following descriptors: not-a-factor, minimal, moderate, considerable, extensive, and maximum-tolerable. These descriptors were taken from the Cooper-Harper Handling Qualities Scale (ref. 53), and were thus familiar to all the test pilots. For analysis, these adjectives were given interval numerical values from -1 to 4, respectively.

Next, the pilots rated the motion fidelity according to the following three categories: (1) Low Fidelity—motion cueing differences from actual flight were noticeable and objectionable, (2) Medium Fidelity—motion cueing differences from actual flight were perceptible, but not objectionable, and (3) High Fidelity—motion cues were close to those of actual flight. These definitions were taken (and slightly modified) from Sinacori (ref. 44) (modification discussed later in sec. 4). For this experiment, pilots had to rely on recollection of their actual in-flight experience. These subjective ratings were given numerical values 0 to 2, respectively.

Finally, the pilots were asked to report whether they perceived any cockpit translational or rotational motion. A zero was assigned if they did not feel a particular motion. Each of the four configurations was flown four times in a random sequence by each pilot.

Table 1. Motion filter quantities for yaw tasks.

Task	Rotation		Lateral		Longitudinal		Vertical	
	K	ω_m (rad/sec)	K	ω_m (rad/sec)	K	ω_m (rad/sec)	K	ω_m (rad/sec)
1 - translational +rotational	1.00	1.0E-5	1.00	1.0E-5	1.00	1.0E-5	0.00	1.0E-5
1 - translational	0.00	1.0E-5	1.00	1.0E-5	1.00	0.2	0.00	1.0E-5
1 - rotational	1.00	1.0E-5	0.00	1.0E-5	0.00	1.0E-5	0.00	1.0E-5
1 - motionless	0.00	1.0E-5	0.00	1.0E-5	0.00	1.0E-5	0.00	1.0E-5
2 - translational +rotational	0.35	0.55	0.35	0.55	0.35	0.55	0.00	1.0E-5
2 - translational	0.00	0.55	0.35	0.55	0.35	0.55	0.00	1.0E-5
2 - rotational	0.35	0.55	0.00	0.55	0.00	0.55	0.00	1.0E-5
2 - motionless	0.00	0.55	0.00	0.55	0.00	0.55	0.00	1.0E-5
3 - translational +rotational	1.00	1.0E-5	1.00	1.0E-5	1.00	1.0E-5	1.00	1.0E-5
3 - translational	0.00	1.0E-5	1.00	1.0E-5	1.00	0.2	1.00	1.0E-5
3 - rotational	1.00	1.0E-5	0.00	1.0E-5	0.00	1.0E-5	1.00	1.0E-5
3 - motionless	0.00	1.0E-5	0.00	1.0E-5	0.00	1.0E-5	1.00	1.0E-5

Results

Using standard terminology, the above experimental design is called a two-factor fully-within-subjects factorial experiment (ref. 54). The two factors were translational and rotational motion. Each of the two factors had two motion levels: present or absent. The combination of the two levels within each factor results in four motion configurations for each task. An analysis of variance was performed on the data taken for each task, with the observed significance levels (p-values) given below. The quantity $F(x,y)$ is the estimated ratio of the effects due to individual subjects, plus the effects due to experimental variation, all divided by the effects due to individual subjects. The values of x and y are the numerator and denominator statistical degrees of freedom, respectively. The p-values represent the probability of making an error in stating that a difference exists based on the experimental results when no difference actually exists. If no difference actually exists, the variations are due to randomness. Typically, differences are deemed significant for $p < 0.05$ (5 chances in 100 of making an error). An

example of how data are processed using the above is given in appendix C.

Task 1: 15° Yaw Rotational Capture

Objective Performance Data. Figure 12 shows a representative time-history of several key variables for Task 1 for both the full motion (Translation+Rotation) and the motionless condition. Peak yaw rates (not shown) for the full-motion run were near 10°/sec. Comparing the full-motion case with the Motionless case shows that the latter had more yaw rotational overshoots about north, higher math model yaw rotational accelerations, and larger control inputs.

Figure 13 depicts, for the four motion conditions, the means (circles and x's) and standard deviations (vertical lines through circles and x's) of the number of times pilots overshoot the $\pm 1^\circ$ heading point about north. The solid and dashed lines connecting the means are drawn to show trends when going from "No rotation" to "Rotation."

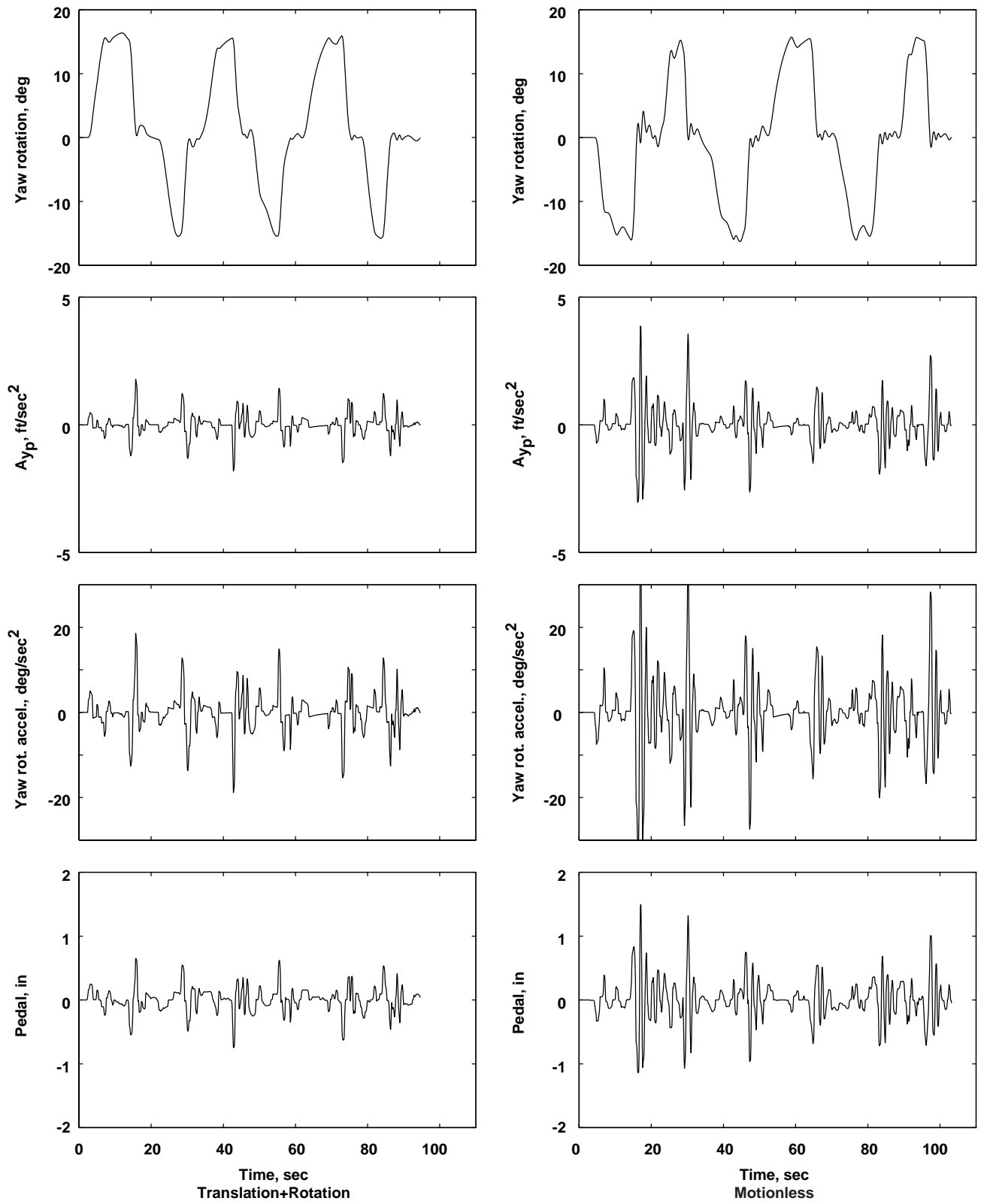


Figure 12. Comparison of full motion and no motion for Task 1.

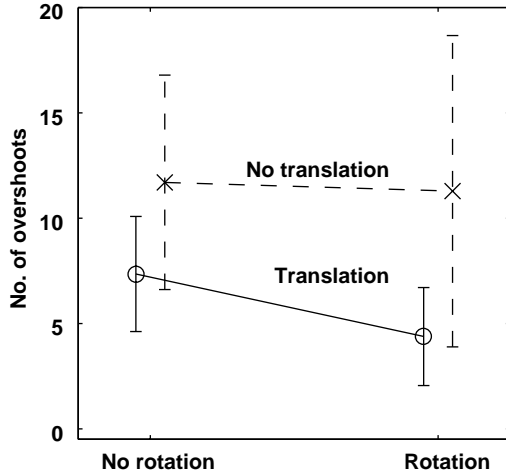


Figure 13. Measured performance for Task 1.

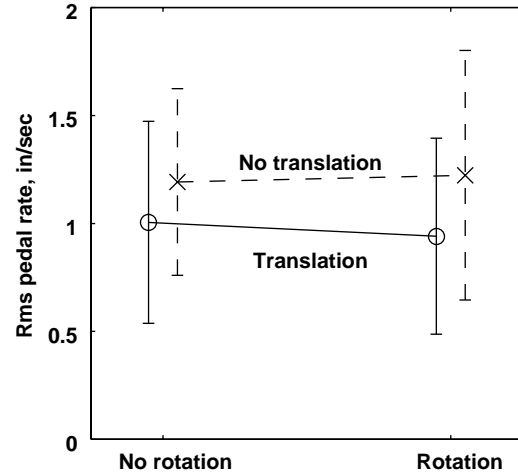


Figure 14. Control rate for Task 1.

So, figure 13 shows that when no rotational and no translational motions were present (Motionless configuration of fig. 11), the mean number of overshoots outside the $\pm 1^\circ$ criterion was 11 per run. When only lateral translational motion was present, the mean number of overshoots was 7 per run, etc. This measure is generally indicative of the level of damping, or relative stability, in the pilot-vehicle system. The analysis of variance for these results shows that when translational motion was added, the decrease in the number of overshoots was statistically significant ($F(1,4) = 9.16$, $p = 0.039$). The decrease in overshoots with the addition of rotational motion was marginally significant ($F(1,4) = 5.58$, $p = 0.077$). Of the six measures to be discussed, this was the only task of the three in which the addition of the yaw platform rotational motion indicated an improvement. However, the statistical reliability of the improvement was marginal. The effects of rotational and translational motion did not interact in this measure (i.e., they were statistically independent).

Figure 14 illustrates the rms cockpit control (pedal) rate for the four motion configurations. Often, this measure is associated with pilot workload, with more control rate being generally indicative that more pilot lead compensation is required. The analysis of variance for these data shows that when translational motion was added, the decrease in pedal rate was statistically significant ($F(1,4) = 18.53$, $p = 0.013$). No significant differences were noted when rotational motion was added, and rotational and translational motion effects did not interact.

It is not surprising that the addition of the lateral translational motion improves the pilot-vehicle performance for this and the later tasks. The addition of the

translational cue not only better emulates the real world cue, but it also provides a strong indication of the vehicle's rotational acceleration (eq. (7)). Thus, the pilot can use this information effectively to place a zero in the open loop of his rotational-rate control in order to ameliorate the effects of high-frequency lags.

Subjective Performance Data. Figure 15 shows the means and standard deviations of the compensation required (i.e., extensive, considerable, moderate, or minimum), as rated by the pilots, for the four motion conditions. When translational motion was added, the compensation that was required significantly decreased from considerable to moderate compensation ($F(1,5) = 6.83$, $p = 0.047$) and no significant differences were found for the addition of rotational motion. Rotational and translational motion did not interact for pilot compensation. These subjective pilot opinions are consistent with the objective control-rate differences just discussed. That is, the addition of translational motion reduced control activity, which in turn likely reduced pilot opinion of the required compensation.

Similar results were obtained for the pilots' rating of motion fidelity, as shown in figure 16. When translational motion was added, the motion fidelity rating improved ($F(1,5) = 7.74$, $p = 0.039$). The fidelity increased from low-to-medium to medium-to-high, on average. Although the data visually suggest an improvement in fidelity with the addition of rotational motion, the improvement was not statistically significant. Rotational and translational motion did not interact in the fidelity ratings.

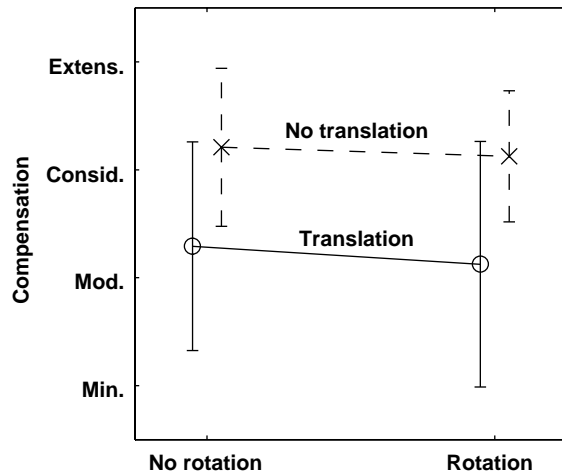


Figure 15. Pilot compensation for Task 1.

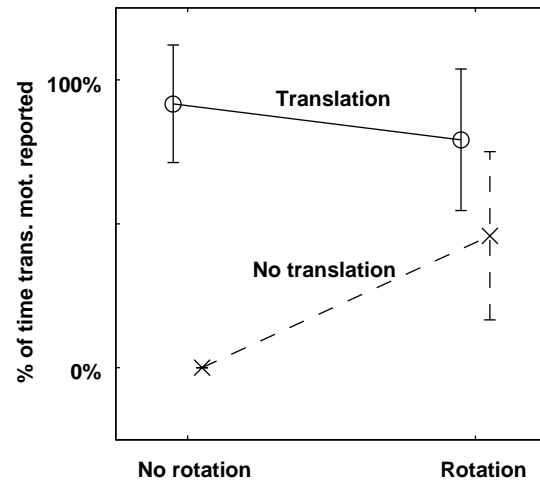


Figure 17. Lateral translational motion perception for Task 1.

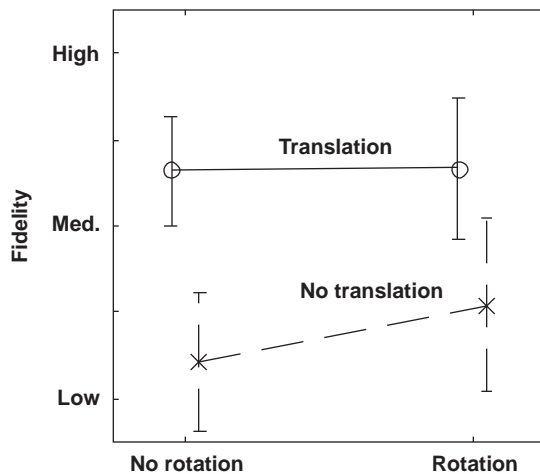


Figure 16. Motion fidelity for Task 1.

Figure 17 depicts whether or not pilots reported lateral translational motion to be present for the four motion configurations. Statistically, the two factors of rotational and translational motion interacted ($F(1,5) = 30.6$, $p = 0.003$). Lateral translational motion was reported an average of 85% of the time when it was present, and the addition of rotational motion did not increase lateral translational motion reports (actually, it decreased lateral translational motion reports from 91% to 79%). On the other hand, whereas lateral translational motion was never reported in the no-motion condition, it was reported nearly 50% of the time when only rotational motion was present.

The influences of rotational cues on lateral translational motion reports may have been a result of the pilots sensing some actual lateral translational acceleration in the rotation-only configuration. The pilot's design eye-point was less than 0.5 ft forward of the motion-system's rotation point. It is possible that depending on the variation in pilots' posture, this small offset may have resulted in their vestibular system registering a translational acceleration. The maximum rotational accelerations for the likely worst case (0.5 ft offset and a $20^\circ/\text{sec}^2$ yaw accelerations, see fig. 12) results in a 0.005-g translational acceleration. This acceleration is small but perhaps just within a pilot's threshold (see appendix A).

Pilot reporting of rotational motion, shown in figure 18, was also affected by an interaction between actual rotational and translational motion ($F(1,5) = 10.4$, $p = 0.023$). Rotational motion was reported 30% of the time when no motion was present. The reporting of rotational motion increased dramatically to 87% when any motion was given. Apparently, when combined with visual cues, the translational motion enhances the onset of a phenomenon calledvection. Vection is visually induced motion; that is, it is the belief that one is moving through a scene when no motion is actually present (a phenomenon first investigated and reproduced in a laboratory by E. Mach in 1875) (ref. 55). A description of how the vestibular and visual cues combine to producevection has been described by Zacharias and Young (ref. 56).

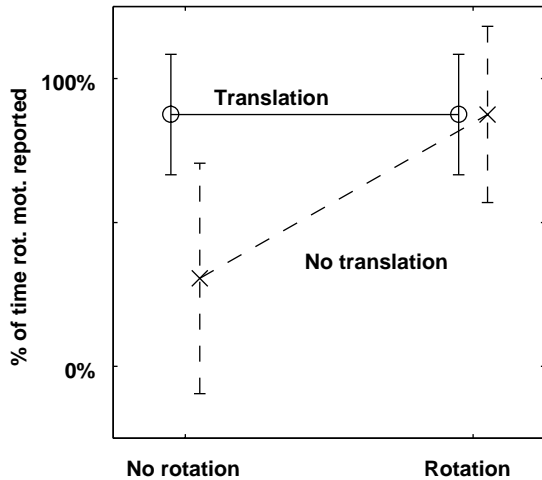


Figure 18. Rotational motion perception for Task 1.

To summarize the results for this task, translational motion was clearly the most important motion variable. Translational motion improved pilot-vehicle performance, lowered control activity, lowered pilot compensation, improved pilot impression of motion fidelity, and caused pilots to believe that rotational motion was present when it was not. The addition of rotational motion showed no statistically significant improvement, with the exception of a marginal statistically significant decrease in the number of overshoots.

Task 2: 180° Hover Turn

Objective Performance Data. Figure 19 is a representative time-history of several key variables for the Translation+Rotation motion and Motionless conditions in Task 2. Peak math model, and thus visual, yaw rates for this turn were 50°/sec (not shown). These rates were, of course, attenuated by the motion system (table 1) so that it remained within its displacement constraints. In the Motionless configuration, an increase in yaw overshoots is noted, which is evident in the displacements, rates, accelerations, and control inputs. These trends are consistent with those of Task 1.

Figure 20 depicts, for the four motion conditions, the means and standard deviations of the number of times pilots overshoot the $\pm 3^\circ$ heading criterion about the runway centerline during the 180° turns. When translational motion was added, the decrease in the number of overshoots was marginally significant statistically ($F(1,4) = 5.40$, $p = 0.081$). Interestingly, in this case, the addition of rotational motion made the performance worse, and this result was statistically significant ($F(1,4) = 13.26$,

$p = 0.022$). Rotational and translational motion did not interact in this measure.

These results are not easily explained; however, it must be remembered that in this task the motion platform never presented the pilots with full math-model motion. It is therefore possible that some false cueing in rotation, owing to the motion filter and its selected parameters, had a negative effect on performance in this case. A rough approximation confirms this possibility. For instance, if one modeled the yaw rotation between 0° and 180° by

$$\psi = \frac{\pi}{2} \sin \omega t \quad (10)$$

then the peak yaw rate would be $(\pi/2)\omega$. Since the peak yaw rates were 50°/sec, this gives a natural frequency of approximately 0.6 rad/sec. This frequency is a reasonable approximation of the heading time-histories, if one discounts the holding times at both 0° and 180° . That is, the periods would be about 10 sec. Since the yaw rotational motion filter for this configuration had a break frequency of 0.55 rad/sec, the motion cue's phase distortion at the task frequency was 90° . It is possible that this distortion was adversely affecting performance.

Figure 21 illustrates the rms pedal rate for this task. The analysis of variance indicated that the decrease in pedal rate was statistically significant when translational motion was added ($F(1,4) = 11.69$, $p = 0.027$). No significant differences were noted when rotational motion was added, and translational and rotational motion effects did not interact.

Subjective Performance Data. The average pilot-rated compensation required for this task is shown in figure 22. Large variations in pilot opinion occurred, but no statistically significant differences were noted. Based on the variation in the data, one cannot say that the motion configurations affected the amount of subjective compensation required. However, the trends shown in figure 22 follow those in Task 1 (fig. 15).

Figure 23 shows the mean motion-fidelity ratings for Task 2. Here motion fidelity was significantly higher when translational motion was present ($F(1,4) = 47.9$, $p = 0.002$), whereas the presence of rotational motion did not affect rated fidelity. Rotational and translational effects did not interact. So, pilots believed that the lack of translational motion was objectionable as compared to flight. However, the lack of rotational motion, as long as there was translational motion, was not perceived as a fidelity degradation.

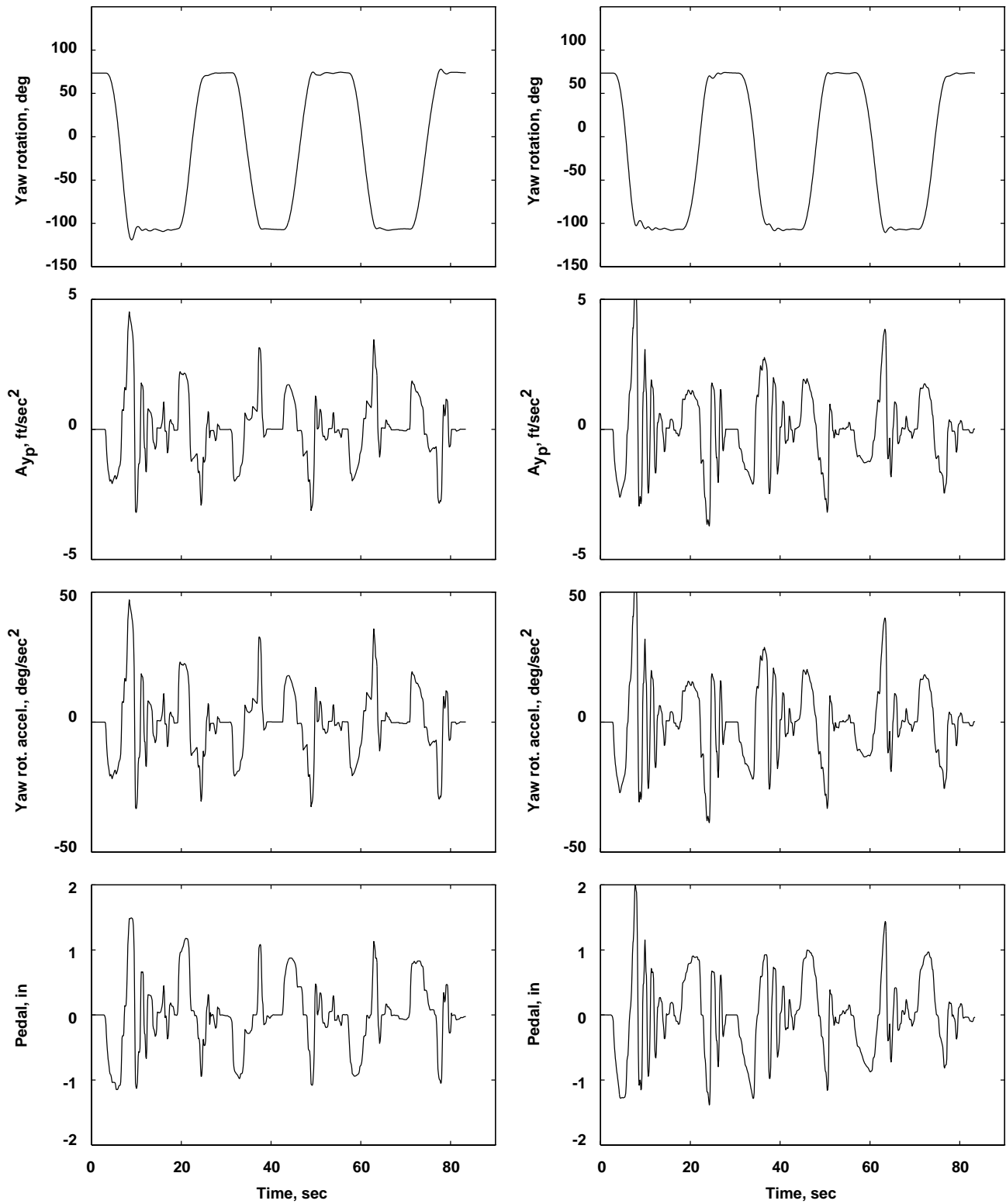


Figure 19. Comparison of full motion and no motion for Task 2.

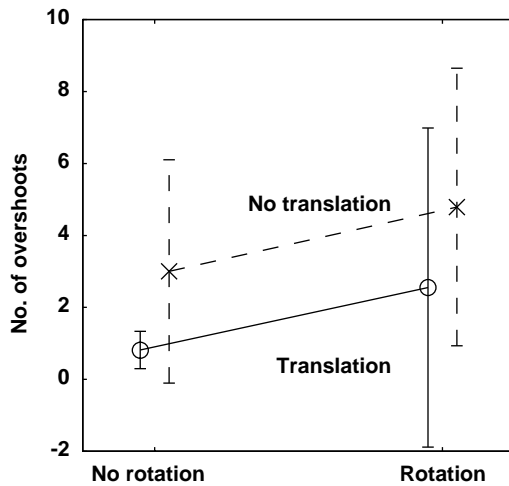


Figure 20. Measured performance for Task 2.

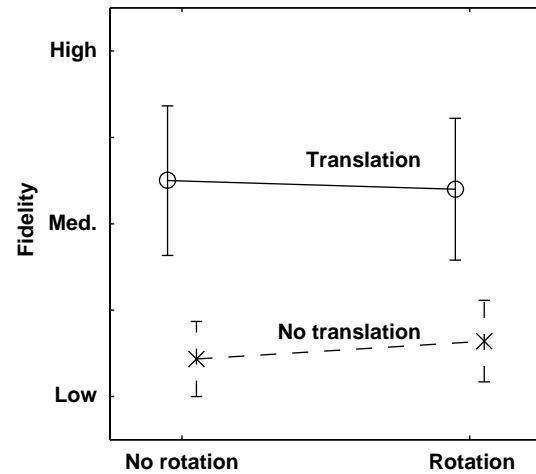


Figure 23. Motion fidelity for Task 2.

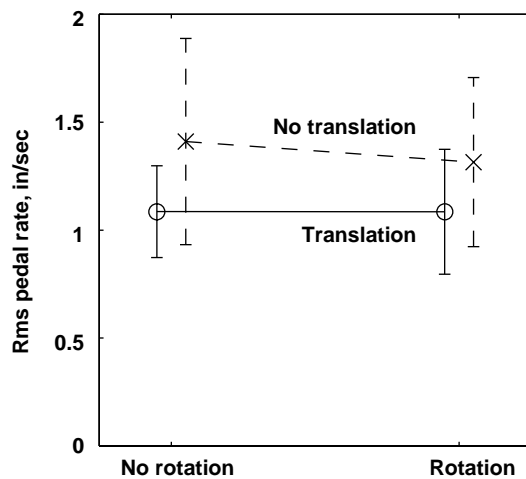


Figure 21. Control rate for Task 2.

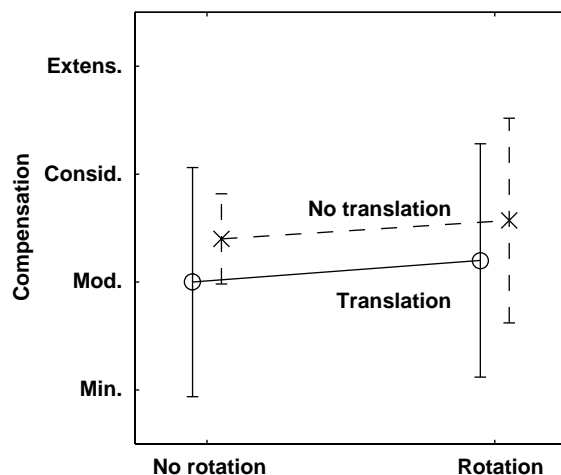


Figure 22. Pilot compensation for Task 2.

Figure 24 illustrates pilot reports of whether lateral translational motion was present. There were significantly more reports of lateral translational motion when it was present (70%), than when it was not (5%) ($F(1,4) = 14.8$, $p = 0.018$). There was no significant effect of rotational motion on lateral translational motion reports, nor was there any significant rotational motion and lateral translational motion interaction (unlike Task 1).

In the reporting of rotational motion, the rotational and translational motion factors interacted (fig. 25) ($F(1,4) = 20.0$, $p = 0.011$). Rotational motion was reported 90% of the time when translational motion was present, both when rotational motion was actually present and when it was absent. Only when translational motion was absent did the presence of rotational motion lead to increased reports of rotational motion. When no motion was presented, rotational reports occurred 27% of the time on average, but increased to 65% of the time when a rotational motion was added.

To summarize the results for this task, lateral translational motion was again the key motion variable. Its addition reduced control activity, improved motion fidelity, and led to the belief that rotational motion was also present when it was not present. These results are similar to those of Task 1, except for the interesting result that the addition of rotational motion degraded performance slightly in Task 2.

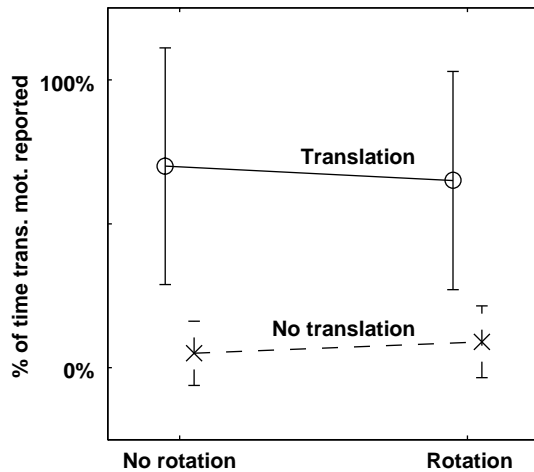


Figure 24. Lateral translational motion perception for Task 2.

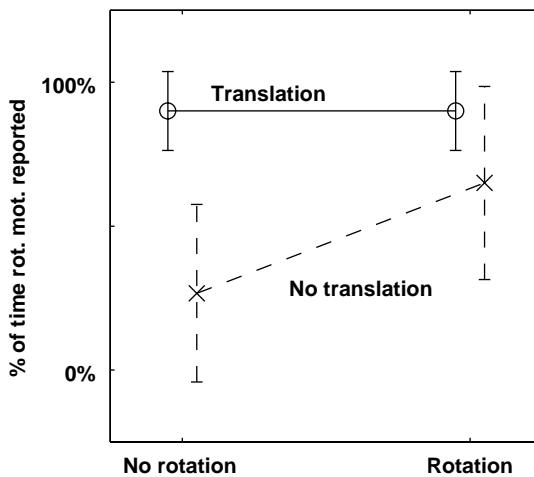


Figure 25. Rotational motion perception for Task 2.

Task 3: Yaw Rotational Regulation

Objective Performance Data. Figure 26 depicts key variables in a sample run for the Translation+Rotation and Motionless conditions in Task 3. The peak yaw rate for this run was $7.5^\circ/\text{sec}$ (not shown). The peak yaw accelerations for this task were similar to those of Task 1, but the rms accelerations were slightly higher in Task 3 than in Task 1 ($5.67^\circ/\text{sec}^2$ versus $4.21^\circ/\text{sec}^2$, respectively). The amount of visual rotation was less in this disturbance-rejection task than in the command task of Task 1. Slightly more acceleration overshoots were present when motion was removed.

Figure 27 depicts, for the four motion conditions, the means and standard deviations of the number of times pilots had an excursion outside $\pm 1^\circ$ about north per run. When translational motion was added, the decrease in

the number of overshoots was statistically significant ($F(1,4) = 8.06$, $p = 0.047$). The addition of rotational motion did not yield a significant difference. The effects of rotational and translational motion did not interact in this measure.

Figure 28 illustrates the pedal rate for the four configurations. Unlike the results for the previous two tasks, the addition of translational motion did not significantly reduce the rms pedal rate. However, the addition of rotational motion actually increased pedal rate ($F(1,4) = 18.74$, $p = 0.012$). The rotational and translational motion effects did not interact. So this is another case in which the addition of rotational motion made matters worse; however, as figure 28 shows, the percentage increase in control rate was not dramatic.

The cause for the performance degradation with the addition of rotational platform motion is unknown. The opposite result occurred in Task 1. No attempts were made to explain why with an analytical model; that is left for future work. However, during the model development, a modeler will face the difficulty of determining how a pilot integrates both the rotational and translational cue.

Subjective Performance Data. Average pilot compensation ratings are shown in figure 29. The improvement in the ratings for the translational motion conditions, relative to those in the rotational motion conditions, was marginally significant ($F(1,4) = 6.38$, $p = 0.065$). The addition of rotational motion resulted in no statistical difference in compensation. The effects of rotational and translational motion did not interact.

The same result occurred for rated fidelity, which is presented in figure 30. The addition of translational motion resulted in an improvement in fidelity ratings that was marginally significant ($F(1,4) = 6.15$, $p = 0.068$). The addition of rotational motion again made no difference. The effects of rotational and translational motion were statistically independent.

Figure 31 illustrates the percentage of the time that pilots reported the presence of lateral translational motion. The addition of translational motion significantly increased the number of reports of lateral translational motion ($F(1,4) = 12.1$, $p = 0.025$). Interestingly, the addition of rotational motion led to a marginally significant decrease in the reports of lateral translational motion ($F(1,4) = 5.4$, $p = 0.08$).

Figure 32 illustrates the percentage of the time that pilots reported the presence of rotational motion. No significant effects were found, with rotation being reported an average of 73% of the time, independent of the motion configuration.

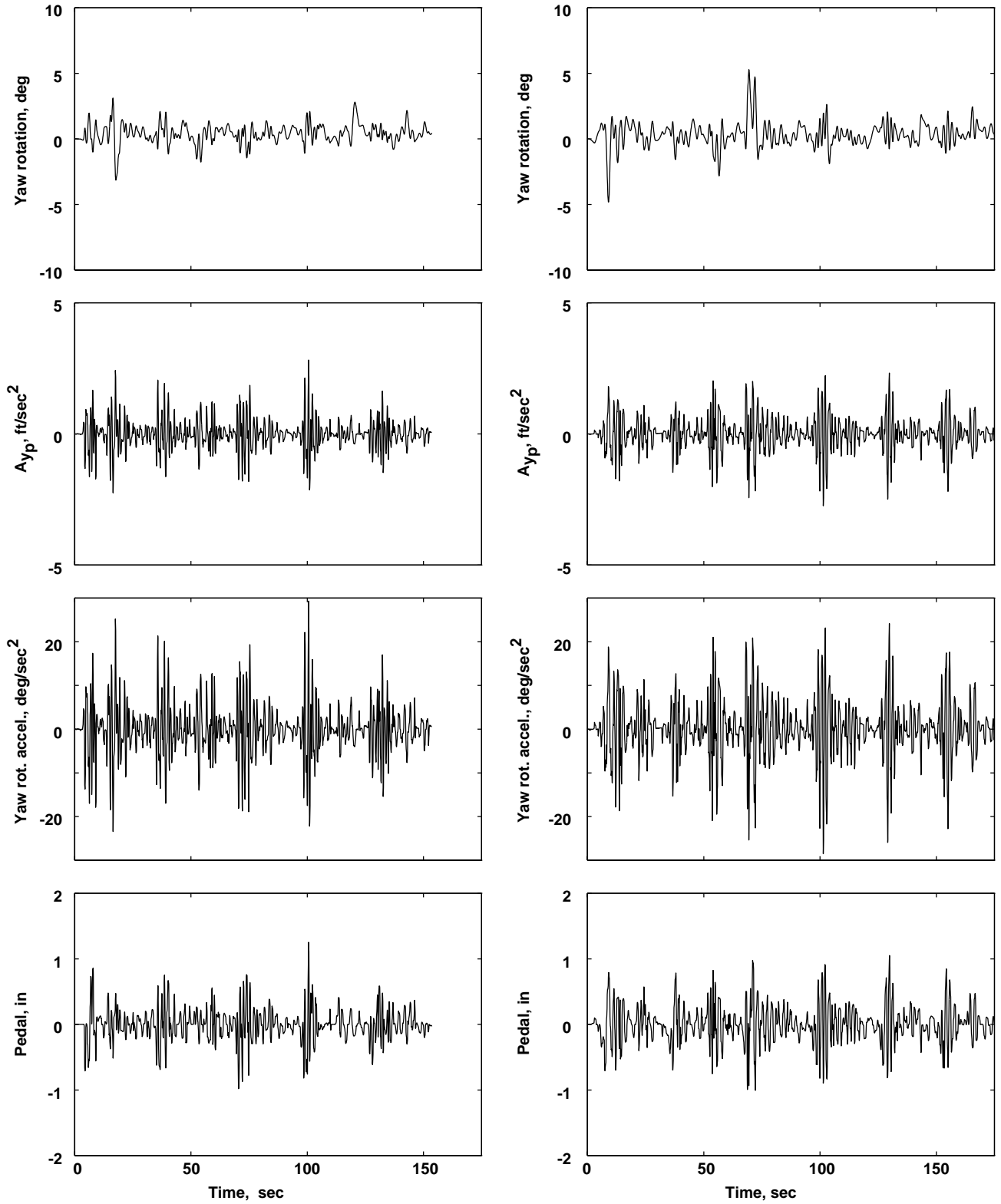


Figure 26. Comparison of full motion and no motion for Task 3.

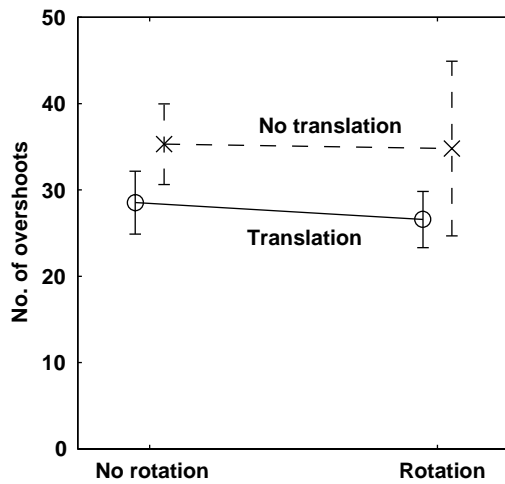


Figure 27. Measured performance for Task 3.

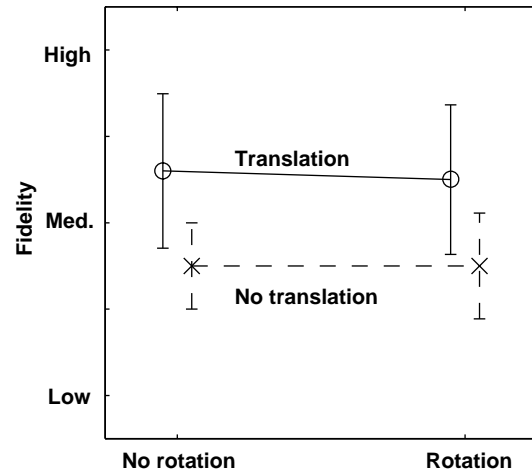


Figure 30. Motion fidelity for Task 3.

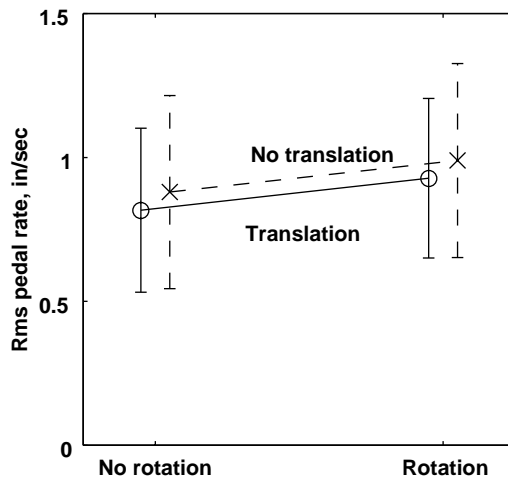


Figure 28. Control rate for Task 3.

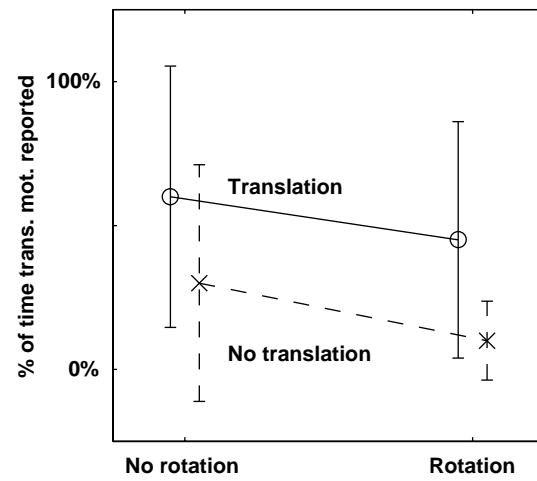


Figure 31. Lateral translational motion perception for Task 3.

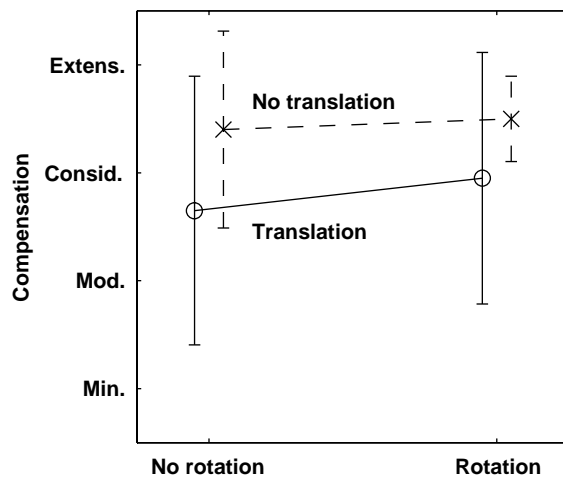


Figure 29. Pilot compensation for Task 3.

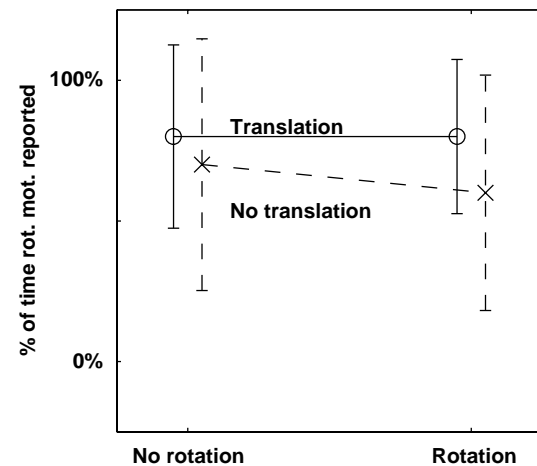


Figure 32. Rotational motion perception for Task 3.

In summary, the results of this task do not reveal many differences from those of Tasks 1 or 2. Lateral translational motion was again the dominant variable. Its addition improved pilot-vehicle performance, although its effect on rated pilot compensation and fidelity was less reliable than it was in the other two tasks. The only statistically significant effect of rotation was a deleterious effect on control activity.

Combined Results

Table 2 summarizes the effects of the presence of lateral translational or yaw rotational motion on the six measurables for the three tasks. All of the improvements in the measures occur for the presence of lateral translational motion, except for one. In that case, a marginally significant effect was noted in pilot-vehicle stability for the addition of yaw rotation. Statistically significant degradations in the measures occurred only for the addition of yaw rotational motion. Interactions between lateral translational and yaw rotational motion occurred only in the lateral translational and yaw rotational motion perception reporting. However, in Tasks 1, 2, and 3, pilots reported (on average) rotational motion being present 87%, 90%, and 80% of the time, respectively, when only lateral translational motion was present.

The claim made as a result of these evaluations is that yaw rotational platform motion is not adding value to helicopter flight simulation. However, the claim that yaw rotational platform motion does not provide a cue is not made. During the course of these studies, a hypothesis

was raised that the pilots simply were not sensing whatever cue the yaw rotational platform motion was providing. As previously stated, each task resulted in enough motion so that the physiological thresholds, as measured in passive situations, were exceeded. However, the possibility remained that, since the pilots were actively a part of the control loop rather than passive observers, those passive thresholds may have risen to the point that the yaw rotational motion platform cue was not being sensed.

This hypothesis is rejected based on the following. To determine if whatever cue the yaw rotational platform motion might be providing was indeed being sensed, an additional motion configuration was evaluated on an ad hoc basis. That configuration simply reversed the sign in the yaw rotational platform motion command. So for math model rotations to the right, the visual scene correspondingly moved to the right, but the platform moved a symmetric amount to the left. This configuration was extremely disliked by all the pilots, some of whom experienced physical discomfort. Thus, what appears to be happening in the typical motion configuration (with correct motion signs) is that the yaw rotational platform motion cue is simply confirming the already compelling rotational cues that come from the visual scene. This conclusion is also supported by the earlier studies performed by the author (refs. 48, 49) in which the pilot was sitting at the rotational center. In that case, no translational cue was present, so the yaw rotational cue was redundant with the visual cue.

Table 2. Summary of yaw task results.

Measure	Task:	Translational			Rotational			Translational/ rotational interaction		
		1	2	3	1	2	3	1	2	3
Pilot-vehicle stability		+	+	+	+	-	○			
Control rate		+	+	○	○	○	-			
Compensation		+	○	+	○	○	○			
Fidelity		+	+	+	○	○	○			
Translational reporting			+	+		○	-	x		
Rotational reporting				○			○	x	x	

+: Significant improvement; +: marginal improvement; -: significant degradation; ○: no effect; x: interaction.

In addition to these compelling visual cues, when lateral translational motion is present, its combination with the visual cues provides more than enough cues to cause the pilot to believe he is rotating when he is not physically rotating. When the yaw rotational platform cue is in the opposite direction, it is no longer providing confirmation, but it is instead providing conflict. Consistent with this explanation is the dictum “bad motion is worse than no motion” in that spurious motion cues destroy anyvection that has been generated by the other motion and visual cues (ref. 9).

Earlier it was stated that Meiry’s yaw experiment (ref. 22) showed that the addition of rotational motion improved performance. It is possible that the difference in experimental setup between that experiment and the one reported here could account for the difference, although the results of Task 1 in the present study did agree with those of Meiry by showing a marginal improvement in performance. In Meiry’s experiment, pilots countered a considerable yaw rotational disturbance (white noise with a 15° rms), did not control a model representative of a helicopter (the model resulted in yaw rate proportional to pilot input at all frequencies), and the visual system was a line on an oscilloscope. So, with this deprived-cue visual system and with only a yaw rotational cue, yaw rotational motion might have helped. However, Meiry’s study did not determine if the lateral translational motion cue could have provided an equivalent substitute for the yaw rotational cue, which was the principal result shown here.

Effect of Results

The effect of these results is twofold. First, for simulators with independent-axis motion drives, that is, dedicated servos for each axis, excluding the yaw platform rotational degree-of-freedom capability would result in a cost savings to manufacturers. To users of motion simulators that already have a yaw rotational degree of freedom, less time, if any, needs to be spent configuring and tuning that axis for a given application.

Second, for simulators without independent-axis motion drives, such as the common synergistic hexapod motion systems (fig. 33), not using the yaw platform rotational degree of freedom allows for more available displacement in the other motion axes. Since the same set of actuators is used to move the platform to a desired position or orientation, the available displacement or orientation of any axis is a function of the displacement or orientation in another axis.

An example of the dependency is shown in figure 34, which was generated by Cooper and Howlett (ref. 40). Loss of available motion in the longitudinal, lateral, and vertical axes also occurs for rotations about the yaw axis. Thus, users should disable yaw rotation and thereby gain additional benefits in axes that provide added value in flight simulation.

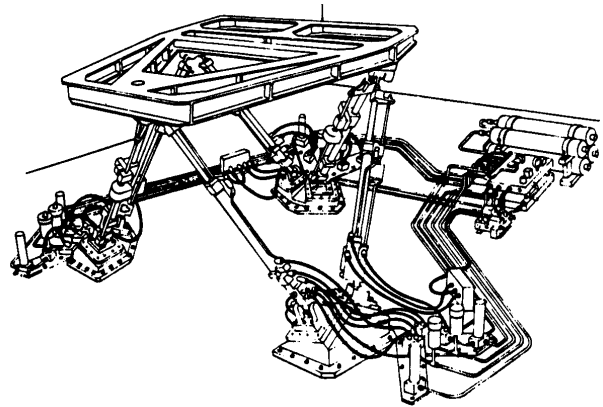


Figure 33. Typical hexapod motion drive system.

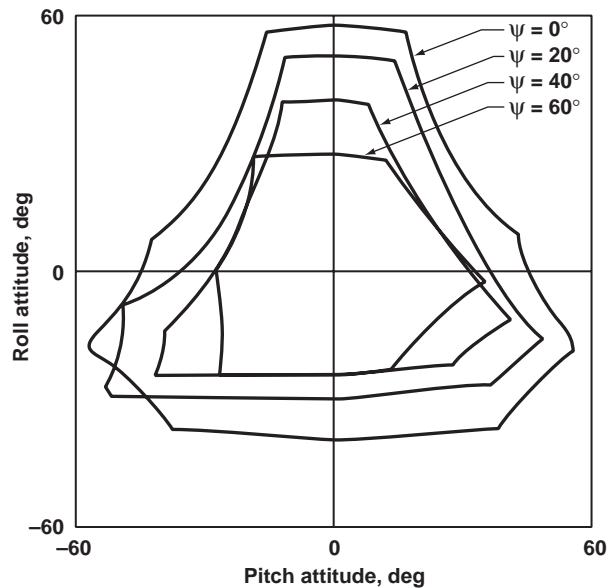


Figure 34. Effect of yaw angle orientation on pitch and roll angles.

4. Vertical Experiment I: Altitude Control

Background

For helicopters, only one study has focused extensively on the vertical axis (ref. 24). In that study, the effects of the motion-filter natural frequency were examined, but almost always with a high-frequency gain of unity. The research described here also examined motion-filter natural frequency, but in addition evaluated the combined effects of motion-filter gain.

The setup of the experiment is described, including a task description, the math model, and the simulator cueing systems. This description is followed by the results, which subsequently validate a revised motion-fidelity criterion for the vertical axis.

Experimental Setup

Task

The vertical task required the pilot to increase aircraft altitude 10 ft. To do so, the pilot used visual cues to place the horizon between two red squares on an object 50 ft away, as shown in figure 35. These sighting objects were used previously, in both flight and simulation, for vehicle model validation (ref. 57). The red region had a height of 0.75 ft, which was the final altitude tolerance.

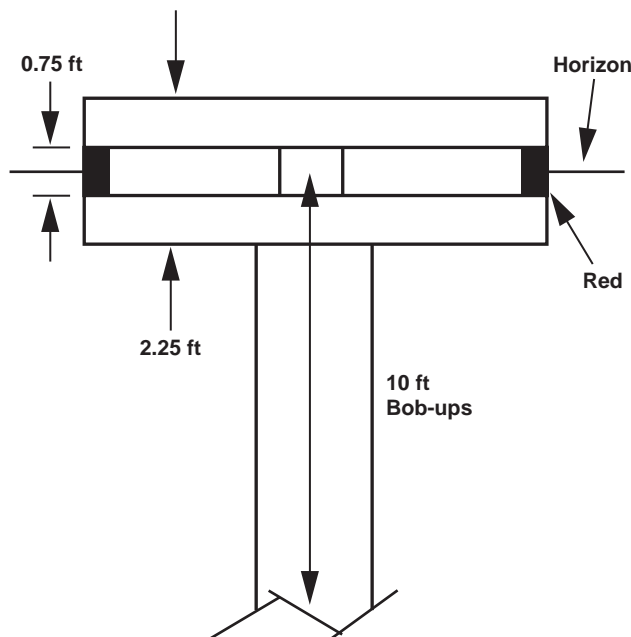


Figure 35. Sighting object for vertical tracking.

An altitude displacement, or bob-up, of 10 ft was chosen for two reasons. First, 10-ft bob-ups could be performed in the VMS without any attenuation of the math model accelerations. This situation is referred to as 1:1 motion, since the simulator cockpit motion is the same motion as that calculated by the vehicle model, and the motion is also the same as that shown by the visual scene. Second, when the aircraft was 10 ft below the target, the target remained in the field of view of the visual scene.

The desired performance standard for this task required that the pilot make only two or fewer reversals outside the red region before stabilizing in the red. Adequate performance required two or fewer reversals outside the top and bottom horizontal boundaries of the objects, which are 2.25 ft apart.

The bob-up task was to be performed as fast as possible. Five bob-ups were completed for each motion-system configuration. Pilots repositioned the helicopter downward to the starting position between each bob-up. This repositioning was performed at the pilot's discretion without performance standards. Thus, the bob-down was not part of the evaluation.

Simulated Vehicle Math Model

The vertical-axis dynamics were selected by averaging the hovering characteristics (at sea level) of five helicopters: the OH-6A, BO-105, AH-1G, UH-1H, and the CH-53D. Heffley et al. (ref. 58) was the source for these dynamics. The resulting vertical-acceleration-to-collective-position dynamics were as follows:

$$\frac{\ddot{h}}{\delta_c}(s) = \frac{9s}{s + 0.3} \quad (11)$$

A delay is usually added to a model such as this to approximate the lag caused by the rotor dynamics, but this delay was instead subsumed by the simulator motion and visual systems. This technique was successfully used in a previous model validation experiment (ref. 59). In addition, no torque or rpm limits were imposed on the pilot. Also, since the task was limited to a single axis, there was no coupling into the directional axis. Atmospheric conditions were calm air, no turbulence, and unrestricted visibility. The math model cycle time was 25 msec.

Simulator and Cockpit

The NASA Ames VMS, described in section 2, was again employed. For this experiment, only the vertical degree of freedom was used. A Singer Link DIG-I image generator provided the visual scene, which was representative of the

state of the art in the late 1970s. This visual image generator was different from that reported in section 3, a result of scheduling constraints at the VMS facility. The image generator that was used did not have a texturing capability. The visual delay from the math model to the visual image was 83 msec (ref. 52), which is a typical delay for flight simulator image systems. Visual lead compensation was not used to reduce the visual delay, the purpose being to more closely match the visual and motion delays. This matching is imperfect, since the vertical-axis frequency response can be approximated by an equivalent time delay of 140 msec (eq. (4)). Thus, in this experiment, the visual response effectively leads the motion response.

The visual field of view was presented on three windows that spanned $\pm 78^\circ$ horizontally and $+12^\circ$ and -17° vertically as shown in figure 36. The center window had the principal objects in the field of view for the task, and the information presented in the left and right windows was limited to polygonal color variations on the ground. The image that the pilot viewed for the task is shown in figure 37.

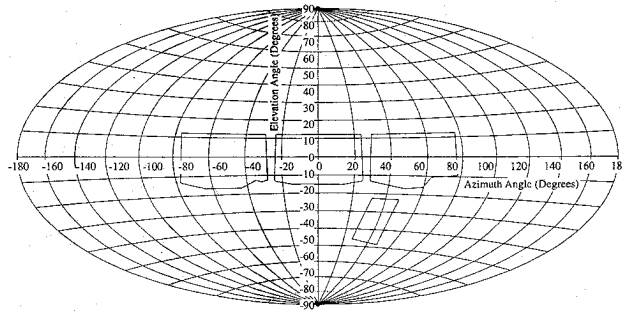


Figure 36. Cockpit field of view for vertical tracking.



Figure 37. Pilot's visual scene for vertical tracking.

A conventional left-hand collective lever was used. It had a travel of ± 5 in, had no force gradient, and the friction was adjustable by the pilot. All flight instruments were disabled so that all cues were from the visual scene and the motion system. Rotor and transmission noises were present to partially mask the motion-system noise. The head-up display shown in figure 37 was stowed for the task. Three NASA Ames test pilots participated; they are hereinafter referred to as pilots A, B, and C. All three fly rotorcraft and had extensive simulation experience.

Motion System Configurations

A second-order high-pass filter, typical of that used in most flight simulators, was placed between the math model vertical acceleration and the simulator-commanded acceleration. It had the form of

$$\frac{\ddot{h}_{com}}{\ddot{h}}(s) = \frac{Ks^2}{s^2 + 2\zeta\omega s + \omega^2} \quad (12)$$

where \ddot{h}_{com} is the commanded vertical acceleration of the simulator cab, \ddot{h} is the math model's vertical acceleration at the pilot's station, K is the motion gain, ζ is the damping ratio, and ω is the filter's natural frequency.

The damping ratio of the above filter was held fixed at 0.7. The two parameters that are used to then keep the motion system within its displacement limits for a given math model and task are K and ω . To reduce simulator motions, either K is reduced or ω is increased. Achieving the proper balance between these two possible ways of reducing the motion, while trying to minimize a loss in motion fidelity, is not well defined. The criterion suggested by Sinacori and discussed in section 1 was used to select the characteristics of the motion configurations.

To validate or modify the criterion, 10 sets of gains and natural frequencies were chosen to span the criterion, as shown in figure 38. The values for the filter are given in table 3. Note that configurations V3 and V4, from table 3, result in gain and phase-distortion coordinates of [0.970, 45.0] and [0.795, 80.0], respectively. Although these filters have unity gain at high frequencies ($K = 1$), the dynamics of the high-pass filter cause the above attenuations and phase distortions at 1 rad/sec, which is the frequency used to plot the motion filters against the criterion.

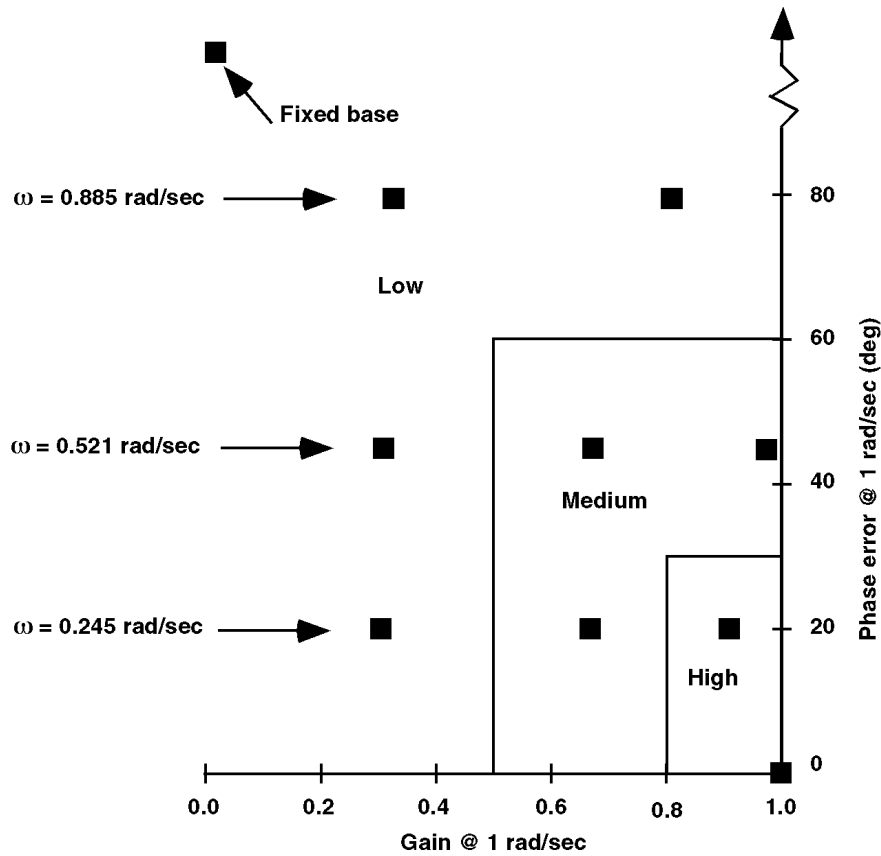


Figure 38. Motion configurations for vertical tracking.

Table 3. Motion-filter quantities for vertical tracking.

Vertical		
Configuration	K	ω (rad/sec)
V1	1.000	0.010
V2	0.901	0.245
V3	1.000	0.521
V4	1.000	0.885
V5	0.650	0.245
V6	0.670	0.521
V7	0.300	0.245
V8	0.309	0.521
V9	0.377	0.885
V10	0.000	—

Procedure

For the pilot to rate the motion fidelity of each configuration, a baseline was established for comparison. The baseline specified that the pilots perform the task first with 1:1 motion; this was a calibration run. Here, the pilots were told that they had 1:1 motion, and that the sensations they were feeling were to be interpreted as the “actual aircraft.” The motion fidelity of all future configurations was then compared to this 1:1 motion baseline configuration. This testing procedure allowed immediate back-to-back comparisons of the effects of motion parameter changes. This procedure mitigates some of the problems that occur in simulation fidelity experiments that compare the actual aircraft to the simulation back-to-back, even when the events occur in the same day.

During the evaluations, the pilots had no knowledge of the configuration changes, except when they were told of the full-motion “calibration runs.” Still, the 1:1 motion case (configuration V1 in table 3) was also evaluated; during its evaluation, the pilot was not told he had the 1:1 configuration.

Pilots A and C completed all the configurations listed in table 3 in one session, Pilot B completed all the configurations in two sessions, and all of the configurations were evaluated by all three pilots. Some configurations were repeated if time permitted. For each configuration, pilots assigned a motion-fidelity rating using the definitions in figure 4. Then, the pilots answered questions regarding the aircraft’s characteristics, their task performance, and the compensation required to perform the task. The pilots were also asked to estimate the relative use of the motion and visual feedback cues.

Results

The results of Vertical Experiment I consist of objective performance data and subjective fidelity ratings. Relevant pilot comments will be added in the discussion of these results.

Objective Performance Data

Again, compelling performance differences are shown between full motion and no motion in figure 39 (configurations V1 and V10, respectively). For the configuration V1 case, well damped, accurate bob-ups were achieved with the vertical velocity remaining within 10 ft/sec; the vertical acceleration remained within 0.5 g, and the collective stayed within 1.5 in. A drastic difference is evident in the no-motion case (V10). Initially, the pilot overshoot the 85-ft desired altitude and then returned to the starting point as he responded to the unfamiliar cues. Since the acceleration feedback cue was the only cue that changed from the full- to the no-motion case, part of the pilot’s collective input must have been a result of that cue. With the acceleration cue removed in the V10 configuration, the pilot had to adjust his compensation based on the new set of cues. With time in the motionless configuration, the performance improved, but even the final repositioning took longer in the fixed-base case than in the full-motion case. These differences have obvious training implications, for the pilot must develop different mental compensation between the two cases. No data were

taken when returning to the full-motion case for recalibration, but pilots commented that relearning the full-motion configuration was easy and natural.

Figures 40 through 49 show phase-plane portraits for each motion configuration. Each portrait shows three runs, one for each pilot, using his best performance run if an evaluation was repeated. Both the bob-up and bob-down are shown. These plots show how the motion changes affected the pilot’s ability to capture the upper desired point smoothly. Ideally, these plots should be well-damped and approximately oval.

Figure 40 indicates that some overshoots were present for the full-motion condition, but overall the trajectories were well damped and smooth. There was reasonably precise control about the 85-ft altitude point, with one instance of a pilot not arresting the vertical velocity soon enough, which caused a position overshoot. Little change in performance, or perhaps a slight improvement, is noted for the slight motion changes of configuration V2 in figure 41.

The high-gain, moderate phase-distortion case of configuration V3 in figure 42 still produces well-damped trajectories on ascents. The acceleration cues for this configuration lead the math model by 90° at 0.52 rad/sec. If the motion between the ascents and descents were sinusoidal, the frequency of the maneuver would be approximately 2 rad/sec. This value is approximated by letting

$$h = 80 + 5 \sin \omega t \quad (13)$$

$$\dot{h} = 5\omega \cos \omega t \quad (14)$$

$$\dot{h}_{\max} = 10 \text{ ft / sec} \Rightarrow \omega = 2 \text{ rad / sec} \quad (15)$$

For the initial phase of the maneuver, therefore, the motion cues would be accurate, but the subsequent stabilization at a particular altitude would produce some miscues, for lower frequency content would be present. Pilots seemed to have more difficulty in returning to the starting point than in the first two configurations; however, this repositioning was not officially part of the evaluations. For the high-gain and high-phase-distortion case of configuration V4 in figure 43, the overshoots were more prominent, and the overall control was much less precise.

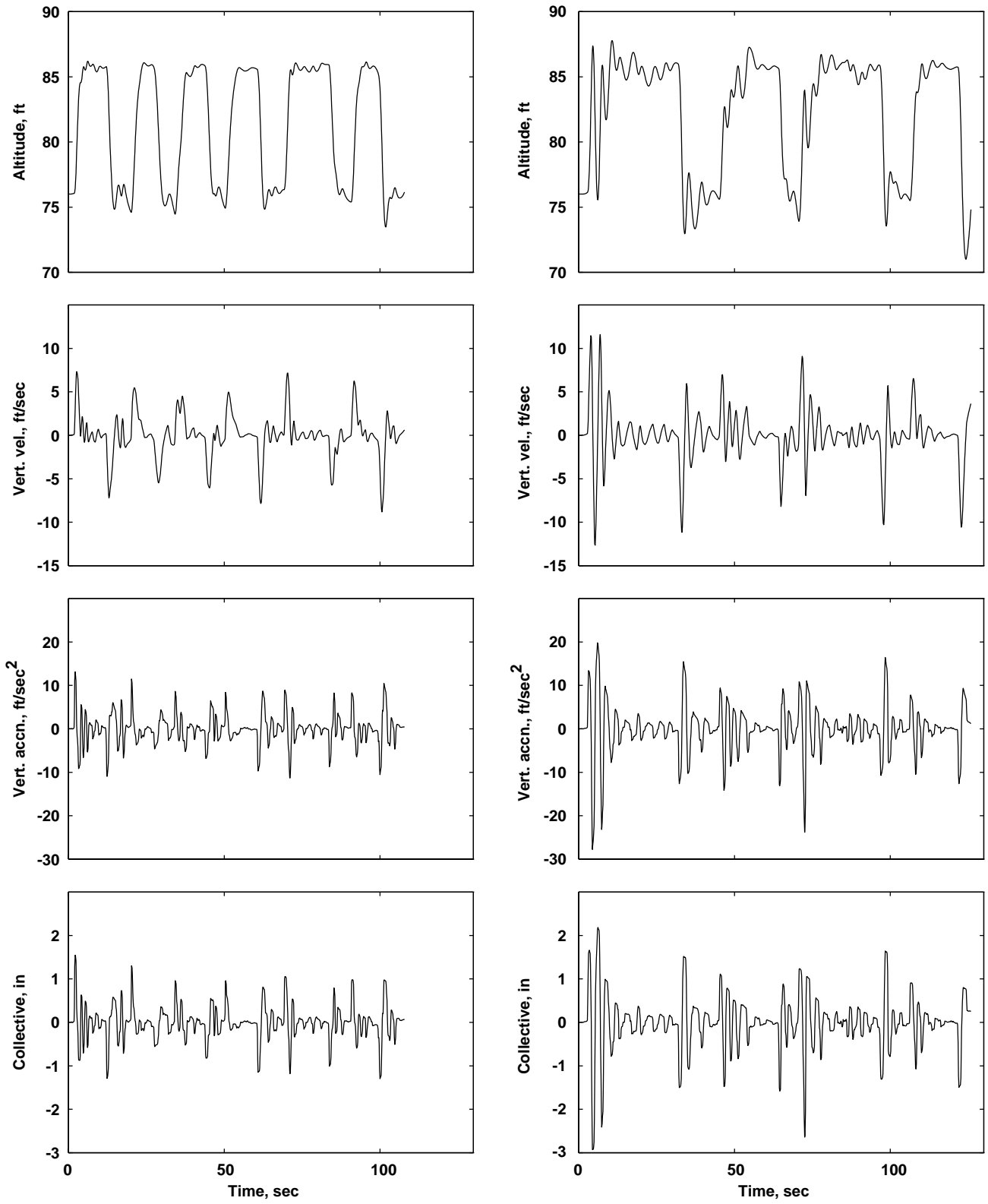


Figure 39. Altitude control: full motion versus no motion.

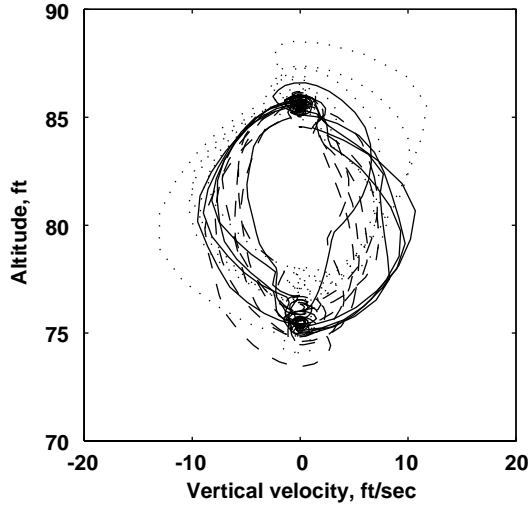


Figure 40. Phase-plane portrait for configuration V1.

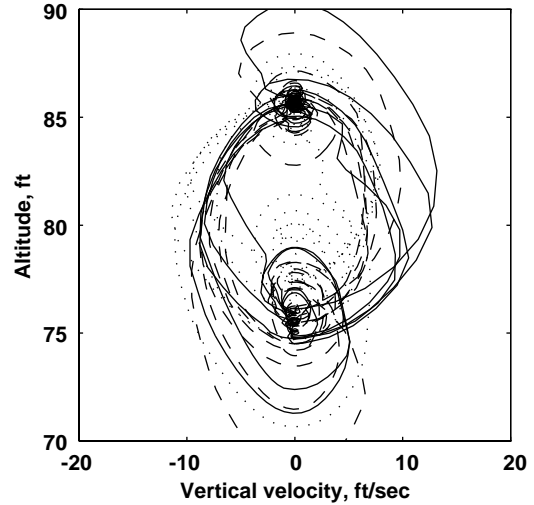


Figure 43. Phase-plane portrait for configuration V4.

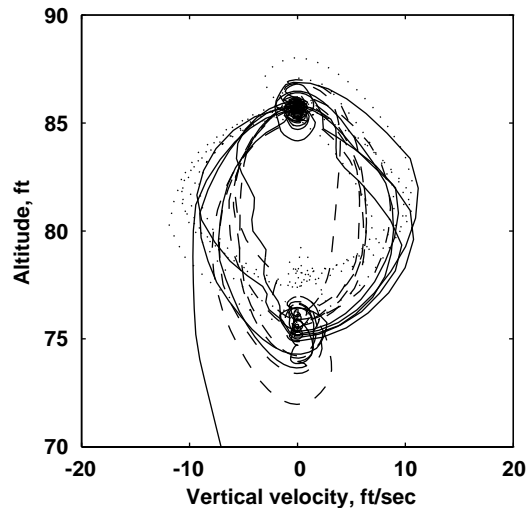


Figure 41. Phase plane portrait for configuration V2.

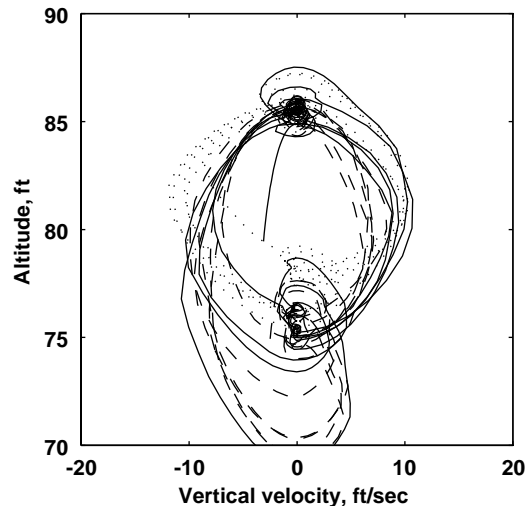


Figure 42. Phase-plane portrait for configuration V3.

For the medium-gain, low-phase-distortion case of configuration V5 in figure 44, the bob-up trajectories show good performance, with the trajectories being similar to those of the full-motion case, or at least similar to those of the V2 case. The gain is lowered to 65% of full motion for the V5 configuration.

Increasing the phase distortion from configuration V5 to configuration V6 caused a slight reduction in the precision around the desired stationkeeping point with a few undershoots of the ascent point as shown in figure 45. The gain reduction in going from V3 to V6 does not appear to degrade performance significantly.

The low-gain, low-phase-distortion case, configuration V7 in figure 46, resulted in less precision with more over- and undershoots than in the previous configurations. Here the gain is at 30% of full motion at high frequencies. Performance definitely decreases when the gain drops from 0.65 in configuration V5 to 0.3 in V7.

The precision in V7 also appears worse than in the V4 case of high gain and high phase distortion. Increasing the phase distortion to the V8 case in figure 47 shows a further reduction in precision from that of the V7 case. Again, the gain of 30% is insufficient, but the combination of the low gain with some phase distortion makes the performance even more degraded.

The low-gain, high-washout case of configuration V9 in figure 48 exhibits a further degradation, the middle of the desired oval being occupied with the aircraft's trajectory.

Finally, the no-motion case of configuration V10 in figure 49 indicates the worst performance of all; the imprecise control of velocity is obvious at both the top and bottom points.

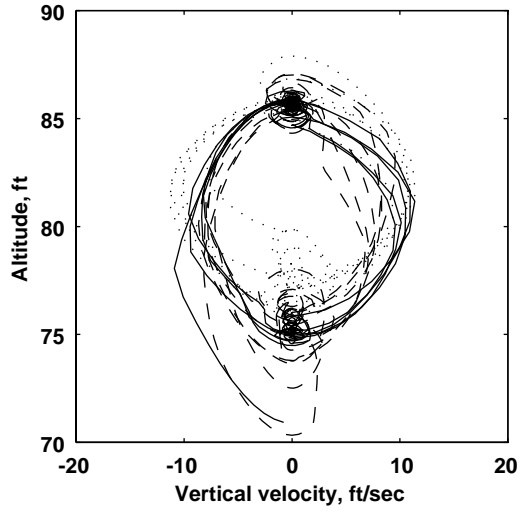


Figure 44. Phase-plane portrait for configuration V5.

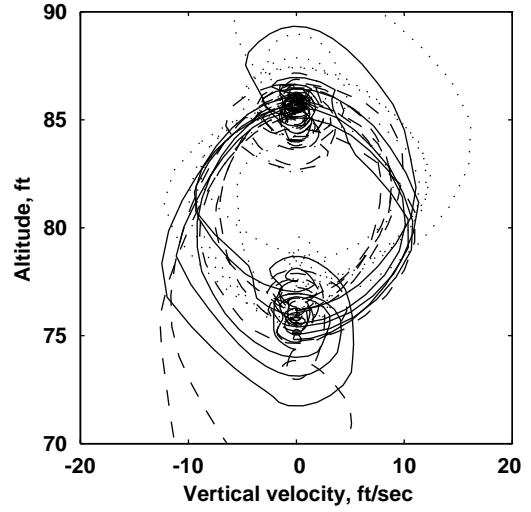


Figure 47. Phase-plane portrait for configuration V8.

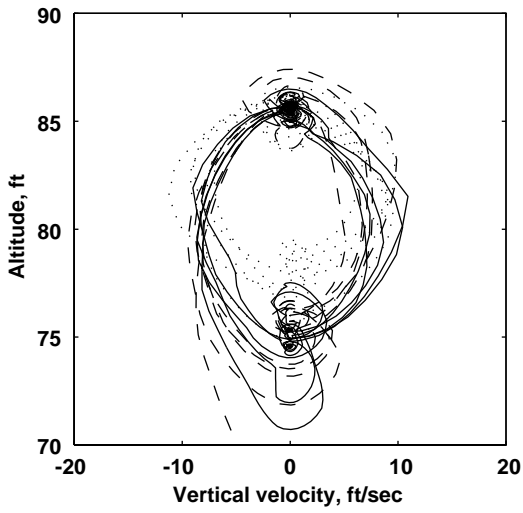


Figure 45. Phase-plane portrait for configuration V6.

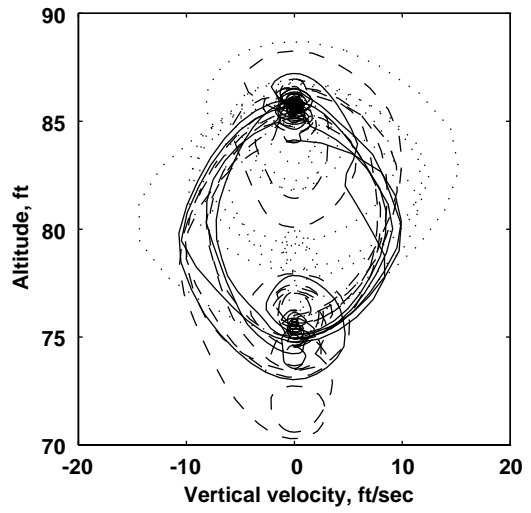


Figure 48. Phase-plane portrait for configuration V9.

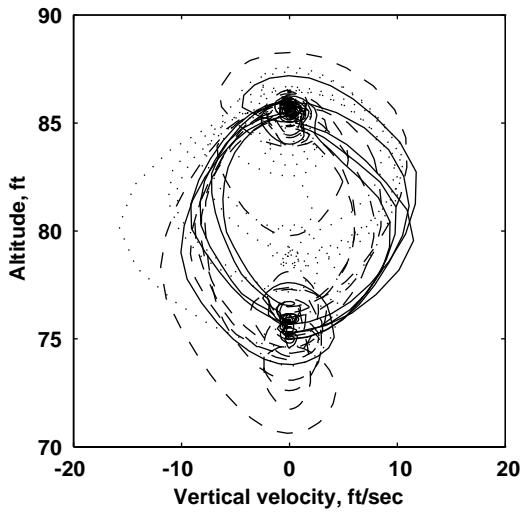


Figure 46. Phase-plane portrait for configuration V7.

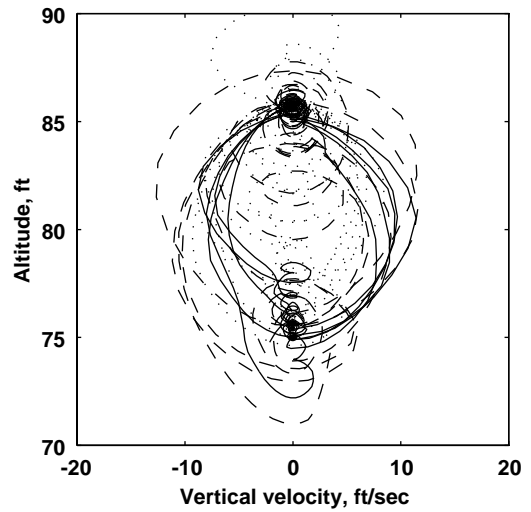


Figure 49. Phase-plane portrait for configuration V10.

Subjective Performance Data

Figure 50 shows pilot motion-fidelity ratings along with the postulated boundaries of Sinacori (ref. 44). The pilots unanimously rated the high-gain, low-washout configurations V1 and V2 as having high fidelity. If either the gain was reduced (as in V5) or the phase distortion increased (as in V3), one of the three pilots reduced his rating to medium. When a combination of this gain and phase distortion was examined, that is, configuration V6, the ratings dropped on average across one level. However, one of the pilots did not perceive differences between the V3 or V5 configuration and the V6 combination.

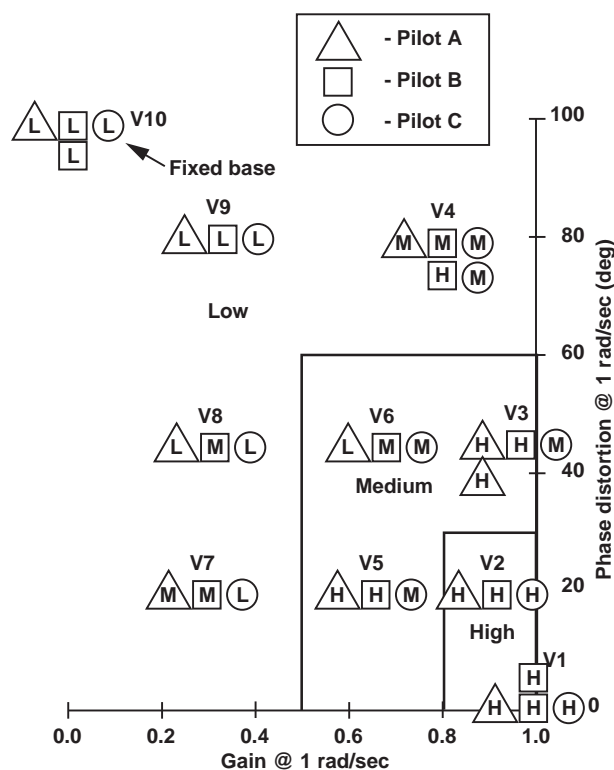


Figure 50. Motion fidelity ratings for altitude control.

The next individual changes in gain or phase from the V3 and V5 cases to the V4 and V7 cases produced, on average, a decrease from high to medium fidelity. However, a combination of these effects, encompassed by the V9 configuration, produced unanimously low fidelity ratings. Unsurprisingly, the fixed-base configuration, V10, also produced unanimously low fidelity ratings.

These ratings suggest that for this task, the fidelity criterion for the vertical axis appears to decrease from high-gain/low-phase-distortion in a direction toward the fixed-base case. The combination configurations V2, V6, and V9 result in ratings predicted by the criterion.

However, either reducing the gain or increasing the phase distortion resulted in fidelity ratings better than predicted, on average.

Combined Results

It is reasonable to suggest a revision to the Sinacori criterion (ref. 44) if objective performance, subjective pilot fidelity ratings, and subjective pilot comments are consistent. Each of the configurations is discussed, and when a consistency exists that does not align with the criterion, then a modification to the criterion is suggested.

With the full-motion case, configuration V1, pilots were consistent in their comments that they achieved desired performance, that compensation was minimal to moderate, and that they felt that they could be very aggressive with the vehicle. All ratings were high fidelity, and the objective performance was good.

For the configuration with a slight decrease in gain and an increase in phase distortion, V2, the comments indicated that a difference was noted. Two of the three pilots noticed a slight decrease in performance, and the compensation increased over that of the V1 case. Yet all pilots rated the configuration high fidelity, since they felt it was "close to visual flight." Here is where the fidelity definitions could be made more precise, because a pilot is faced with a potential dilemma with a configuration that has noticeable but not objectionable differences (medium fidelity definition), yet is close to visual flight (high fidelity definition). Pilots apparently felt that when it was necessary to group the ratings into three categories, the V2 configuration was in the most favorable category. Yet they all perceived a difference. It appears that the pilots may have been sensitive to the differences in the immediate acceleration because of collective input. This initial acceleration is proportional to the high-frequency motion gain, and it is reasonable that the 10% change between these configurations could be noticed. It is also reasonable that the variation was not objectionable.

For the high-gain and moderate phase-distortion case, configuration V3, all pilots noticed the necessity to change their control input technique. Two pilots noticed the unpredictability, or the "slipperiness," of this configuration. Only one downgraded the fidelity rating to medium. The objective performance did not change appreciably in the bob-up, but difficulty was perceived in repositioning downward. Although the ratings indicated the configuration was high fidelity, the comments and the performance did not agree. Thus, the V3 configuration should not be placed in the high-fidelity region.

Increasing the phase distortion further to the V4 configuration resulted in a perceived degradation in

performance, and this is evident from the phase-plane data. The aggressiveness level was reduced, and the required compensation increased. Two of the three pilots noticed a phasing difference between the visual and the motion cues, yet with all of the above, they rated this configuration no worse than medium. However, one pilot thought that it was close to being objectionable. Considering the comments and the performance, it appears that the fidelity was closer to low than the rated medium, and thus no change is suggested.

Comparing these near-unity motion gain results with the only other set of high quality experimental data for helicopters (ref. 24) shows similar trends. That experiment showed that for tracking a randomly moving target, while the open-loop crossover frequency remained nearly invariant with increases in motion-system phase distortion, the phase margin increased by 30° when going from a motion phase distortion of 108° to a phase distortion of 16° . For a phase distortion of 43° , which is similar to configuration V3, a phase margin degradation of 15° was measured. The comments and objective performance data from the present experiment, for these cases, indicated a similar trend in stability degradation, yet the subjective fidelity ratings for this task still rated the V4 configuration as medium fidelity.

In another experiment (ref. 60), for aircraft with poor longitudinal flying qualities in a landing task, it was observed that phase distortions higher than 90° caused “essentially uncontrolled touchdowns.” Thus, considering previous data and the lack of consistency in this experiment’s objective and subjective results for these configurations, it seems appropriate to retain the hypothesized fidelity breakpoints suggested by Sinacori (ref. 44) for the near-unity gain configurations.

Returning to the low phase-distortion configuration with moderate gain, V5, pilot comments and objective performance generally indicated no degradation from the full-motion case. Only one pilot rated the fidelity as medium (owing to a slight vertical oscillation). From the consistency of these results, it appears that when the phase distortion is less than 30° , lowering of the gain required for high motion fidelity from 0.8 to 0.6 is appropriate.

Keeping essentially the same motion gain, but increasing the phase distortion to configuration V6 resulted in comments indicating a performance loss because of a reduction in precision and aggressiveness. Fidelity ratings of medium are consistent with Sinacori’s hypothesized boundaries (ref. 44).

A reduction of gain to 0.3, but with a low phase distortion in configuration V7 resulted in adequate performance, fears of overshooting, and comments that the

motion was almost unusable. These comments were repeated for the remaining configurations, V8 and V9; the objective performance worsened as the phase distortion increased. From the comments and ratings, configurations V7, V8, and V9 were consistent with Sinacori’s hypothesized boundaries (ref. 44). Therefore, regardless of the phase distortion, a gain of 0.3 results in low fidelity.

Referring to the fixed-base configuration, V10, two pilots said that they put the control input in the wrong direction during the run. Pilots were generally stunned at the effects of the total loss of motion. During the 1:1 calibration runs, one pilot made a comment prior to the evaluations that “The visual scene is so compelling at conveying the error that it seems to primarily be a visual task . . . I would expect the effects of motion to be minor.” Another pilot commented after the fixed-base configuration “I have never experienced such a dramatic disconnect from reality as during that configuration, as compared to the full-motion case.” Thus, caution should be used when interpreting a priori conjectures on the value of motion, even when given by experienced test pilots with considerable simulation experience.

Motion cues were certainly perceived by the pilots in all but this fixed-based configuration. This is evident from the performance and comments, but it is also consistent with tests that have determined the vertical-acceleration sensing threshold to be in the 0.09-0.27 ft/sec² range (ref. 19). This threshold was exceeded in all but the fixed-base configuration.

Suggested Revision to Fidelity Criteria

Based on these results, a revision to the vertical axis of Sinacori’s criterion is suggested in figure 51. Here, the changes consist of lowering the gain required when the phase distortion is low. The gain for the high-fidelity region is reduced to account for the results of the V5 configuration. The medium-fidelity region has been extended to a lower gain, but kept above that of the V7 configuration, which has a gain of 0.3. These suggestions are consistent in trend with the data of Mitchell and Hart (ref. 47), which indicated a preference for low-gain, low phase-distortion motion over high-gain, high phase-distortion motion. Also, the fidelity boundaries have been rounded to account for the reduction in fidelity when a gain attenuation is combined with phase distortion. The determination of exactly where the rounding should begin and end requires additional data.

Also, slight wording changes are suggested to the motion-fidelity definitions of figure 4 to alleviate the previously mentioned difficulties in their use. The word “disorientation” should be removed; it caused some pilots to shy

away from the low rating. Although a configuration may have been objectionable, the pilots felt no disorientation. The suggested rewording, as noted on figure 51, should suffice, since any disorientation experienced would be expected to receive an “objectionable” description.

Significant differences in measured performance and in perceived fidelity were evident across these configurations. The analytical model discussed in appendix B predicted a

performance decrease when the motion filter natural frequency increased. However, the predicted bandwidths of the primary loop did not differ by a factor of 1.5, which was the general guideline suggested for determining dissimilarity between motion configuration responses (ref. 61). Although this analytical model is perhaps the most reasonable available, this experiment demonstrated that additional data are needed in order to continue its refinement and validation.

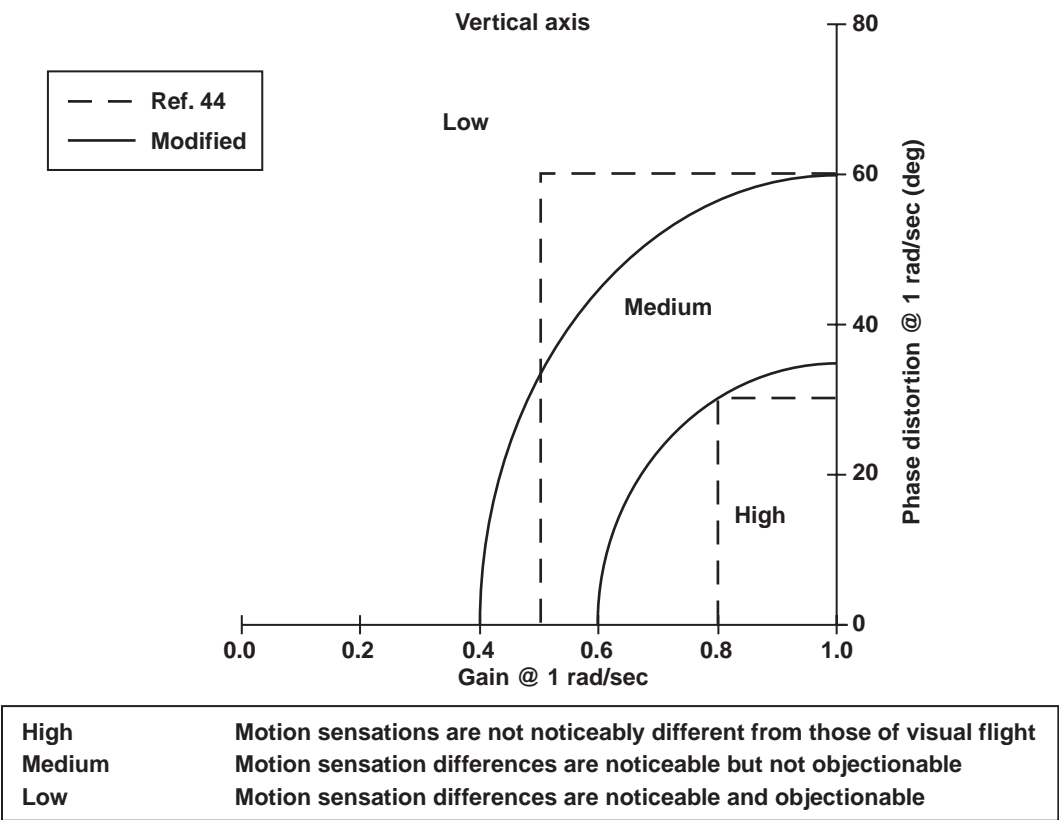


Figure 51. Suggested vertical criterion and fidelity definitions.

5. Vertical Experiment II: Compensatory Tracking

Background

In Vertical Experiment I, the global performance effects of motion-filter gain and natural frequency variations were examined during tracking. In Vertical Experiment II, a more detailed examination of the same filter variations was conducted for a new task: key pilot-vehicle frequency-response metrics were measured during combined tracking and disturbance regulation. This procedure allowed for the influence of the motion-filter changes to be examined simultaneously for these two important piloting tasks. The task and experimental apparatus are first described. Then, objective pilot-vehicle performance metrics and subjective motion-fidelity ratings are discussed.

Experimental Setup

Task

Figure 52 shows the display presented to the pilot. The object was to null the error between the moving target aircraft and the horizontal dashed line that was fixed to the pilot's aircraft.

A system block diagram depicting how the error developed is shown in figure 53. Two external inputs were used in a scheme similar to that developed by Stapleford et al. (ref. 26).

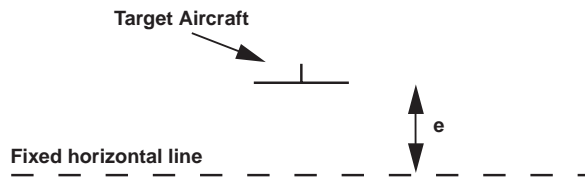


Figure 52. Pilot's display for vertical compensatory tracking.

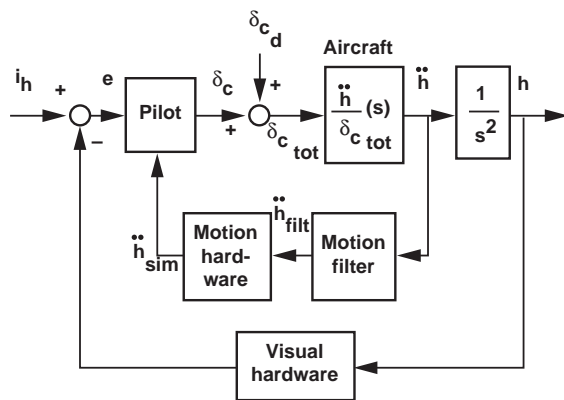


Figure 53. Vertical compensatory loop.

The target was driven by a sum-of-sines (SOS) input, and the vehicle was disturbed by a separate SOS input that was summed with the pilot's collective position. These SOS's were as follows:

$$i_h(t) = 2.573 \sin(0.15t) + 2.202 \sin(0.34t) + 1.563 \sin(0.64t) + 0.923 \sin(1.13t) + 0.411 \sin(2.05t) + 0.150 \sin(3.56t) + 0.040 \sin(6.32t) \text{ feet} \quad (16)$$

$$\delta_{cd}(t) = 0.029 \sin(0.28t) + 0.058 \sin(0.49t) + 0.999 \sin(0.80t) + 0.167 \sin(1.50t) + 0.209 \sin(2.67t) + 0.201 \sin(4.63t) + 0.148 \sin(8.50t) \text{ inches of collective} \quad (17)$$

Each component of each SOS completed an integral number of cycles in the task time-length of 204.8 sec. A warm-up period of 10 sec preceded the run, and a cool-down period of 3 sec followed the run. To prevent the pilot from separating target motion from disturbance motion, the disturbance input, δ_{cd} , was selected so that its resulting altitude spectral content (when filtered by the vehicle dynamics) matched the target shaping function (refs. 26, 41). If the pilot is able to separate the target motion (which is sensed only visually) from the disturbance motion (which is sensed visually and vestibularly), previous research has shown that pilots may alter their behavior and potentially ignore the motion cues when nulling the target motion (ref. 26). The above spectral matching is an attempt to prevent this behavior.

The above shaping function was determined empirically. The compromised result of this shaping was that the highest frequency component of the target input was below the simulator's visible threshold of 3–4 arc min, and the lowest component of the disturbance input was below the vestibular translational acceleration detection threshold of 0.01 g's (ref. 28). As shown in figure 53, the pilot received two external cues for use in zeroing the target error, e : a visual cue, and a motion cue. The dynamics between the pilot input and these cues are discussed in the sections that follow; however, only the block labeled "motion filter" was modified in this experiment. The details of these blocks will be described later.

Although the pilot was instructed to null the displayed error constantly, the desired performance for the task was to keep the error within one-half the height of the target vertical tail for half of the run length. The target was placed 100 ft in front of the aircraft, and the height of the vertical tail was 3 ft.

Simulated Vehicle Math Model

The vertical-axis dynamics were the same as for Vertical Experiment I given by equation (11). Again, only this single degree of freedom was modeled, and the pilot controlled this degree of freedom with a collective lever in the cockpit.

Simulator and Cockpit

The simulator and cockpit were also the same as for Vertical Experiment I. All flight instruments were again disabled. Six NASA Ames test pilots participated (three of the six being the same three who participated in Vertical Experiment I), hereinafter referred to as pilots A–F. All pilots had extensive rotorcraft flight and simulation experience.

Motion System Configurations

The second-order high-pass motion filter given by equation (12) was used. The gains, damping ratio, and natural frequencies evaluated were the same as for Vertical Experiment I, which are given in table 3.

Procedure

All configurations were tested in blind evaluations, and they were randomized. Pilots were asked to rate the

motion fidelity of each configuration, using the motion-fidelity definitions given in figure 4. Between each configuration, in order to calibrate or recalibrate themselves to the true vehicle model response, pilots flew the model with full motion (configuration V1) in a visual scene depicting objects of known size (shown in fig. 35). All six pilots flew all 10 configurations.

Results

Objective Performance Data

Time-histories and standard deviations of several pertinent variables for a full-motion case (V1) and a no-motion case (V10) are shown in figure 54. Both of these runs were made by the same pilot. This comparison reveals that when going from full motion to no motion, the target error, vehicle acceleration, and collective displacement all increase. Rather than compare time-histories across the 10 cases and six pilots, several pilot-vehicle performance metrics were determined, and the statistical significance was evaluated.

First, since the two sum-of-sines inputs were statistically independent, two effective open-loop pilot-vehicle describing functions may be determined (ref. 41). One open-loop describing function applies to the target errors caused by target motion; it is determined by calculating the ratios of the Fourier coefficients of $h(j\omega)/e(j\omega)$ at the

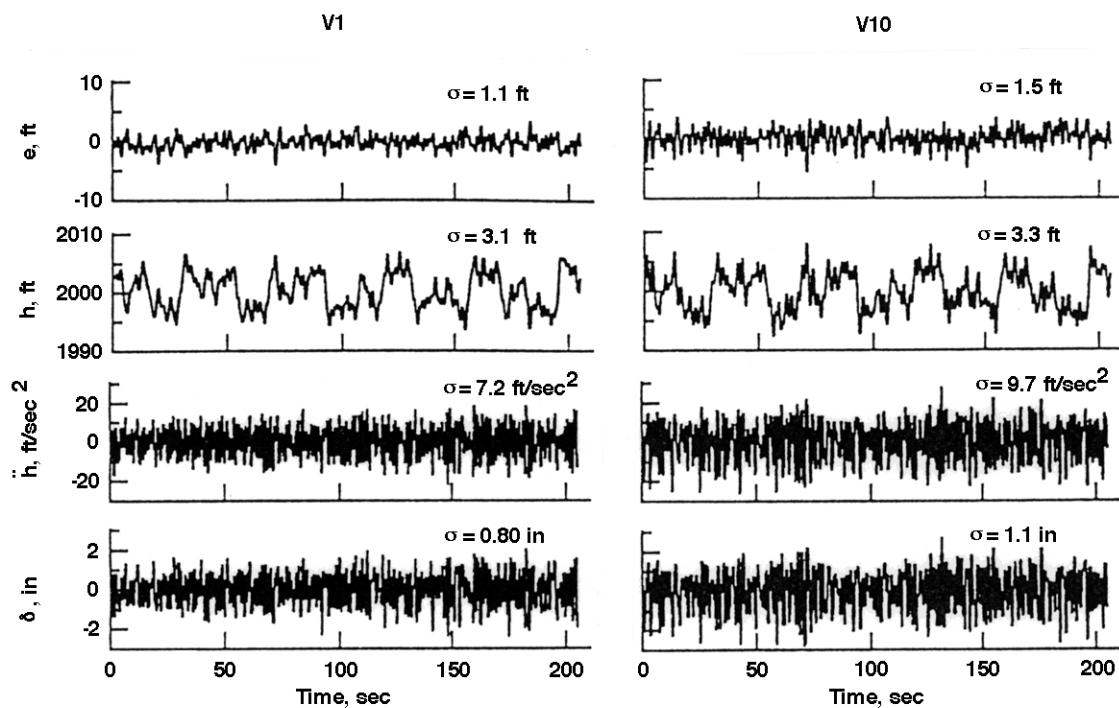


Figure 54. Compensatory tracking: full motion versus no motion.

target input frequencies. The other describing function applies to target errors caused by the disturbance input; it is determined from the ratios of the Fourier coefficients of $-\delta_c(j\omega)/\delta_{ctot}(j\omega)$ at the disturbance input frequencies. These two describing functions are referred to the “target following” and “disturbance rejection” describing functions hereinafter.

From these describing functions, open-loop crossover frequencies and phase margins were determined by linear interpolation. Figure 55 shows the magnitude and phase responses of the disturbance-rejection describing function. The data for this example are from the full-motion run (V1) in figure 54. Linear interpolation between the data at the appropriate frequencies (shown in fig. 55) gives a crossover frequency of 3.3 rad/sec and a phase margin of 28°.

The above two measures provide useful information about the character of the pilot-vehicle response. In particular, the crossover frequency is a rough measure of how fast the error is initially zeroed; the higher the crossover frequency, the faster the initial nulling of the error. The

phase margin is a rough measure of the damping ratio of the error response; the higher the phase margin, the more damped the error response.

Each of these open-loop describing functions includes a different combination of both the pilot’s internal visual and motion compensation applied to the visual error and to the acceleration feedback (refs. 26, 41). Although only the motion cues were changed here, the pilot’s internal compensation may change in an attempt to account for degradations in either the visual or motion cues. The overall effect of these changes on pilot-vehicle performance and opinion are given next.

Target Following. The target-following crossover frequencies are given in figure 56 for all of the configurations. For easy reference, the motion-filter gain K and natural frequency ω , rounded to one decimal place, are indicated above each bar. The mean value (bar height) and standard deviation (horizontal line above bar) are shown, each determined from six values. Each of the six values corresponds to the individual average for each pilot across his runs. Upon examining the variance ratio, or F-test

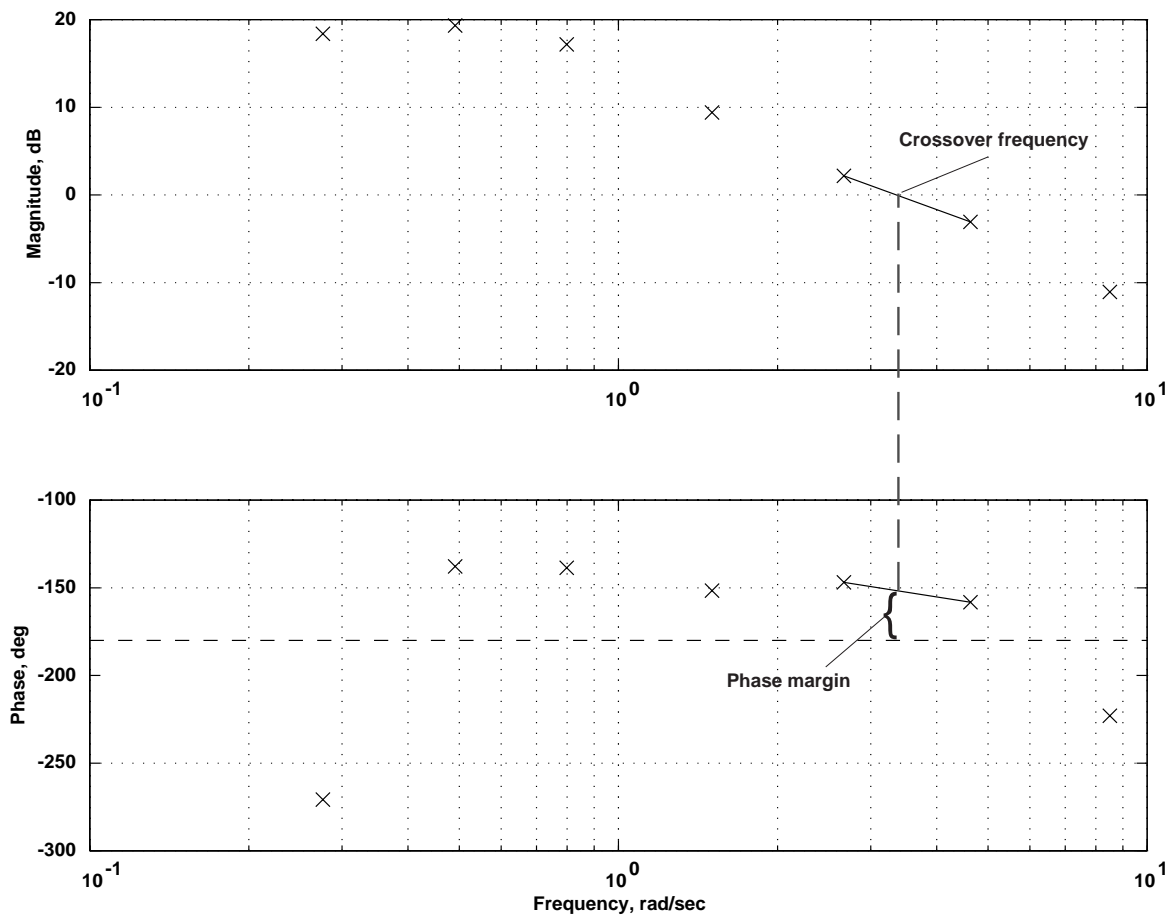


Figure 55. Example disturbance-rejection describing function.

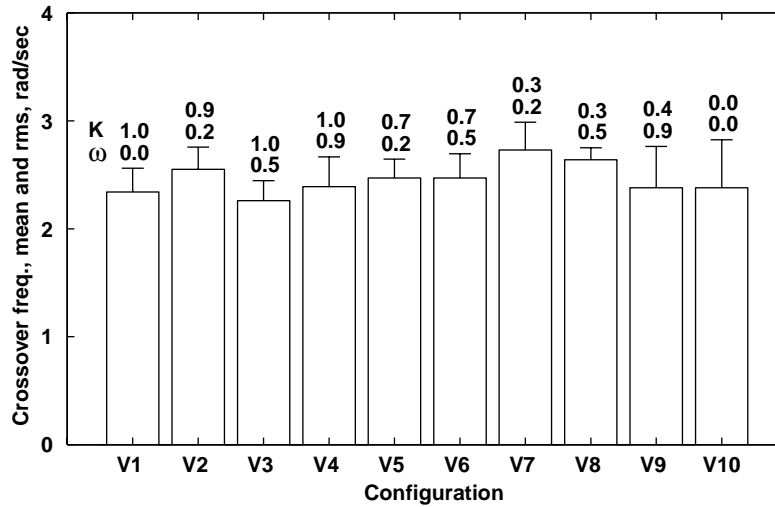


Figure 56. Target-following pilot-vehicle open-loop crossover frequencies.

(ref. 54), for these data, the differences among the configurations were not significant at the 5% level. In addition, no coherent trend was present among the motion-filter variations. This result agrees with, and extends, the results of Bray (ref. 24), which indicated an invariance in target-following open-loop crossover frequency for motion filter natural frequencies between 0.2 and 1.25 rad/sec with $K = 1$ for all configurations. The results from the present experiment indicate that this invariance across natural frequency variations also holds for motion-gain changes. Thus, it appears that the initial quickness with which the pilot closes the target-tracking loop does not depend on the motion cue. That result is intuitive; it might be expected that the speed with which this loop is closed would be based on a pilot's mental model of the speed

with which the loop should be closed. The pilot initiates and generates his own motion in this loop.

Figure 57 shows the target-following loop phase margins for all configurations. Unlike the target-following crossover results, statistical differences are present in the phase margins, although the range of the means is only 10° . The largest phase margin occurred with the full-motion condition (V1), and phase margin was progressively lost as K was reduced and ω_m was increased. Using the Newman-Keuls method (ref. 62) to determine which means are statistically different from each other at the 5% level, the results indicate that configurations V1 and V3 were different from V4 and from V6–V10, and that configurations V2 and V5 were different from V8.

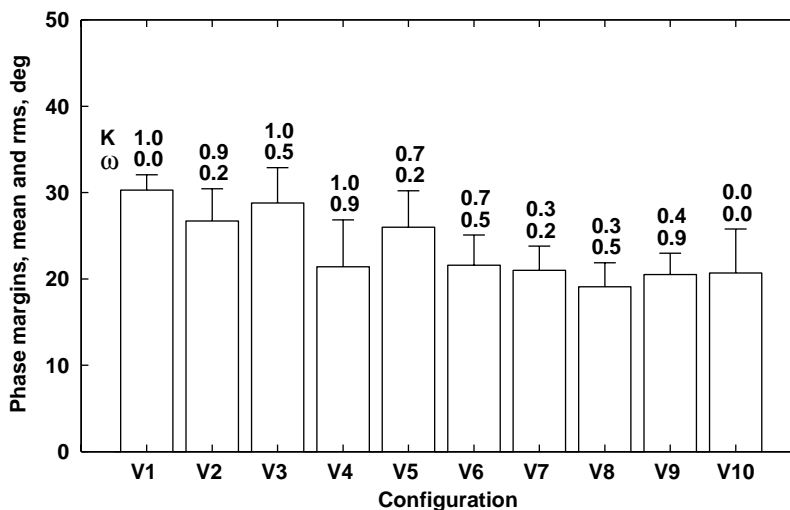


Figure 57. Target-following pilot-vehicle open-loop phase margins.

These results are partially consistent with those of Bray (ref. 24), which indicated that target-tracking phase margin degraded as ω_m was increased from 0.2 to 1.25 rad/sec at a unity gain ($K = 1$). However, Bray's results exhibited larger variations in the measured phase margins, including an almost 20° variation between $\omega_m = 0.2$ and 0.5 rad/sec. Only a slight difference was measured in this experiment between the nearly equivalent V1 and V2 motion configurations.

These phase-margin target-following results suggest that the resulting damping of the error to a nulled steady-state value is affected by motion variations. This result is consistent with the results in section 4. That is, as the quality of the motion improved in that purely target-following task; the principal effect on performance was in damping (see figs. 40–49).

It was also suggested in section 4 that the high-fidelity portion of the Sinacori criterion should include configuration V5. The performance results shown here for target following are consistent with that suggestion.

Disturbance Rejection. Pilot-vehicle open-loop crossover frequencies for the disturbance-rejection loop are shown in figure 58. The crossover magnitudes appear to be roughly ordered by phase distortion level, that is, by successive increases in ω_m . The statistical results reveal that at the 5% level, configurations V1, V2, and V7 all had higher crossover frequencies than the fixed-base case V10. Again, these results are consistent with the configurations tested by Bray (ref. 24), and they extend those results by suggesting that the open-loop crossover

appears to be affected by changes in ω_m at all levels of motion-filter steady-state gain K .

Figure 59 shows the disturbance-rejection loop phase margins. Here the configurations are ordered by progressive reductions in K . Statistically, configuration V3 was better than any of the other cases, and configurations V1 and V4 were better than V10. Bray showed, for $K = 1$, that the low and high phase distortion cases have roughly the same phase margin, with perhaps a slight peaking at moderate amounts of phase distortion. Here, more relative peaking in phase margin was observed for the V3 case than was found by Bray. The crossover frequency for V3 was reduced, which alone might contribute to an increased phase margin; however, V4 had a low crossover frequency, but not an accompanying phase-margin peak. With the unknown details of the pilot feedbacks, the V3 configuration must be coupling in with the vehicle dynamics in a manner different from that in the other configurations.

The overall disturbance-rejection results suggest three points. First, the speed at which the disturbance is rejected is affected primarily by the high-pass motion filter's natural frequency. Second, motion-filter gain appears to affect the relative damping of the disturbance-rejection loop, rather than being driven more by filter natural frequency as in the target-following loop. Third, both the lowest crossover frequency and the lowest phase margin of the disturbance-rejection loop occurred in the no-motion case.

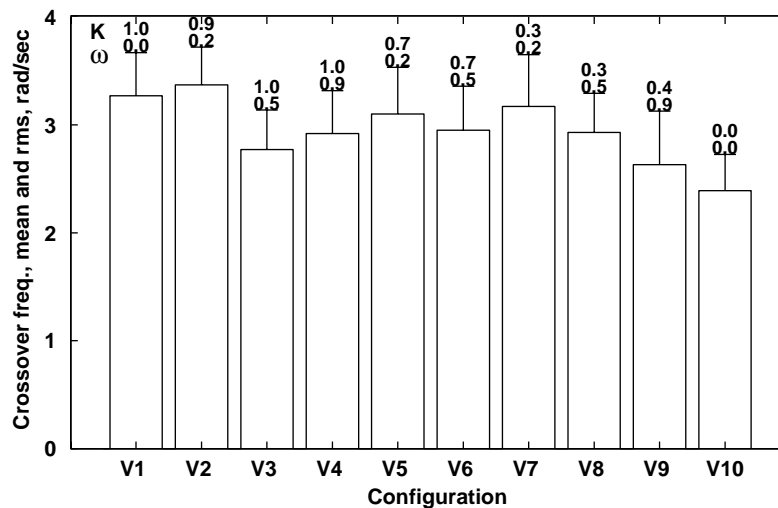


Figure 58. Disturbance-rejection pilot-vehicle open-loop crossover frequencies.

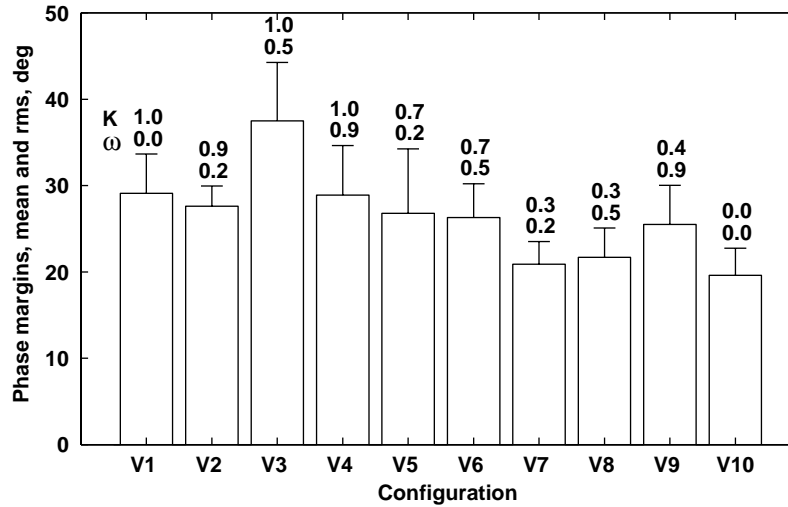


Figure 59. Disturbance-rejection pilot-vehicle open-loop phase margins.

Total Tracking Error. Vertical tracking errors are shown in figure 60. This error accrues from both the target and the disturbance inputs. The four lowest errors occurred for the lowest phase-error configurations, but the differences between any two of the motion configurations were not large. The Newman-Keuls results indicated that

all of the motion configurations, V1–V9, had better performance than the no-motion V10, while no tracking-error differences were present among the V1–V9 configurations at the 5% level. Hence, the biggest effect on error reduction was simply the presence of motion rather than its characteristics.

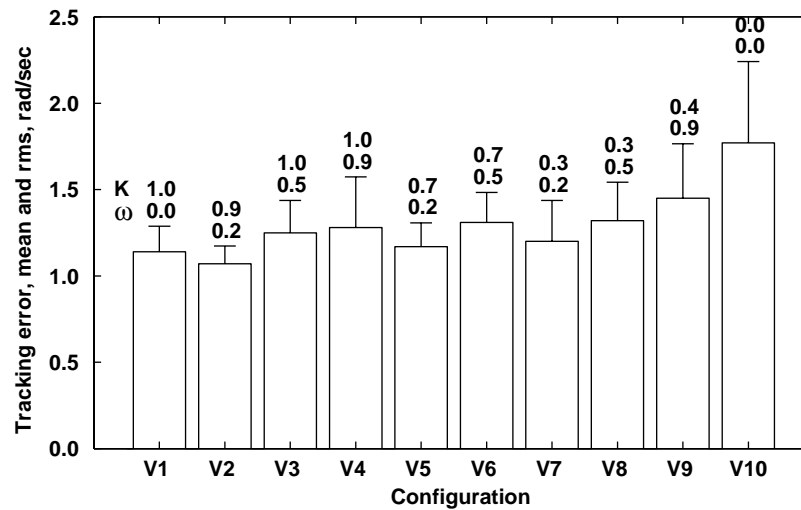


Figure 60. Vertical tracking errors.

Subjective Performance Data

Figure 61 provides the motion-fidelity ratings using the definitions stated earlier. The ratings are divided into “high,” “medium,” “low,” and “split,” where split refers to a pilot assigning inconsistent ratings for repeated runs of the same configuration. Split ratings only occurred for the V1 configuration; this was more likely, because configuration V1 had more repeat evaluations than the other cases. The ratings indicate that no pilot perceived the $K = 0.3$ cases to be high fidelity. Configuration V2 received the best overall ratings, and also had the lowest mean tracking error as shown earlier. Configuration V3 surprisingly received two low ratings; V4 received no low ratings. Configuration V6, which is essentially a combination of the natural frequency of V3 and the gain of V5, was rated worse than either V3 or V5. No configurations in which the high-pass filter’s high-frequency gain was less than 0.3 was judged to be high fidelity. All pilots rated the fixed-base condition to be low fidelity.

Summarizing the results of this section, the presence and quality of motion influenced both target tracking and disturbance rejection. Motion-filter natural frequency affected both target tracking and disturbance rejection, whereas motion gain affected only disturbance rejection. Overall, the results from this dual task are consistent with those presented in section 4.

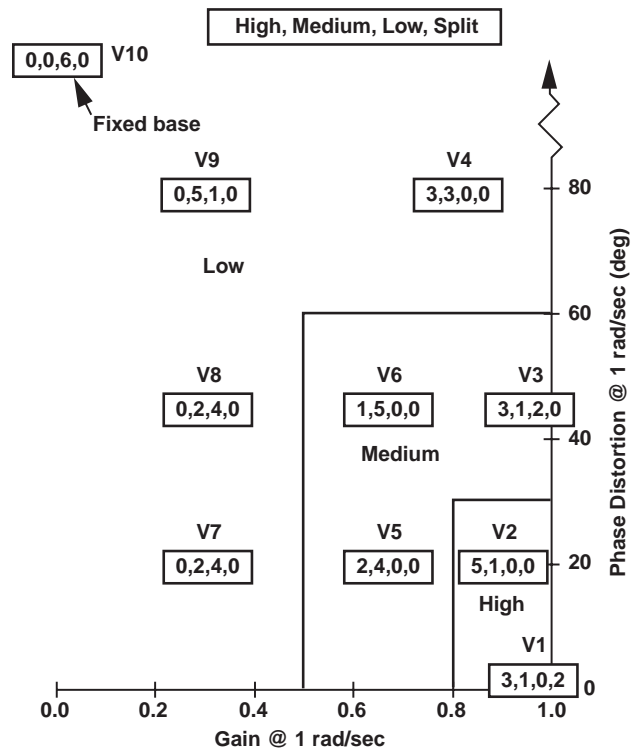


Figure 61. Pilot motion fidelity ratings for vertical task.

6. Vertical Experiment III: Altitude and Altitude-Rate Estimation

Background

Relative to flight, simulation has perennially produced less effective control of altitude and altitude rate. Fixed-wing landings in simulation usually have higher runway position dispersions and higher mean touchdown velocities than in flight. Bray showed that with a 16-in black-and-white television monitor, simulator vertical displacements of at least ± 20 ft are required in order to achieve the desired fidelity in the landing task (ref. 60).

In helicopter simulations, pilots often comment that the vertical damping (as perceived from the visual and motion cues) is less than it is in flight (refs. 59, 63–65). Since the math models have often been developed and validated from in-flight measurements, attempts to determine the cause have focused on the simulator visual and motion cues.

Often, the assumption is made that pilots obtain vehicle acceleration information from the motion system, and rate or position information from the visual system, as shown in figure 62. Thus, decreasing motion gain or increasing washout frequency is assumed not to affect the outer rate and position loops. In this work, an experiment was designed to test this assumption by exploring the effects of visual scene properties and vertical motion on the estimation of altitude and altitude rate.

Experimental Setup

Five factors were incorporated in Vertical Experiment III: (1) reposition direction, (2) initial altitude, (3) presence of vertical motion, (4) visual scene level-of-detail control, and (5) visual scene mean object size.

Tasks

The experiment involved two tasks.

1. In the first task, the altitude repositioning task, pilots were instructed either to double or halve their initial altitude. The initial altitudes were 15.6, 18.3, and 21.0 ft. Altitude was the only degree of freedom under the pilot's control. No time requirement was placed on the task, and no requirements were imposed on overshooting or undershooting what the pilots felt to be their doubled (or halved) altitude.
2. In the second task, the altitude-rate control task, pilots were instructed to climb or descend at a

constant rate of 3 ft/sec. The climbs started at an altitude of 7.5 ft and ended at 42.5 ft. The descents started at an altitude of 42.5 ft and ended at 7.5 ft. These unusually specific altitudes were selected to allow one-to-one motion and visual cues in the Vertical Motion Simulator.

For both tasks, all instruments were disabled so that pilots would have to estimate their altitude and altitude rate from the visual scene, motion system, or cockpit collective movement. Although pilots would ordinarily accomplish these tasks in flight by referring to an instrument that measures either altitude or altitude rate, these instruments were intentionally disabled so that the possible value of the motion and visual cueing variations could be determined.

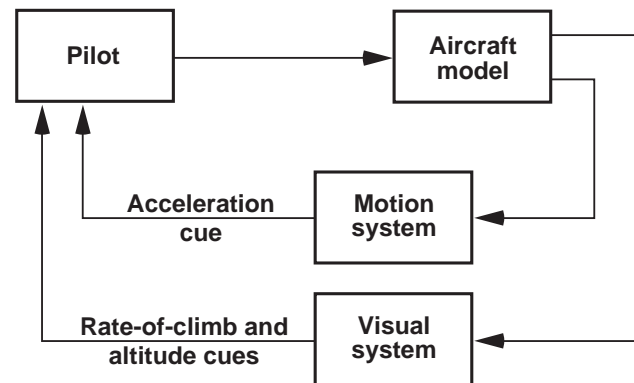


Figure 62. Typical assumptions in the apportioning of simulation cues.

Simulated Vehicle Math Model

The math model represented the AH-64 Apache helicopter:

$$\begin{bmatrix} \ddot{h} \\ \dot{z}_1 \end{bmatrix} = \begin{bmatrix} -0.122 & -118 \\ 0.0 & -12.9 \end{bmatrix} \begin{bmatrix} \dot{h} \\ z_1 \end{bmatrix} + \begin{bmatrix} 14.6 \\ 1.00 \end{bmatrix} [\delta_c] \quad (18)$$

The state z_1 was added to approximate the effects of dynamic inflow into the rotor. All other displacements and orientations were held fixed at zero.

Simulator and Cockpit

The simulator and cockpit were the same as for the yaw experiment described in section 3. The Evans and Sutherland CT5A visual system was used, but both the hardware and software were modified to achieve the visual variations described below.

Design of Visual Scenes

Simulated scenes are typically less dense (fewer objects per degree of field of view) at lower altitudes than at higher altitudes. In flight, objects invisible at high altitudes become visible at low altitudes, as the angle that the object subtends at the eye becomes larger. When this subtended angle exceeds an optical resolution threshold, the object can be seen. These changes in detail cannot be represented accurately owing to the required computational load in the image generator. Instead, visual databases, which are sets of objects, are stored and then faded in and out of the scene according to range. This fading is adjusted so that the transitions between databases appear natural. How an image generator accomplishes this fading of objects is called “level-of-detail management.”

For this experiment, visual databases were constructed of green polygons on a brown ground plane. These polygons were randomly positioned at locations within a 430-ft radius forward of the aircraft. Each database was associated with a particular altitude band (2.5-ft band). These bands occurred between altitudes of 5 and 45 ft. As the vehicle moved between these 2.5-ft altitude bands, one database smoothly faded out while the new database faded in.

For each altitude, whether or not a polygon was displayed at that altitude depended on which of two visual thresholds was used. The “small” visual threshold allowed objects to be drawn when their vertical visual angle spanned at least 0.1° ; the “large” visual threshold allowed objects to be drawn when their vertical visual angles spanned 0.2° .

In either case, the polygons were all rendered in a common set. That is, the polygons were all distributed on a ground plane; whether or not they were then drawn depended on the visual threshold used. Thus, at the 0.1° threshold, more polygons were drawn than in the 0.2° threshold. The polygons that would appear in the 0.2° threshold would also appear at the 0.1° threshold. Four different ground planes of polygons, two each for the two visual thresholds, were used so that any effects found would not be due to some unfortuitous and unusual random placement of the polygons.

Three levels of “level-of-detail management” were evaluated: high, medium, and low. For the high condition, 62 polygon sizes were distributed exponentially in the database with diameters between 0.025 ft and 17.23 ft.

The exponential spread was determined according to the relation

$$d_i = 17.23(0.9)^i \quad i = 0, 1, \dots, 61 \quad (19)$$

where d_i is the diameter of the i th polygon.

These 62 polygon sizes were placed in the common database in the following manner. First, the largest polygons were randomly placed until a specified portion of the unfilled area was filled. Then, polygons of the next largest size were randomly placed in the remaining area until that same proportion of the unfilled area was filled. This continued, allowing no overlapping regions, until polygons of all 62 sizes were placed. Since the image generator could display a maximum of 1350 polygons at 60 Hz, the proportion parameter was selected such that this maximum was not exceeded.

For the medium condition, the polygon sizes were distributed evenly, not exponentially, between 0.025 ft and 17.23 ft. For the low condition, only a single database was presented at all altitudes, so no fading in and out occurred. For the low condition, two sets of only three polygon sizes were used: one set had polygon diameters of 3, 5.23, and 7.46 ft. The other set had polygon diameters of 6, 10.45, and 14.9 ft. These sizes were chosen using the following rationale. First, the largest polygons in each set spanned 0.1 and 0.2 visual degrees at the 45-ft altitude. Second, the smallest polygon in the large set of sizes spanned approximately twice as much visual angle as the small polygon in the small set.

Analytical Evaluation of Visual Scenes

Several metrics were used to evaluate the efficacy of using these procedures in constructing the databases. First, the number of visible polygons is plotted for each of three 10° elevation bands (in fig. 63). These three 10° elevation bands between 0° and 30° below the horizon nearly span the field of view represented by the cockpit windows. As shown, in the high condition, the number of polygons visible is nearly constant versus altitude for each elevation band. However, it is difficult to compare the medium and low condition in terms of the level-of-detail represented. For the medium condition, the number of polygons visible always increases with altitude, but in the low condition, the number of polygons in the 0° – 10° elevation band decreases with increasing altitude.

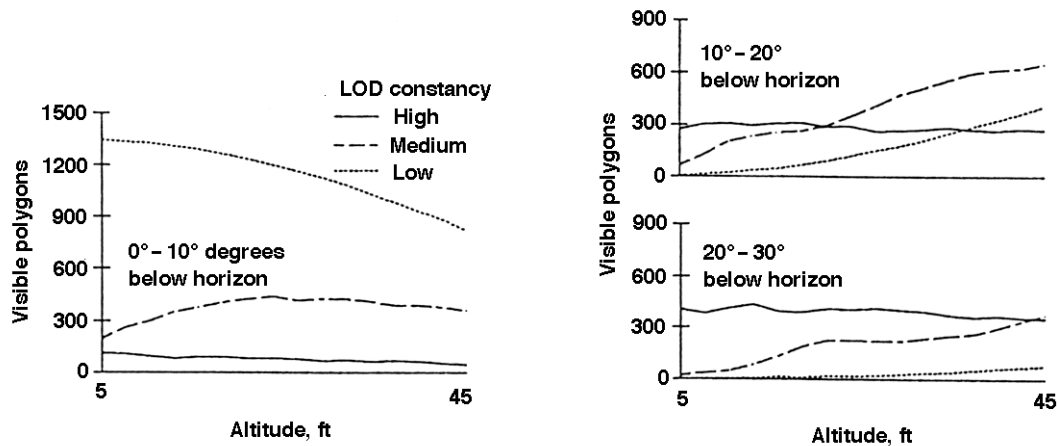


Figure 63. Visible polygons for the three level-of-detail visual databases.

Another metric, mean visual form ratio, was also examined. Mean visual form ratio is the average angular width divided by angular length. It is simply a function of altitude and range to an object. Figure 64 shows that the mean form ratio was invariant for the high condition, decreased slightly with altitude for the medium condition, and dramatically decreased with altitude for the low condition.

Motion System Configurations

Two motion configurations were presented: full motion and no motion.

Procedure

Five NASA Ames test pilots flew the two tasks. All of the pilots had extensive rotorcraft and simulation experience. Pilots signaled the initiation and conclusion of the task by pulling a trigger on the centerstick. The pilots

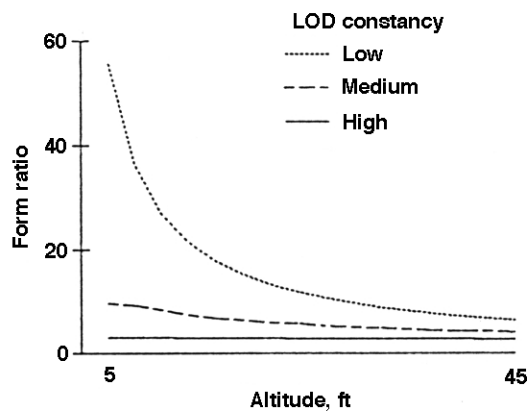


Figure 64. Mean visual form ratio for the three level-of-detail visual databases.

participated in one or two sessions per day, with each session lasting 1 to 2 hr. Pilots received training during their first session and a short refamiliarization on subsequent sessions. These training sessions used several high level-of-detail databases constructed especially for training purposes (they were not used in the data collection). Pilots evaluated the configurations in a randomized order.

Results: Objective Performance Data

All of the results for the altitude repositioning task were analyzed using a repeated measures analysis of variance (ref. 54). For this task, the pilot's altitude repositioning error was determined by

$$\% \text{ repositioning error} = \frac{\left[\begin{array}{c} \text{actual altitude change} \\ - \text{desired altitude change} \end{array} \right]}{\text{desired altitude change}} \quad (20)$$

Figure 65 shows the mean percent repositioning error for three of the five experimental factors: vertical motion presence, reposition direction, and initial altitude. Across all visual databases, accuracy in altitude repositioning improved when motion was present ($F(1,4) = 39.347$, $p = 0.003$), with an overall tendency to overshoot the desired altitude change. This result was very surprising, for conventional wisdom would suggest that estimating the required altitude change would be a purely visual task. It would be expected, based on the results of Vertical Experiments I and II, that the trajectory quality between the two final altitude points would be improved with motion (motion allowing the generation of lead, thus improving the open-loop phase margin). However, it was not expected that the presence of motion would affect the

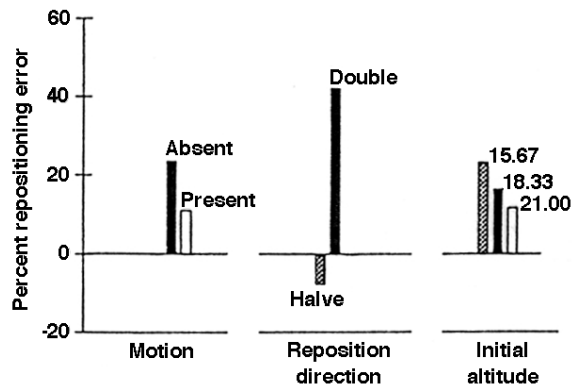


Figure 65. Altitude repositioning error.

altitude endpoint. Apparently the pilot was combining the visual and motion cues in a way that improved his estimate of the vehicle's state.

In comparing climbs versus descents, pilots were better at halving the altitude than they were at doubling it ($F(1,4) = 23.339$, $p = 0.008$); there was a tendency to ascend too high when doubling altitude and to descend too little when halving altitude. Finally, figure 65 shows that better accuracy resulted when starting at higher initial altitudes ($F(1,4) = 14.064$, $p = 0.002$); there was an overall tendency to overshoot the desired altitude. Interestingly, there were no statistically significant main effects found when varying the level-of-detail quality among the databases, nor for the minimum resolution size.

No main effects were found for visual scene level-of-detail manipulations, but there was a statistically significant interaction between level-of-detail and initial altitude ($F(4,16) = 3.451$, $p = 0.032$). Figure 66 illustrates this interaction. For the ascents, the final altitude more closely matches the desired doubled altitude as the level-of-detail becomes more constant. Only for the 21-ft initial-altitude descents did the high constancy level-of-detail database not result in the best repositioning performance. So, it appears useful to attempt to have the visual system mimic the level-of-detail changes, as one would experience in the real world.

Altitude-Rate Control Task. The performance measurement for the altitude-rate control task was mean absolute vertical rate during the climb or descent. Only data between vehicle altitudes of 10 and 40 ft were used, thus eliminating the initiation of either the climb or the descent.

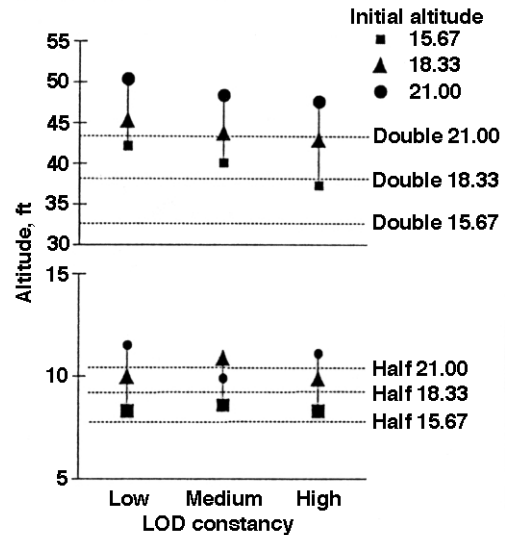


Figure 66. Altitude reposition versus level-of-detail and initial altitude.

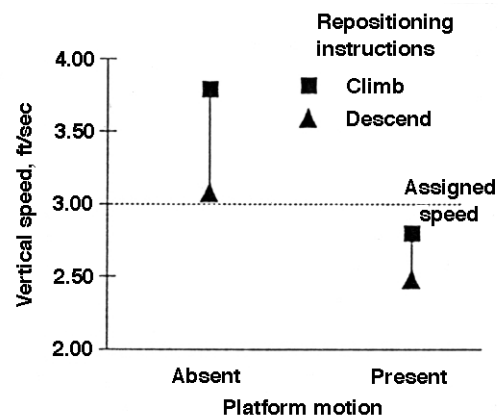


Figure 67. Vertical speed dependence on motion and movement direction.

Statistically, there were significant effects for the presence of vertical platform motion ($F(1,4) = 78.846$, $p = 0.001$) and for movement direction ($F(1,4) = 14.806$, $p = 0.018$). There was also a significant interaction between these two factors ($F(1,4) = 12.379$, $p = 0.024$). Figure 67 shows these effects. Note that the vertical rates were slower with motion than without motion, and that the vertical rates were slower when descending than when climbing. The presence or absence of platform motion had a stronger effect on performance than the movement direction.

Figure 68 shows the mean vertical speeds versus altitude for all of the pilots for the four combinations of movement direction and motion presence. These profiles illustrate that for climbs, vertical speed increased with increasing altitude, and that the increase was more pronounced when motion was absent. What seems to be occurring is that the presence of platform motion reduces the influence of optical flow rate changes on a pilot's control of vertical speed. Optical flow rate when moving vertically (the angular rate at which objects move visually in elevation) is proportional to vertical speed divided by altitude (ref. 66). So, at constant vertical speed, optical flow rate continuously decreases during a climb. If pilots try to maintain a nearly constant optical flow rate, they will increase speed with increasing altitude.

The theory that pilots try to maintain a constant optical flow rate is supported by Johnson and Awe (ref. 67). They found that during a fixed-base simulation in which pilots were asked to maintain speed that the pilots often slowed as their altitude decreased. Since Figure 68 shows

this same tendency, but less so with motion, it is believed that the acceleration cue mitigates the attempt to maintain a constant optical flow rate. Manipulations in level-of-detail did not affect the pilots' ability to control vertical rate.

Summarizing the experiment discussed in this section, platform motion improved pilots' accuracy in the altitude repositioning task, which was surprising. It is hypothesized that an integration of the visual and the motion cues is occurring, and that the integration affects a pilot's estimate of altitude and altitude rate. The specifics of this integration are still unknown. That is, future work is needed to determine how many of the altitude and altitude-rate cues are derived from the visual and how many are derived from the motion system. Still, this study showed that one cannot ascribe any of the vertical states to a single cue. The overall conclusion is that for the control of altitude in simulation to be more like that of flight, vertical motion should be provided.

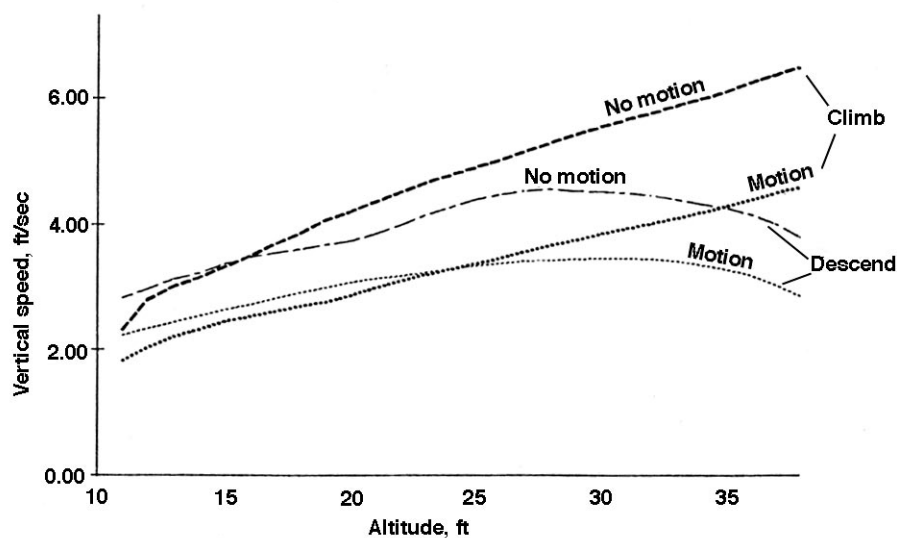


Figure 68. Mean vertical speed versus platform motion and movement direction.

7. Roll-Lateral Experiment

Background

In flight simulation, the roll and lateral translational degrees of freedom are treated together for several reasons. First, owing to the motion platform geometry, a certain amount of lateral translational motion must accompany a rolling motion to locate the center of rotation properly. Second, for coordinated maneuvers, in which the body-axis lateral aero-propulsive forces are zero, lateral translational platform motion provides an acceleration to counteract the “leans” that would result from only rolling the cockpit.

Figure 69 shows a coordinated and an extremely uncoordinated case (roll only) with a pendulum hanging from the top of a rolling flight simulator cockpit. In both cases, altitude remains constant. In the coordinated case, the platform moves laterally with an acceleration of $g \tan \phi_{\text{plat}}$; however, the body-axis lateral component of the aero-propulsive force is zero which keeps $a_y = 0$. Sustaining the platform acceleration to maintain this coordination consumes available lateral displacement quickly.

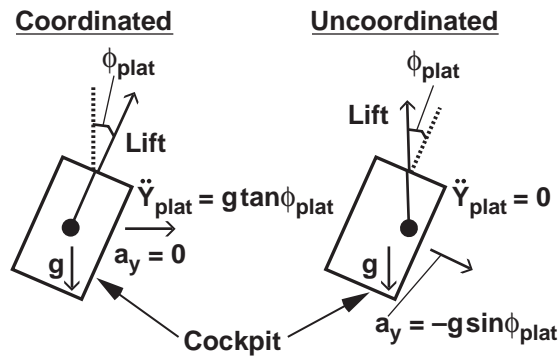


Figure 69. Coordinated vs. uncoordinated flight.

Most motion-base flight simulators are hexapods with similar displacement capabilities. In these devices, sufficient lateral translational platform travel is not available to simulate exactly the motion cues that a pilot would receive in coordinated flight. To reduce the amount of lateral displacement used, platform drive commands use several methods. In one method, the roll angle of the motion platform is reduced relative to the model (and thus the visual scene). This requires less lateral travel, since less lean-due-to-roll motion is present. In the second method, less than the full amount of lateral translational

motion required for coordination is used. The purpose of his study was to investigate the trade-off between these two options.

Experimental Setup

Task

Constant-altitude lateral side steps were performed between two points 20 ft apart. A positioning sight in the visual scene allowed pilots to use parallax to determine their positioning error precisely. The desired positioning performance standard was ± 3 ft about the desired hover point (which was 20 ft away), and the adequate performance standard was ± 8 ft. The task had to be completed in less than 10 sec for desired performance and in less than 15 sec for adequate performance. Pilots pressed an event marker on the center stick when they felt they had acquired the station-keeping point. They were instructed that pushing this button meant that they were within the position error for desired performance, and that they believed they would remain within the desired performance standard.

Simulated Vehicle Math Model

The math model had only two degrees of freedom. Altitude remained constant at 25 ft; heading, pitch, and longitudinal position remained constant at zero. Pilots controlled the vehicle with lateral displacements of a center stick only. The equations for motion were

$$\ddot{\phi} = -4.5\dot{\phi} + 1.7\delta_{\text{lat}} \quad (21)$$

$$\dot{v} = g \sin \phi \quad (22)$$

where v is the body-fixed velocity in the y direction (lateral). These equations represent a typical helicopter math model that is fully coordinated at the aircraft's c.m., since no lateral aero-propulsive forces are present ($a_y = \dot{v} - g \sin \phi$). Actual helicopters have a drag owing to lateral translational velocity, and they also produce a side force at the rotor which contributes to a rolling moment. Each of these real-world effects causes uncoordinated flight during a side-step maneuver. This experiment used a fully coordinated model, since the objective was to examine the effects of uncoordinated simulation cues caused by simulator platform displacement limitations. Thus, these real-world effects were intentionally absent. So the model represented a vehicle in which only applied torques created rolling motion (similar to an AV-8B-like concept) with no drag owing to velocity (which is small near hover).

For the experiment, the pilot's abdomen was located at the aircraft's c.m. The roll-axis dynamics given above, when combined with the visual system delay of 60 msec, had

satisfactory (Level 1) handling qualities as predicted by the U.S. Army's Rotary Wing Handling Qualities Specification (ref. 50).

Simulator and Cockpit

The experiment again used the NASA Ames Vertical Motion Simulator, but only the roll and lateral axes. The lateral axis has ± 20 ft of travel, and the roll axis has $\pm 18^\circ$ of displacement. The roll and lateral axis dynamic characteristics were dynamically tuned with feedforward filters in the motion software to synchronize the two axes as much as possible. For this experiment, each motion axis had an equivalent time delay of approximately 60 msec, as measured using techniques developed by Tischler and Cauffman (ref. 46). The cockpit was configured with a center stick only. No instruments were present, so the pilot had to extract all cues from the motion system, the visual system, and the inceptor (center-stick) dynamics. The center-stick dynamics were measured to be

$$\frac{\delta_{\text{lat}}}{F_{\text{lat}}} (s) = \frac{1}{0.6} \frac{s^2}{s^2 + 2(0.8)s + 8^2} \quad (23)$$

where δ_{lat} and F_{lat} are the displacement and force, respectively, at the pilot's grip.

For the visual system, the Evans and Sutherland ESIG 3000 image generator was used. The visual time delay was adjusted so that it was 60 msec in order to match the equivalent motion time delay in the roll and lateral axes. The simulator cab was the same as that used in section 4, so the field of view is that shown in figure 36.

Motion System Configurations

Figure 70 shows the relevant motion-platform drive laws. That is, the simulator-roll-angle command differed from the math model only by a gain (i.e., no frequency-dependent motion attenuation from a washout filter was present). The platform moved laterally to reduce the false lateral acceleration caused by platform roll angle. Only a gain was applied on this lateral translational platform command as well. In practice, both a gain and a high-pass filter are used, but these effects were not examined.



Figure 70. Motion platform logic for roll/lateral task.

As such, the cues felt by the pilot were all in phase with the visual scene. Usually, this is not the case, because high-pass (washout) filters introduce a distortion between not only the motion and visual cues, but also between motion cue axes.

For small angles, the motion system mechanization of figure 70 results in a false lateral specific force given by

$$a_{y_{\text{plat}}} = g(K_{\text{lat}} - 1)K_{\text{roll}}\phi \quad (24)$$

Thus, as expected, decreasing lateral translational gain increases the false cue. However, for a given K_{lat} , increasing the roll gain, K_{roll} , also increases the false lateral translational cue. So, increasing the roll gain improves the fidelity of the roll acceleration cue, but if the subsequent lateral translational motion is not coordinated, the improvement comes at the expense of increasing the false lateral translational cue.

Table 4 shows the combinations of roll and lateral translational motion gains that were tested. Figure 71 shows these combinations with arrows indicating predicted fidelity trends for the variations in the motion gains. As K_{roll} increases, the fidelity of roll accelerations and rates would increase, but at a given K_{lat} , coordination would decrease, as the leans resulting from roll would increase. From the earlier equation for $a_{y_{\text{plat}}}$, the false lateral specific force for a given roll attitude decreases along the diagonal.

Table 4. Motion gains tested for roll/lateral experiment.

K_{lat}	K_{roll}
0.0	0.0
0.4	0.2
0.4	0.4
0.4	0.6
0.6	0.2
0.6	0.4
0.6	0.6
0.8	0.2
0.8	0.4
0.8	0.6
1.0	1.0

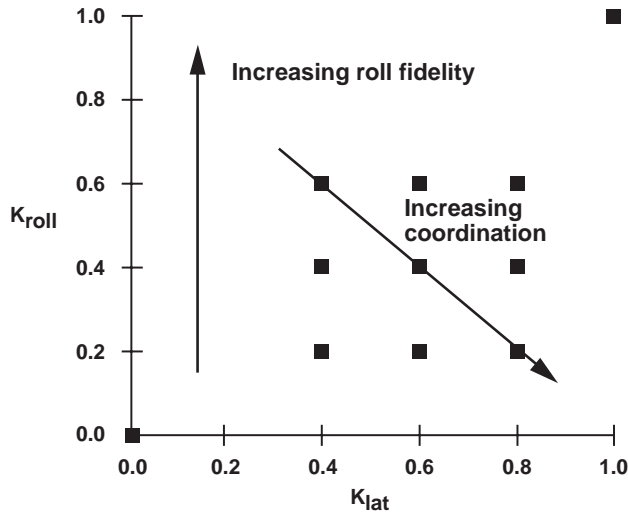


Figure 71. Configurations and fidelity effects for roll/lateral experiment.

Procedure

Three test pilots participated in the study. The pilots were from NASA Ames, the Federal Aviation Administration, and Lockheed-Martin. All pilots had significant flight and simulation experience. The NASA and the FAA pilot had extensive helicopter experience, and the Lockheed Martin pilot had experience in hovering jet aircraft.

Pilots practiced with a motion configuration selected randomly at the beginning of each test period. During the trials, each of the three pilots evaluated the configurations in a random order. Pilots rated each configuration after performing the task with that configuration three times.

Pilots subjectively evaluated the configurations in two categories: motion fidelity and handling qualities. For motion fidelity, they used the scale developed by Sinacori (ref. 44), but with the modifications suggested in Vertical Experiment I. The scale is shown in table 5. To rate the handling qualities, the Cooper-Harper scale was used (ref. 53). An overview of the scale is given in appendix D.

Table 5. Revised motion fidelity scale.

Fidelity rating	Definition
High	Motion sensations are like those of flight
Medium	Motion sensations are noticeably different from flight, but not objectionable
Low	Motion sensations are noticeably different from flight and are objectionable

Results

Objective Performance Data

Again, compelling performance differences occurred between full motion and no motion, as shown in figure 72. The solid lines in the figure represent full motion ($K_{roll} = K_{lat} = 1$), and the dotted lines represent no motion. When transitioning from full to no motion, performance degraded, and the magnitude and rate of control inputs increased. Pilot-vehicle performance degradation typically becomes more marked as the dependency on the pilot for control and stabilization increases. The magnitude and rate of control input increases, because the pilot is now trying to extract vehicle state information kinesthetically (via sensing position and forces in the limb-manipulator system), since the platform cues that supplied lead information directly (from vehicle acceleration) are now missing. These tendencies are consistent with the other studies in this report.

Figure 73 illustrates how overall positioning performance varied with the configurations. Pilots assigned numerical values to designate performance levels: a 1 for desired performance; a 2 for adequate performance; and a 3 for inadequate performance. Since pilots flew three runs for each configuration, their performance for each one of the three runs was assigned a value. Thus, if adequate performance was achieved on all three runs, the score was 6. Mean and standard deviations are shown.

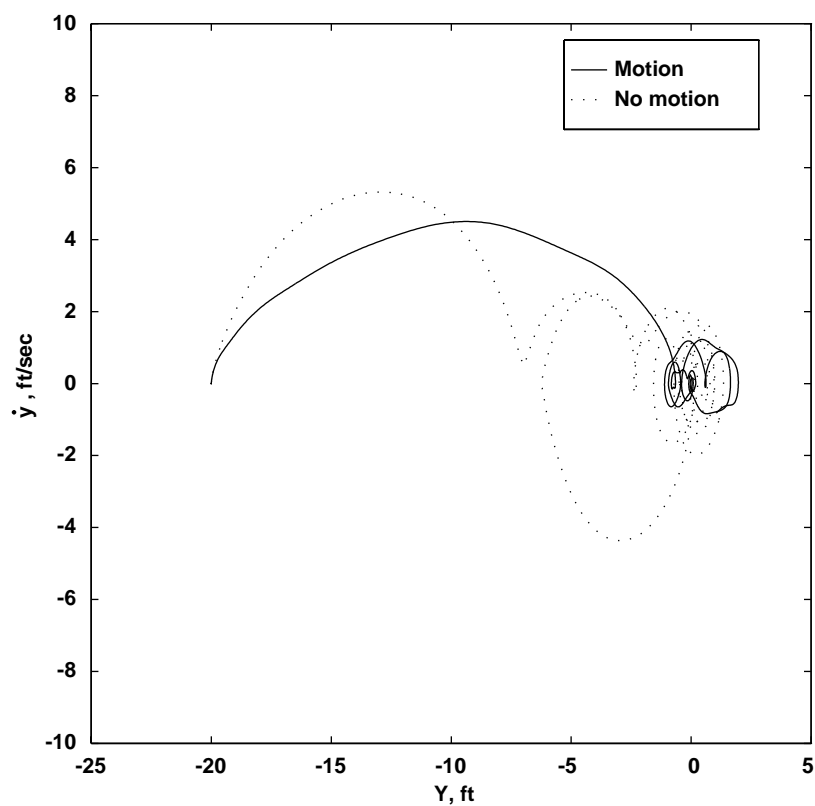
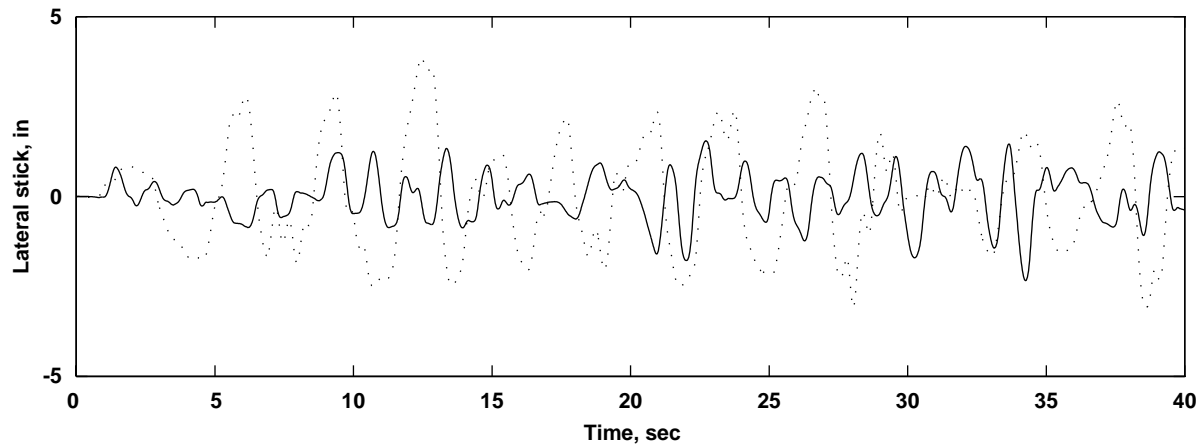


Figure 72. Full motion vs. no motion for roll/lateral experiment.

The objective positioning performance varied little with configuration. Most pilots were able to achieve desired performance for the runs, except for the fixed-base run. Two of the three pilots did not obtain desired performance consistently without motion.

Lateral stick rms position averages are shown in figure 74. The highest average rms values are for the fixed-base condition. As the amount of motion increased, the resulting rms stick position generally decreased.

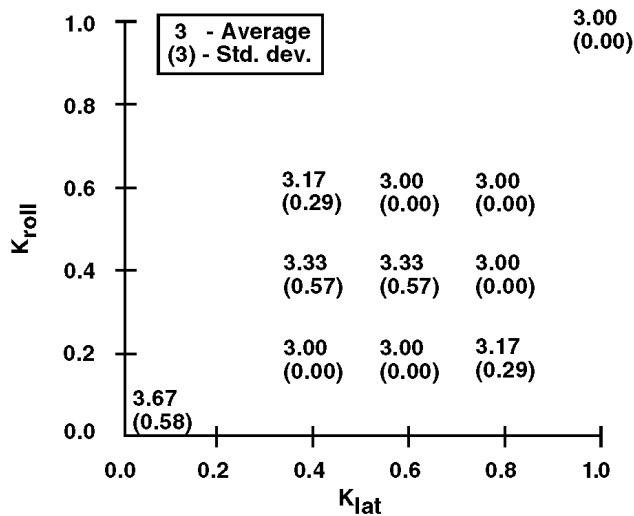


Figure 73. Positioning performance for roll/lateral experiment.

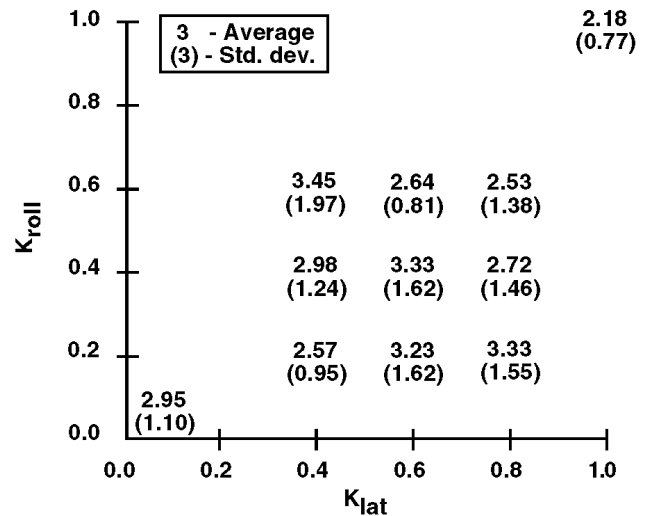


Figure 75. Rms lateral stick rate for roll/lateral experiment (in/sec).

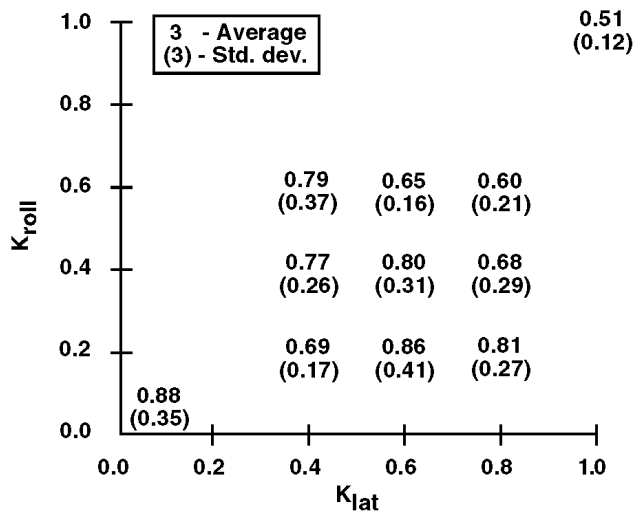


Figure 74. Rms lateral stick position for roll/lateral experiment (in.).

Figure 75 shows how rms of the lateral stick rate varied over the configurations. Each value represents the average of the three rms values (one for each pilot) for a concatenation of three time-histories (one for each run). The fixed-base condition resulted in higher rms stick rates than the larger motion conditions ($K_{lat} = 1/K_{roll} = 1$; $K_{lat} = 0.8/K_{roll} = 0.6$; $K_{lat} = 0.8/K_{roll} = 0.4$; $K_{lat} = 0.6/K_{roll} = 0.6$). Comparisons with and among the remaining configurations are less clear.

Subjective Performance Data

Figure 76 shows how the motion fidelity ratings changed versus roll gain and lateral translational gain. Numerical values of 1, 2, and 3 were assigned to fidelity ratings of Low, Medium, and High for determining the averages. All pilots rated the fidelity of the fixed-base case as Low. In general, as the amount of motion increased (increasing both K_{lat} and K_{roll}) the rated motion fidelity improved. Interestingly, as K_{roll} increased for a fixed K_{lat} , fidelity improved. This situation increases the false lateral specific force cue, which would suggest a fidelity degradation. However, it appears this degradation was more than compensated for by an increase in roll fidelity.

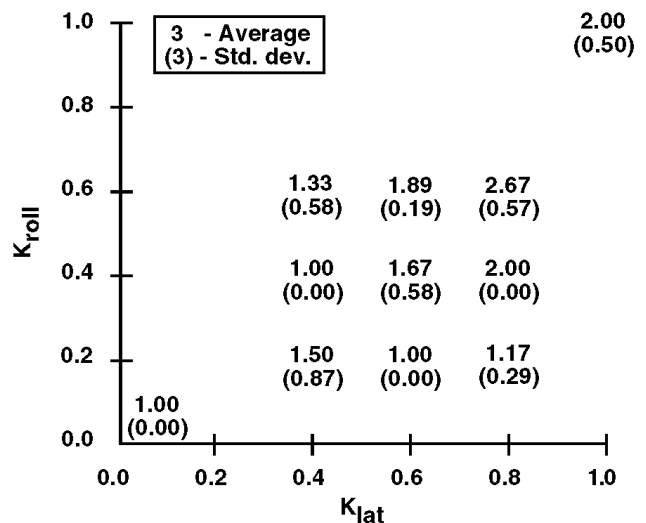


Figure 76. Motion fidelity ratings for roll/lateral experiment.

The configuration that received the best ratings was for $K_{lat} = 0.8/K_{roll} = 0.6$. This configuration was rated better than the 1:1 configuration. A possible reason for the 1:1 configuration not being rated the best could be the amplification of simulation artifacts at the extremes of the motion-system envelope, as discussed later.

Figure 77 presents the average Cooper-Harper ratings for all configurations. The trend of these results follows closely with those of the motion fidelity results. This consistent trend might be expected, because reductions in perceived fidelity may lessen performance, increase workload, or both. Sometimes pilots can try to substitute other cues, such as the kinesthetic cues from the force-feel systems, for cues that have been reduced or eliminated. However, if this substitution does not result in reduced performance, it can likely increase workload. Taking Cooper-Harper ratings, as discussed in appendix D, is ideal for capturing such a trade-off.

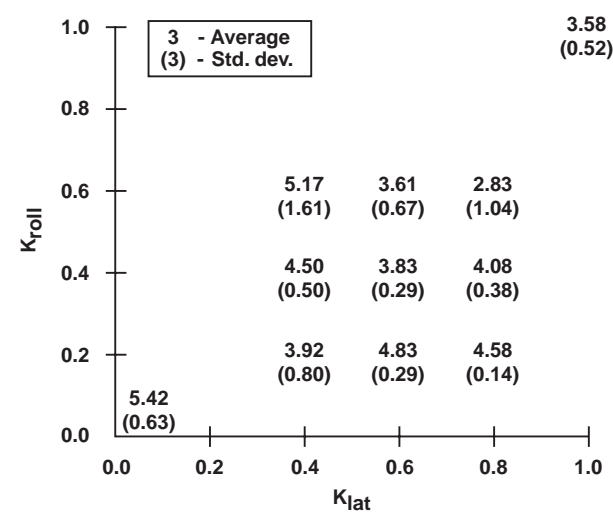


Figure 77. Cooper-Harper ratings for roll/lateral experiment.

Substantial differences resulted in going from the best configuration (again $K_{lat} = 0.8/K_{roll} = 0.6$) to the worst configuration (fixed base). The best configuration elicited satisfactory handling qualities (Level 1, which are ratings less than 3.5), and the worst configuration elicited adequate handling qualities (Level 2, which are ratings between 3.5 and 6.5). Again, as the amount of motion increased, the handling qualities improved.

Proposed Roll-Lateral Specification

The motion-fidelity results map well into a combination of the revised motion-fidelity criteria of Vertical Experiment I, which are shown in figure 78. Since this

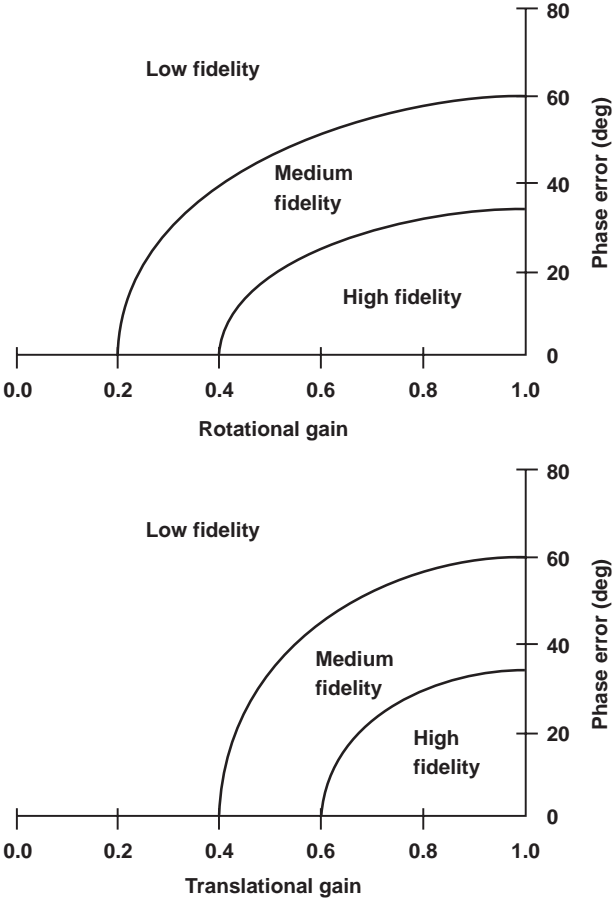


Figure 78. Revised motion fidelity criteria from Vertical Experiment I.

experiment evaluated the effects of gain, and not the effects of high-pass filter break frequency, the abscissas in figure 78 can be combined as shown in figure 79. The average motion-fidelity ratings for the tested configurations are also shown on this combined specification.

In general, the combined specification matches well with the data. The dividing line between High and Medium fidelity would be at 2.5, and the dividing line between Medium and Low fidelity would be 1.5. An instance that does not match well is for the $K_{lat} = 0.4/K_{roll} = 0.2$ configuration for Pilot 1. This configuration would be predicted to be on the borderline of Low and Medium, and this pilot rated the configuration High and Medium in his two evaluations. The other two pilots rated it Low, which matches prediction. Interestingly, Pilot 1 decreased his rating to Low if additional lateral translational motion was provided at the same roll gain. Because an increase in lateral translational motion should not decrease the fidelity, the ratings of Pilot 1 for this one point may be due to a random effect, like the order of configurations that were presented to him.

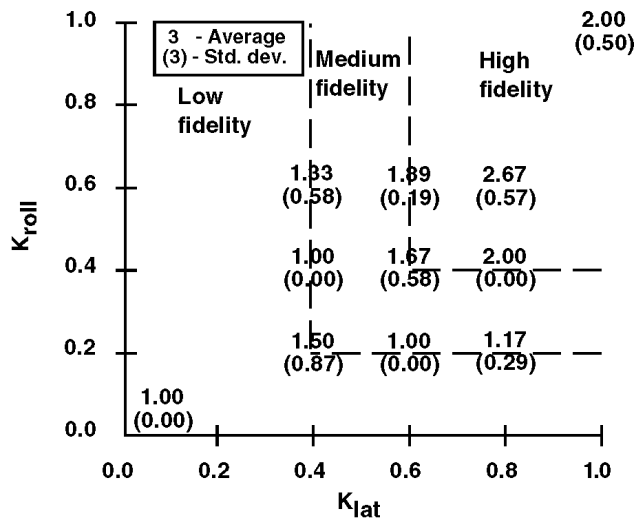


Figure 79. Proposed combined specification for roll/lateral gains.

The second poor match is for the full-motion ($K_{lat} = 0.4/K_{roll} = 0.2$) configuration. On average, the pilots rated the fidelity of this configuration Medium. A possible reason that Medium, instead of High, ratings were given is that some of the undesired side-effects of providing extremely large motion were noticed. An example of a VMS artifact is the rack-and-pinion noise that is proportional to lateral-track velocity. Pilots commented on the noise, and since it represents a sensation noticeably different from flight, a rating of Medium fidelity results. Since the $K_{lat} = 0.8/K_{roll} = 0.6$ configuration effectively results in 48% of the lateral translational motion used in the 1:1 case, artifacts such as the above are reduced significantly. Another possible side-effect is the imperfect high-frequency coordination between the roll and lateral axes; for high-frequency tracking, using high gains can reveal a noticeable, but not objectionable, sensation (i.e., the definition of Medium fidelity). Still, with these two exceptions, the criterion in figure 79 correlates well with the data.

8. Discussion of Overall Results

General Discussion

These experiments showed the powerful effect that platform motion has on pilot-vehicle performance and on pilot opinion in flight simulation. Often, the quantitative measures have supported the pilot's subjective measures, which adds confidence to the results. In addition, frequency-response analyses offer an explanation of how the characteristics of the motion filter affect closed-loop performance.

The powerful effect of motion was shown even when the pilot was creating his own motion, which was the case in all of the tasks except the disturbance-rejection task discussed in section 5. This result conflicts with the views of Hunter et al. (ref. 14) and Puig et al. (ref. 15). The difference between these two views is almost certainly a result of differences in vehicle dynamics. At low speed, fixed-wing aircraft on stabilized paths do not require as much compensation from a pilot as do helicopters. In addition, the tasks that helicopters perform often require the pilot to control all six degrees of freedom of the vehicle simultaneously. Improved fidelity of external cues, such as motion cues, aid in the effective pilot control of the vehicle. Thus, motion requirements cannot be defined by task alone. Both the task and the vehicle must be considered in concert.

This report has illustrated the performance and opinion differences that arise when simulator motion is provided, but it has not shown if there is any training benefit to the use of motion. It is possible that training in a more difficult task environment (no motion) may actually shorten or improve training. For instance, learning to balance a short inverted pendulum can train a person to balance a long inverted pendulum easily. However, if lack of motion causes a bad habit to be learned, then that would certainly argue against training without motion. The effectiveness of training without motion would require a careful transfer-of-training study.

Among the motion configurations tested, it was the translational motion that always had a strong effect. Yaw rotational motion was shown to be a redundant cue, and less roll motion was more acceptable (when comparing percent of full motion) than less lateral translational

motion. Requiring less motion in the rotational axes is still consistent with the revised set of the Sinacori criteria that were suggested in this report.

A question arises as to why only one of the three rotational cues is redundant. That is, why is yaw rotational motion redundant, but pitch and roll motion useful? A possibility is that the pitch and roll rotational cues (as sensed by the inner ear) are no more important than the yaw rotational cue, yet their usefulness arises from the additional cues concomitant with pitch and roll motion. These additional cues have two sources.

First, pitch and roll motion cues interact with the gravity vector, as discussed in section 7. Very few simulators can remove the specific force cue that arises from either pitch or roll attitude. As such, evaluating the effect of the angular cue only is challenging; it has only been investigated by Jex et al. (ref. 41) in which subjects rolled while lying on their backs (thus the gravity vector did not change relative orientation during an orientation). Although that study showed an effect of roll, this could be due to another factor (in addition, it might be argued that compelling roll visual cues were not present in that study, as only a horizon line was present).

The other factor is the tangential acceleration that results from the moment arm between the roll center of rotation and the motion sensors on a human. It is not possible to eliminate the effect of these tangential accelerations completely, for the human motion sensors are in different locations (inner ear, neck, buttocks, limbs). Some experiments have isolated the head by fixing it in an apparatus and subsequently performing reorientations about that axis, but those were not piloted experiments. Thus, when pitching and rolling, isolating the angular cue from the translational cue is difficult if not impossible. It is only in yaw that many of these cross-coupling effects into the translational axes are lessened (but perhaps not removed completely, as discussed in sec. 3). Thus, the above reasons may explain why the requirements on the yaw axis are different from pitch and roll.

Although the longitudinal axis was not examined in these studies, no reason is offered as to why the requirements in that axis might be different from those in either vertical or lateral translation.

Proposed Fidelity Criteria versus Results of Previous Research

Since a cornerstone of the results presented herein was the modification and validation of the fidelity criteria in figure 78, placing those criteria in the context of other work is important. The results of previous work are discussed in section 1, and figure 80 correlates the previous work with the new criteria suggested here. In figure 80, the points tested and found to have at least adequate fidelity are shown. The word “adequate” is chosen in an effort to make a consistent comparison with the earlier work. Much of the earlier work attempts to define a boundary between adequate and inadequate rather than breaking down adequate into three categories such as High, Medium, and Low fidelity. However, it is appropriate that the user should strive to stay away from Low fidelity, which would certainly be termed as inadequate, for the motion sensations are objectionable. Thus, in comparing the previous work with the proposed criteria, an inconsistency would be present if previous work stated that an “adequate” motion system setup was in the proposed Low fidelity region.

In the rotational axes, the criteria apply only to pitch and roll; yaw was found to be redundant. Only the work of Bergeron (ref. 38) evaluated a range of yaw configurations, which was discussed earlier. The only inconsistency between the previous work and the criteria suggested is the work by Shirachi and Shirley (ref. 42). Their experiment did not vary motion-filter natural frequency, which provided 62.5° of phase distortion at 1 rad/sec, which is 2.5° in excess of the Medium fidelity boundary. Still, the boundary at 60° should remain, for both the work of Stapleford et al. (ref. 26) and Bray (ref. 27) support it. If Shirachi and Shirley had evaluated conditions with less

phase distortion, those conditions might have been preferred.

In the translational axes, a “region of uncertainty” extends into the Low fidelity region; this does not suggest an inconsistency, however, because that area simply was not evaluated by Jex et al. (ref. 43). However, a “delayed side force” region cuts off an area in Medium fidelity. The delayed-side-force region applies to the sway axis when that axis is used to eliminate the specific force that arises from platform roll. That region was not explored in section 7, and it may merit additional examination. However, the delayed-side-force region is certainly adequate when trying to represent true math model cues, as shown in the vertical experiments discussed in sections 4 and 5.

There is another inconsistency in the translational axis when compared to the results of Cooper and Howlett (ref. 40). The displacement of their simulator was clearly limited as shown by their boundary “too much displacement.” And their report states “Pilot criticism to motion anomalies during returns from steady maneuvers still is a problem.” So, their region of “best compromise” is likely to be based on their simulator’s capability. It is interesting to note that their rotational axis filter is well within the High fidelity region. Since their platform is synergistic (angular motion usurps translational motion and vice versa), figure 80 suggests that they might relax their angular motion in order to gain translational motion. This change might allow both angular and translational axes to be in the Medium fidelity region for some maneuvers, rather than one in High and one in Low. The remaining comparisons in figure 80 for the translational axes are favorable. In general, the suggested criteria are reasonably consistent with those of previous work.

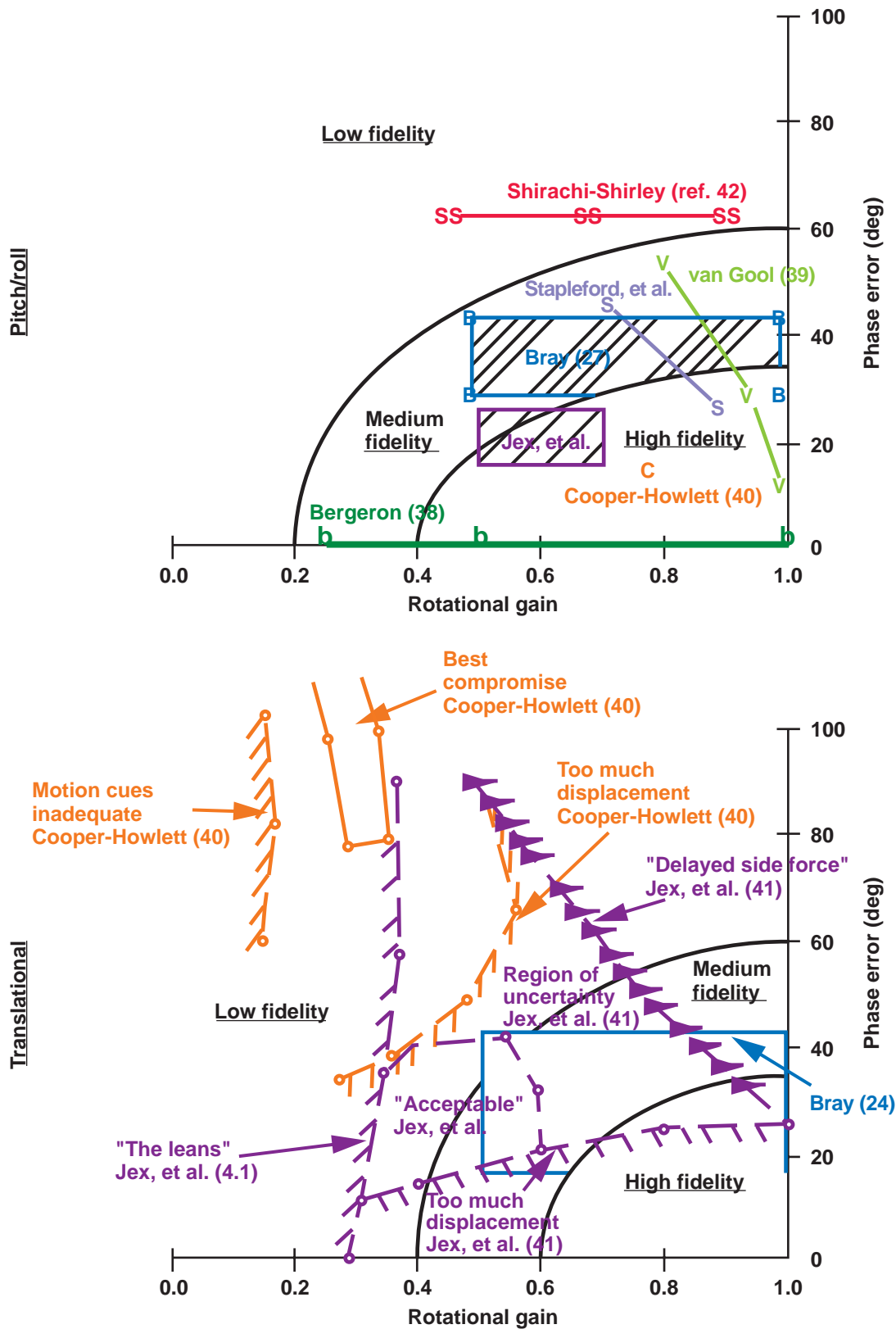


Figure 80. Comparison of previous work with suggested criteria.

A General Method for Configuring Motion Systems

Based on these experiments, on the experience attained in their development, and on the discussion above, figure 81 suggests a step-by-step method for users who configure motion systems. In figure 81, boxes that are dashed, and underlined words in the boxes, represent suggested additions to current practice as a result of the research described in this report. This method is in contrast to the current trial-and-error method that is often used by motion-tuning experts and in subjective pilot evaluations. A recent improvement to the trial-and-error method has been suggested through the use of an expert system by Grant and Reid (refs. 68, 69). However, their method does not explicitly use motion-fidelity criteria as does the method proposed here.

First, the task needs to be analyzed to determine if fundamental motion frequencies are present. Some tasks

have a predominant task frequency. For instance, nap-of-the-Earth flight over regularly varying terrain can necessitate low-frequency heave cues (the frequency determined by hill separation divided by vehicle forward speed). In these instances, the motion-filter natural frequency and gain should not be set independently in an attempt to satisfy the motion-fidelity criteria. Otherwise, pilots do not feel like they are falling or climbing when the visual scene indicates they are falling or climbing. Setting the motion-filter natural frequency should take priority over setting the gain. The filter natural frequency should be selected such that less than a 30° phase error at that predominant task frequency exists. Then, the motion gain can be selected by trying to maximize the criteria shown in figure 78. Once these two parameters are selected, the motion-filter configuration should be evaluated with a pilot flying the task in simulation to determine if simulator excursions reach their physical limits. If the physical displacement limits are reached,

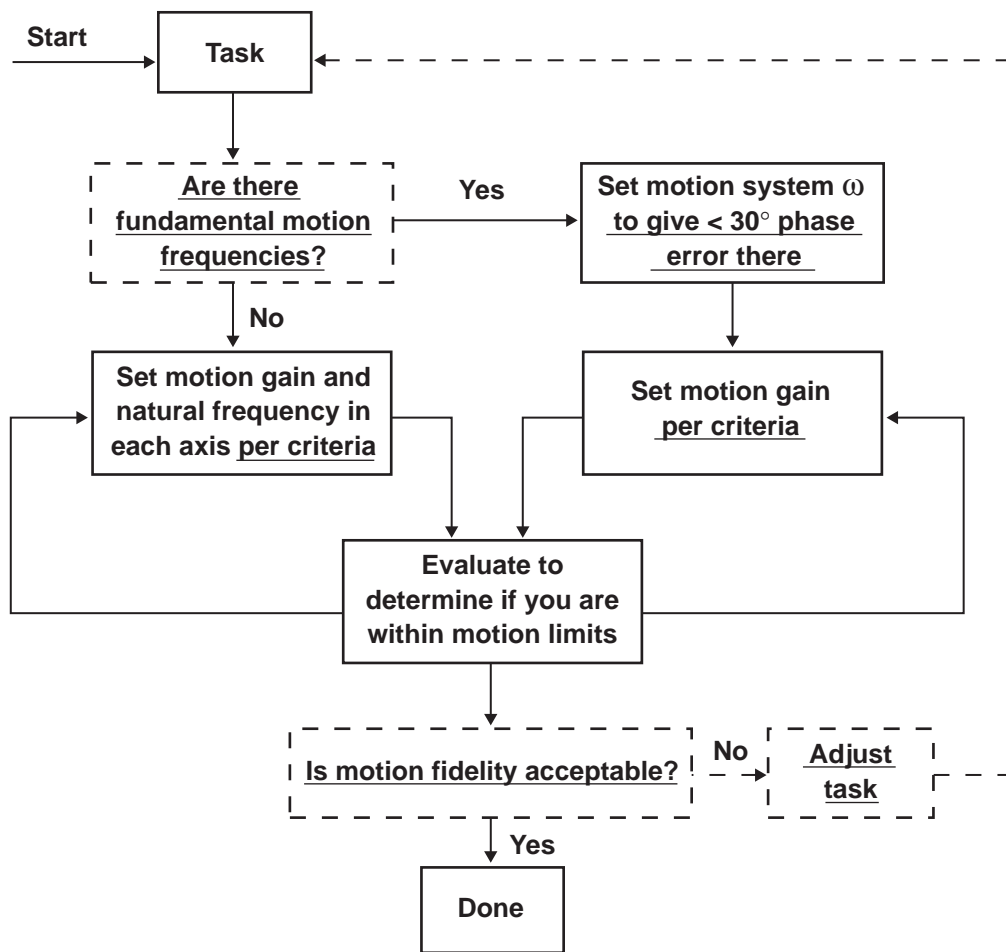


Figure 81. Method for configuring motion systems.

then the motion gain should be lowered until the ensuing motion remains off the limits.

If fundamental motion frequencies do not exist, then the gain and natural frequency of the motion filter can be set independently. In this instance, the highest fidelity should be sought in accordance with the criteria in figure 78.

Iteration with a pilot still needs to be performed to determine the reachable fidelity level. At the end of either of these paths, a certain achievable fidelity level will be reached.

If the desired fidelity level cannot be achieved for a given simulator's displacement capability, then the user should consider changing the task. Often the task is considered a given and is treated as inviolate, since its origins may be from flight test experience. However, trying to extrapolate simulator results to flight when the simulator can only duplicate the task with low fidelity will usually result in a poor extrapolation.

Poor extrapolations from simulation to flight have occurred frequently because of a control sensitivity that is

too high. Pilots improperly perceive vehicle sensitivity to control stick inputs if tasks are not developed in concert with a simulator's displacement capability. Rather than change the task, the simulator's gain is reduced, which gives the pilot a false reading of the true sensitivity.

If the process of developing a task is considered as a feedback process with the attained simulator fidelity as a performance metric, then modifying both the motion cues and the task itself should be considered. It may be the only method for achieving high simulation fidelity.

Extrapolations to flight can then be made with improved confidence.

Generally, this method should serve as a useful guide for configuring motion systems and for selecting tasks to minimize differences between simulation and flight.

Although the method is iterative, it is possible that its combination with the expert system ideas of Grant and Reid (refs. 68, 69) might prove useful.

9. Conclusions

Summary

The five piloted helicopter simulation experiments described in this report produced several important results. Four of the six degrees of freedom were examined: roll, yaw, lateral, and vertical. These experiments were performed on the world's largest displacement flight simulator, making it possible to perform many of the tasks with the motion and visual cues matching exactly. Using these experiments as a baseline allowed the effects of degraded motion cues to be examined.

Representative helicopter math models were used; in some cases, the models were derived from flight test data. Experienced test pilots were the experimental subjects, and both objective and subjective data were employed in developing the principal conclusions that follow.

1. Yaw rotational platform motion has no significant effect on hovering flight simulation. The presence of yaw platform rotational motion did not contribute to significant improvements in pilot-vehicle performance, control activity, pilot-rated compensation, or pilot-rated motion fidelity.
2. Lateral translational platform motion has a significant effect on hovering flight simulation. In contrast to yaw rotational cues, the presence of lateral translational motion did contribute to improvements in pilot-vehicle performance, reductions in control activity, lower pilot-rated compensation, and higher pilot-rated motion fidelity.
3. Lateral translational platform motion combined with visual yaw cues made pilots believe yaw platform rotational motion was present when it was not. This visual and motion cueing combination gave pilots a strong sensation that both rotational and lateral translational motions were present. It is believed that more rapidvection was produced by the lateral translational motion cue. Thus, for hovering flight simulation, one should represent the lateral translational acceleration cue, for it is important to all the aspects of pilot-vehicle performance and pilot opinion. The same point cannot be made for yaw-axis rotational motion. As such, since many of today's hexapod motion platforms achieve both lateral translational and yaw rotational motion with the same set of limited-travel actuators, a high weighting should be placed on representing the former cues rather than the latter. An alternative to modifying today's hexapod motion platforms is to develop a new simulator configuration that emphasizes limited

translational motion. Because lateral and vertical translational motions are the most prevalent, placing a cab on the end of a cantilevered arm that can rotate in azimuth and elevation would provide these motions. Different length arms could be used depending on the vehicle capability, the evaluation requirements, or both.

4. Vertical platform motion has a significant effect on pilot-vehicle performance, control activity, and motion fidelity. Pilots were surprised at the performance results and at how their technique had to change when all motion was removed. Two of the three pilots made collective inputs in the wrong direction when flying fixed base. Until the value of vertical motion was demonstrated, pilot subjective impressions were that the vertical task was primarily visual. Thus, caution should be used when interpreting piloted subjective impressions of the value of motion. From these vertical-axis results, a revised specification was developed that better correlated with existing experimental results.
5. Vertical motion cues affected altitude estimation. Pilots, when asked to double or halve their altitude, had their performance significantly affected by vertical platform motion. With vertical motion, pilots more accurately doubled and halved their altitude. Until now, it was generally accepted that steady-state altitude estimation was derived from visual cues only. A hypothesis is that the pilot estimates vehicle state using all the available sensory inputs. As a part of this, some significant weighting is applied to acceleration cues that provide a component of the pilot's position estimate.
6. A specification for roll-lateral motion requirements was developed. For a side-step task that exactly reproduced motion and visual cues, significant performance and opinion differences resulted as motion was removed. A combination of translational and rotational gain specifications provided a good prediction of motion-fidelity ratings.

Recommendations for Future Work

1. Two additional degrees of freedom, pitch and surge, should be examined. The results for these two coupled axes are expected to be similar to those of the coupled roll and lateral axes.

2. The specification demarcations between high, medium, and low fidelity were determined based on the granularity of the points tested. Further efforts are needed to determine the curves that divide the fidelity regions more precisely.
3. Controlled experiments should be performed on several representative hexapod platforms to quantify the performance benefits of allowing increased motion in the other axes when turning the yaw rotational displacement off.
4. Continued attempts should be made to model the pilot-vehicle system in the simulator environment. Several unusual results, such as the performance degradation with the addition of yaw rotational motion and the improved estimation of height with the addition of vertical motion have been shown here. Future models need to account for these findings.
5. Does learning to fly a helicopter on a substandard or suboptimal motion platform increase total training costs, or does it pose a safety hazard? To answer these questions, a careful transfer-of-training study needs to be performed.

Appendix A—Human Motion Sensing Characteristics

Models of how the semicircular canals and the central nervous system combine in the perception of angular movement have been treated in several research summaries (refs. 28–31). Subtle differences exist among the model structures reviewed. Significant differences, sometimes by several orders of magnitude, exist among measured numerical values in the respective structures. This appendix discusses factors that are important in pilot-vehicle dynamics modeling and in understanding human perception of motion in flight simulation.

A model for angular velocity sensation is shown in figure A1. The semicircular canals are roughly orthogonal to each other, and each behaves like an overdamped torsional pendulum (ref. 32). The output of each block is the deflection of the canal's cupula, and when it reaches a threshold deflection, a sensation develops. Van Egmond et al. (ref. 32) determined the time constants for yaw to be 0.1 sec and 10 sec. The low-frequency poles shown in figure A1 are those determined in a later study by Jones et al., who assumed that the torsional pendulum dynamics developed a sensation of angular velocity (ref. 33). The dynamical differences among axes do not have a satisfying physical explanation and may lie at the behavioral level as suggested by Zacharias (ref. 31). The delay from the central nervous system was included by Levison et al. (ref. 35) for the yaw axis and was carried over to the other axes. The thresholds shown are based on a summary given by Zacharias (ref. 31).

Differences among individuals have been noted in both the dynamics and the thresholds, and it is known that the thresholds can vary up to an order of magnitude, depending on whether a subject has to perform a task (such as flying a simulator) (ref. 36).

While the semicircular canals act as effective rate gyros, the utricles in the inner ear act as effective linear accelerometers. Peters (ref. 28) provides a block diagram of the sensing path for the utricles, which is shown in figure A2. The transfer function was developed by Meiry (ref. 22) with a subject experiencing longitudinal motion only. No dynamic data have been determined in the vertical or lateral axes. The dynamics of the utricles act as a bandpass filter between 0.1 and 1.5 rad/sec. The cutoff frequency of 1.5 rad/sec suggests that high-frequency accelerations must be sensed by the tactile mechanisms

in the body and not by the vestibular system. A wide variance exists in the literature for the translational specific force sensing threshold, which is d_{\min} in figure A2. Peters reviewed thresholds from seven sources and found that they ranged from 0.002 and 0.023 g's (ref. 28).

In addition to these vestibular models, nonvestibular motion sensing plays a prominent role in motion perception. Gum states that "For man in flight the component of the vestibular apparatus, semicircular canals and otolith, do not seem to be very reliable or useful force- and motion-sensing mechanisms" (ref. 30). He summarizes nonvestibular models, with a model of the control of lateral head motion shown in figure A3. Here, the head is essentially an inverted pendulum with respect to the pilot's body that is strapped into a moving cockpit. Taps of the physiological feedback system that regulates the head position serve as an effective motion cueing source. The closed-loop dynamics of the head-control model have a real-axis pole at 3 rad/sec with the rest of the poles at frequencies higher than 10 rad/sec. Thus, the bandwidth of the head-positioning control is twice that of the vestibular system.

The final sensing model covers body pressure sensing; very few quantitative data are available to describe its dynamic response. The body-pressure model shown in figure A4 is from Gum (ref. 30); it has a natural frequency of 34 rad/sec. This bandwidth would make the body's pressure response dynamics the highest of all of its motion-sensing capabilities. The 1-sec time-constant high-pass filter in the model is due to the adaptation effect wherein the receptors in the skin lose their sensitivity to sustained acceleration.

These models represent the latest research findings in the field of motion sensing, but they are incomplete and have limitations. Zacharias points out that there have to be studies to develop an integrated cueing model (ref. 31).

To summarize, substantial work in human sensory modeling has provided useful, but incomplete, information for predicting motion platform effects on pilot-vehicle performance and workload. Rather than use these detailed sensory models, appendix B illustrates that some useful trends can be predicted by using a higher-level structural model of the pilot. Yet, as will be shown, this model fails to predict a pilot's sensitivity to some key motion parameters. All of this points to the need for additional empirical data.

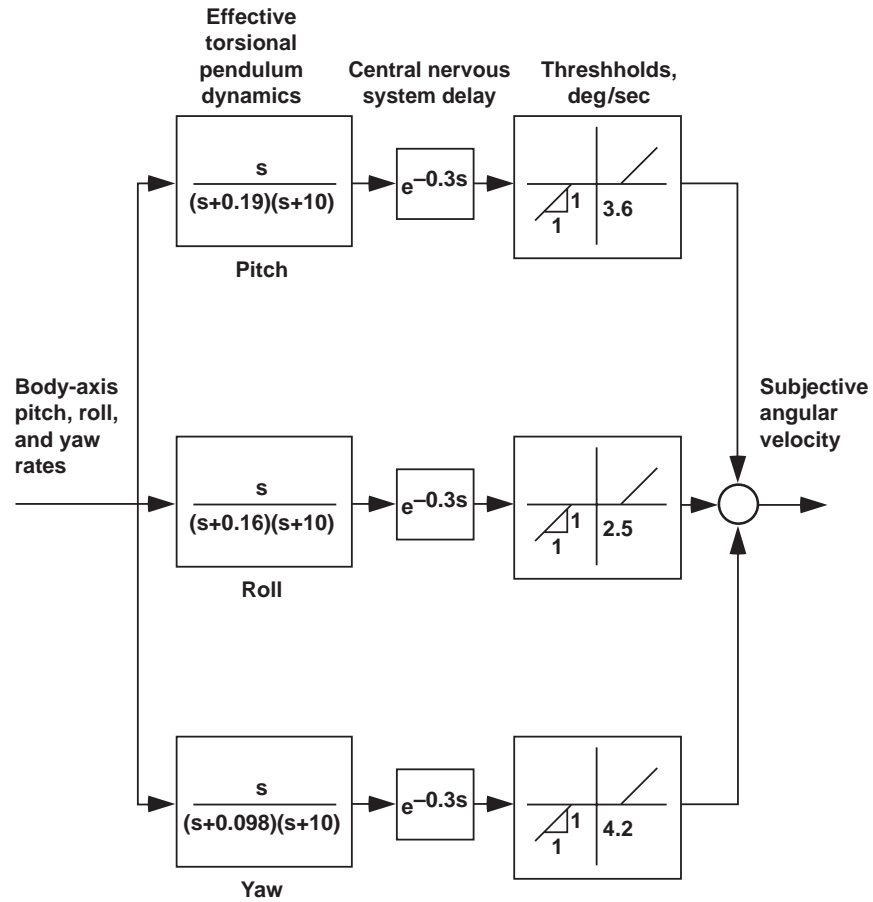


Figure A1. Model of angular velocity sensation.

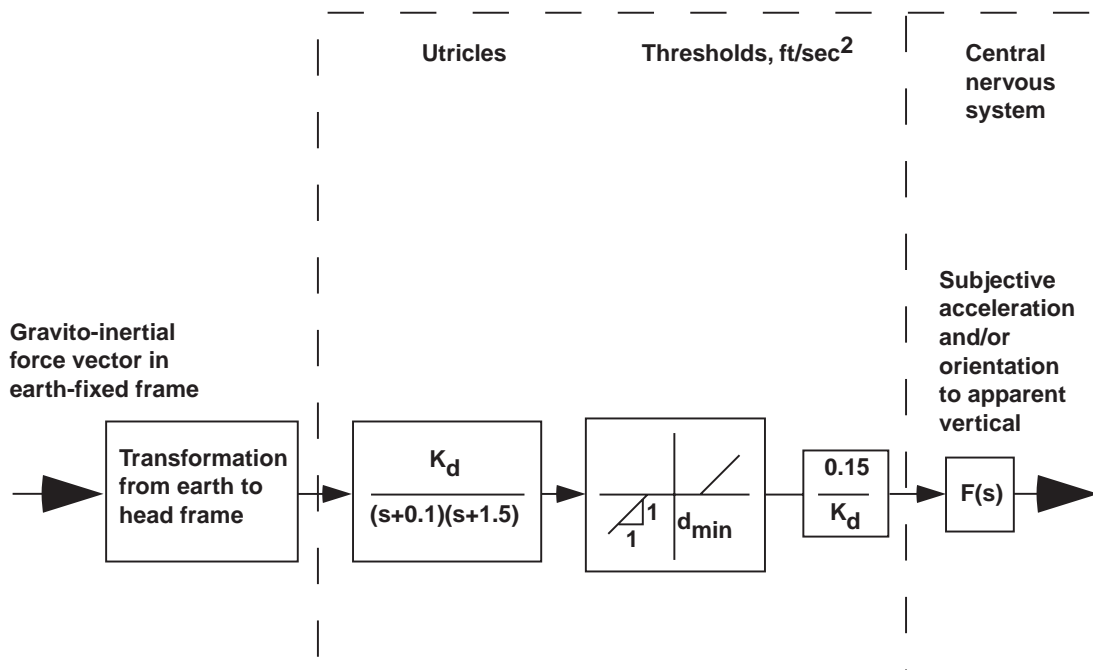


Figure A2. Model of specific force sensation.

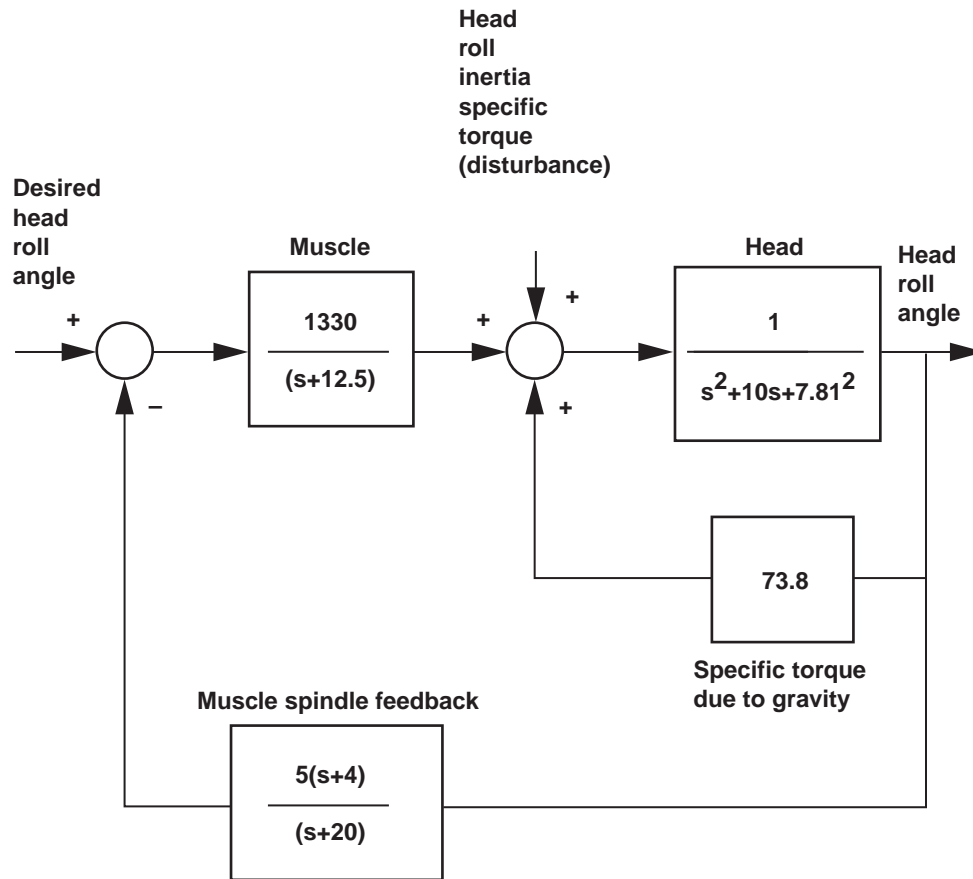


Figure A3. Lateral head motion control model.

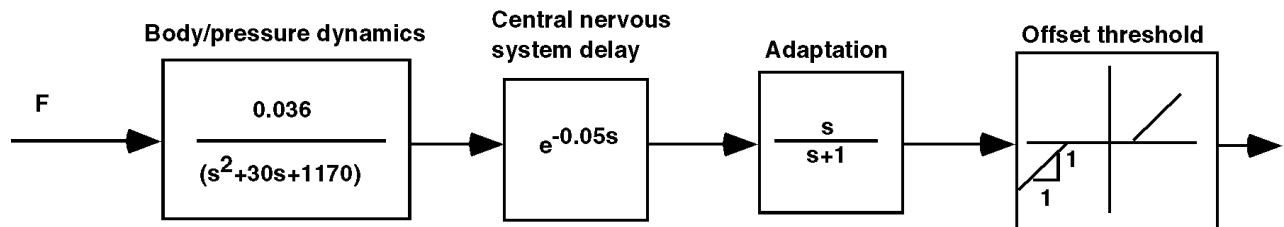


Figure A4. Body-pressure sensing model.

Appendix B—Height Regulation Analysis with Previous Model

To acquire insight into the potential effects of motion on a pilot during the performance of a task, a state-of-the-art analytical model was used. The model was applied to the experiment described under Vertical Experiment I (sec. 4). The task in that experiment was an altitude reposition during hover, so it was a single-axis task. A plausible interconnection of the relevant system dynamics in the task is shown in figure B1. Here the pilot desires to attain the commanded altitude, h_c . Based on the motion and visual cues, the pilot then adjusts his collective control position δ_c to zero the difference between his actual and commanded altitude. All of the elements and connections in figure B1 are adequately known except for the pilot element.

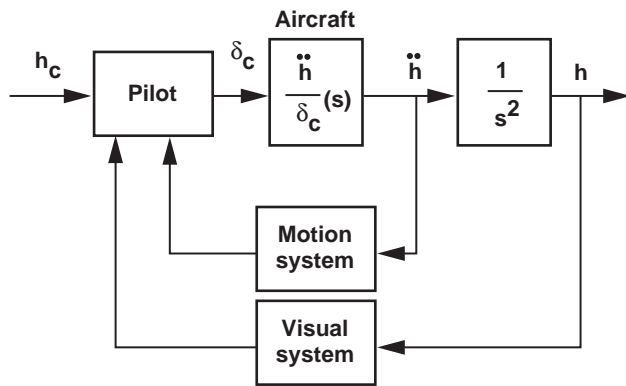


Figure B1. Altitude reposition block diagram in simulation.

In particular, what is not known is how the pilot uses the motion and visual cues to estimate vehicle state. Although the motion system has only acceleration as its input, and the visual system has only position as its input, what are each of these system's effective outputs? It is reasonable to assume that the motion system provides a salient acceleration cue and that the visual system provides a strong position cue. It is often assumed that the visual system also supplies the velocity cue via the time-rate-of-change of the displayed positions. And certainly at a steady-state velocity, the motion system provides no cue.

These very assumptions are made by Hess and Malsbury (ref. 61) as shown in their "structural model of the pilot," which is reproduced in figure B2 in the context of the altitude repositioning task discussed in section 4.

The pilot is assumed to close loops around vertical acceleration, vertical velocity, and vertical displacement.

In the model, the acceleration is derived solely from the motion feedback; however, it might be argued that acceleration could also be derived from the second time-derivative of the displacement. In the acceleration feedback path, two dynamical elements are shown. The first is a high-pass motion filter, which attenuates motion at all frequencies via K and at frequencies below ω . Both of these parameters are adjustable in a given simulation facility based on the task demands and the facility's motion displacement capability. The second dynamic element is the motion-system servo hardware. Using the frequency-response testing techniques developed by Tischler and Cauffman (ref. 46), the simulator has vertical-axis drive dynamics (approximately) of

$$\frac{\ddot{h}_{sim}(s)}{\ddot{h}_{com}(s)} = \frac{(8)(26)}{(s+8)(s+26)} \quad (B1)$$

The vehicle vertical velocity and displacement are derived from the visual system, which is represented by an 83-msec time delay. Hess and Malsbury point out in reference 61 that the vertical velocity sensing assumption affects the primary control loop, but that it is currently not known how to select the appropriate division of the vertical velocity estimation between the motion and visual cues, which is a motivation for Vertical Experiment III described in section 6.

The pilot gains shown in figure B2 are selected based on a set of adjustment rules proposed by Hess and Malsbury. For these tasks, only the high-pass filter was changed, and using the adjustment rules results in the change of three variables $K_{\ddot{h}}$, $K_{\dot{h}}$, and K_h . The gain $K_{\ddot{h}}$ is determined so that the lowest damping ratio of any oscillatory roots in the $\ddot{h}(s)/\ddot{h}_c(s)$ transfer function is at least 0.15. This value of damping ratio is selected to represent a trade-off between stability and high-frequency phase-lag reduction (ref. 70). In reference 70, Hess points out that requiring an identical damping ratio of this loop for all configurations reduces the sensitivity of the modeling procedure to the particular value chosen.

Then, with the motion loop closed, $K_{\dot{h}}$ is determined so as not to violate the combination of a phase margin of 45° and a gain margin of 4 dB in the vertical velocity open-loop $\dot{h}_{cue}(s)/\dot{h}_c(s)$. These values are selected by Hess to achieve adequate stability margins for the vertical-velocity loop. Again, Hess states that requiring all configurations to have the same level of relative stability (same phase and gain margin) reduces the sensitivity of the model to the particular values chosen.



For the five motion configurations that encompassed the motion-filter natural frequency changes, the predictions of the model are shown in table B1. The motion-filter configurations, V1, V2, V3, V4, and V10 are fully

Note that the analytical model predicts a reduction in the vertical-velocity closed-loop bandwidth, from 6.36 to 4.27 rad/sec, as the motion feedback degrades from near full-motion to no motion. For the no-motion case, V10, the pilot has to increase his visual velocity feedback, which results in a higher crossover frequency than before, but in a lower closed-loop bandwidth.

Table B1. Analytical pilot-vehicle characteristics.

Configuration	K_h (1/sec)	$K_{\dot{h}}$ (1/sec)	$K_{\ddot{h}}$	$\dot{h}_{\text{cue}} / \dot{h}_e \omega_c$ (rad/sec)	\dot{h} / \dot{h}_c BW (rad/sec)
V1	0.323	0.542	0.217	1.20	6.36
V2	0.299	0.565	0.240	1.24	6.24
V3	0.335	0.595	0.215	1.33	6.13
V4	0.385	0.636	0.213	1.50	5.85
V10	0.795	0.725	0.000	3.10	4.27

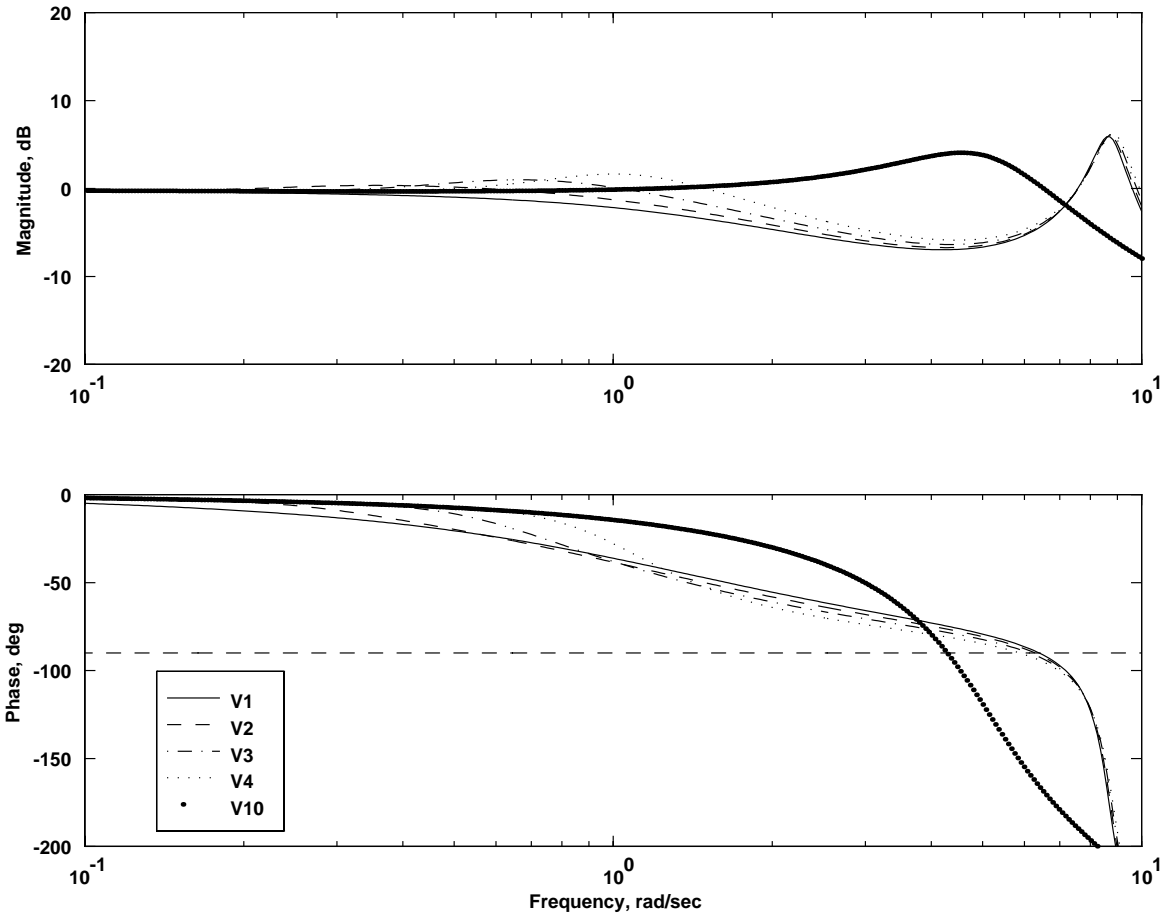


Figure B3. Closed-loop vertical-velocity frequency responses.

If the changes in the closed-loop system roots are examined for the above configurations, the effective heave damping goes from -1.4 sec^{-1} for the full-motion case (V1) to -1.1 sec^{-1} for the V4 configuration. The location of this root accounts for much of the bandwidth difference. This root is also the principal root of interest in the pilot's control of altitude. The corresponding effects on

the other roots are minimal. The heave damping argument, however, does not hold for the no-motion case (V10). In fact, although the bandwidth is less in this case, the damping of the primary closed-loop roots is good.

The above model also predicts a degradation in closed-loop performance from degradations in the motion filter alone.

Figure B4 illustrates how the closed-loop vertical-velocity roots migrate as the motion filter changes. However, these closed-loop poles are those that result when the model's gains are fixed at the full-motion (V1) condition for all the remaining conditions (V2, V3, V4, V10). This situation was examined to show the effect of the motion filter alone without pilot adaptation. Only the region near the origin is depicted, since the poles and zeros far from the origin exhibit negligible change.

Two effects of the motion filter alone are noticed. First, the effective heave damping is reduced as the motion filter's natural frequency increases. This result also occurs when the adjustment rules of the model are followed. Second, pole-zero dipoles form in which the separation between the pole and zero become more prominent as the motion filter is made more restrictive (going from V1 to V4). As the filter natural frequency increases, these dipoles encroach upon the pilot-vehicle crossover frequency. Thus, a broad range of integrator-like characteristics in the crossover region does not occur. So if the pilot wanted to

achieve a similar, but slower, closed-loop response, more than just a simple gain change on his part would be necessary. He would also have to adjust his dynamic compensation, which would likely entail an increase in workload or a reduction in his opinion of simulator fidelity. As expected, the closed-loop bandwidth without using the pilot adjustment rules becomes worse. The bandwidth of the V10 configuration is 3.60 rad/sec without the adjustment rules versus 4.27 rad/sec with them.

Since this model was applied to Vertical Experiment I (sec. 4), it is interesting to compare the phase-plane time-histories from that experiment (figs. 40–43, 49) with the phase-plane time-histories that the model predicts. The model's predictions for the five configurations analyzed (V1, V2, V3, V4, and V10) are shown in figure B5. Although the model shows degradations as the quality of the platform motion becomes worse, the model poorly represents the experimental results in two ways. First, the model introduces a pronounced underdamped oscillatory

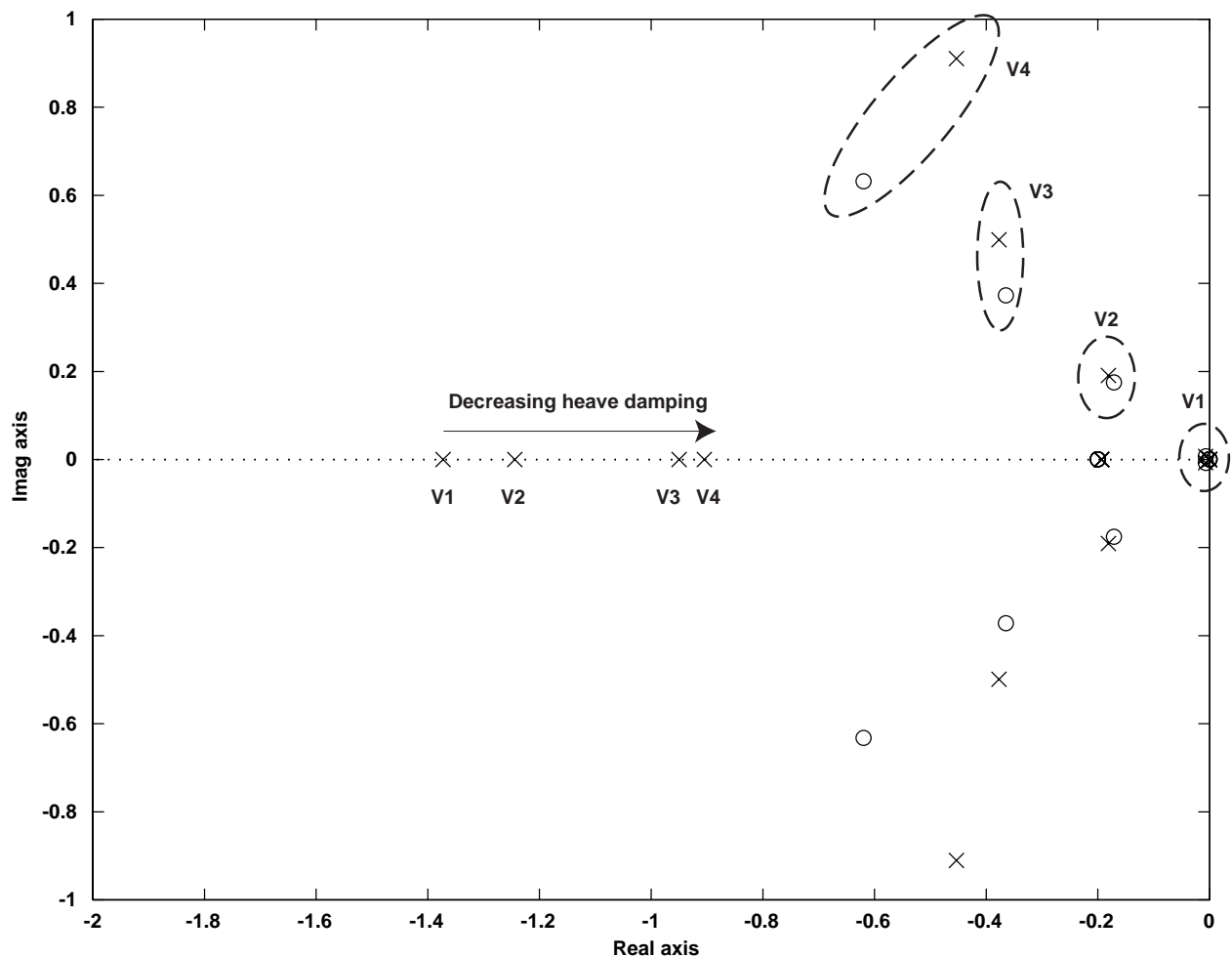


Figure B4. Closed-loop vertical-velocity spectrum versus motion filter changes.

mode for the V1-V4 configurations, which has a frequency of 8 rad/sec. This mode is not present in the experimental results, which show a reasonably smooth response during the ascent. Second, the model does not predict the oscillatory behavior that occurs experimentally at the terminal altitude point (85 ft), which is especially prevalent in the motionless (V10) configuration. The adjustment rules need to be modified in the model in an attempt to match the experimental results. This modification is left for future work.

It should be clear that some key assumptions are made in the development of this model, such as which parts of the simulator system provide which cues, and the adjustment

rules are somewhat of an art. The bottom line is that today's models are incomplete and certainly not validated. The lack of adequate analytical models has been noted by others. Breuhaus pointed out that it is a dubious assumption that one knows all of the important cues and their interrelationships (ref. 72). Heffley et al. stated that when a modeler begins to assemble all of the components that are believed to influence the pilot-vehicle loop in simulation that one notices the fragmentary nature of, and the serious gaps in, the quantification of the component characteristics (ref. 73). More empirical results from systematic and realistic investigations are needed before useful analytical models can be created.

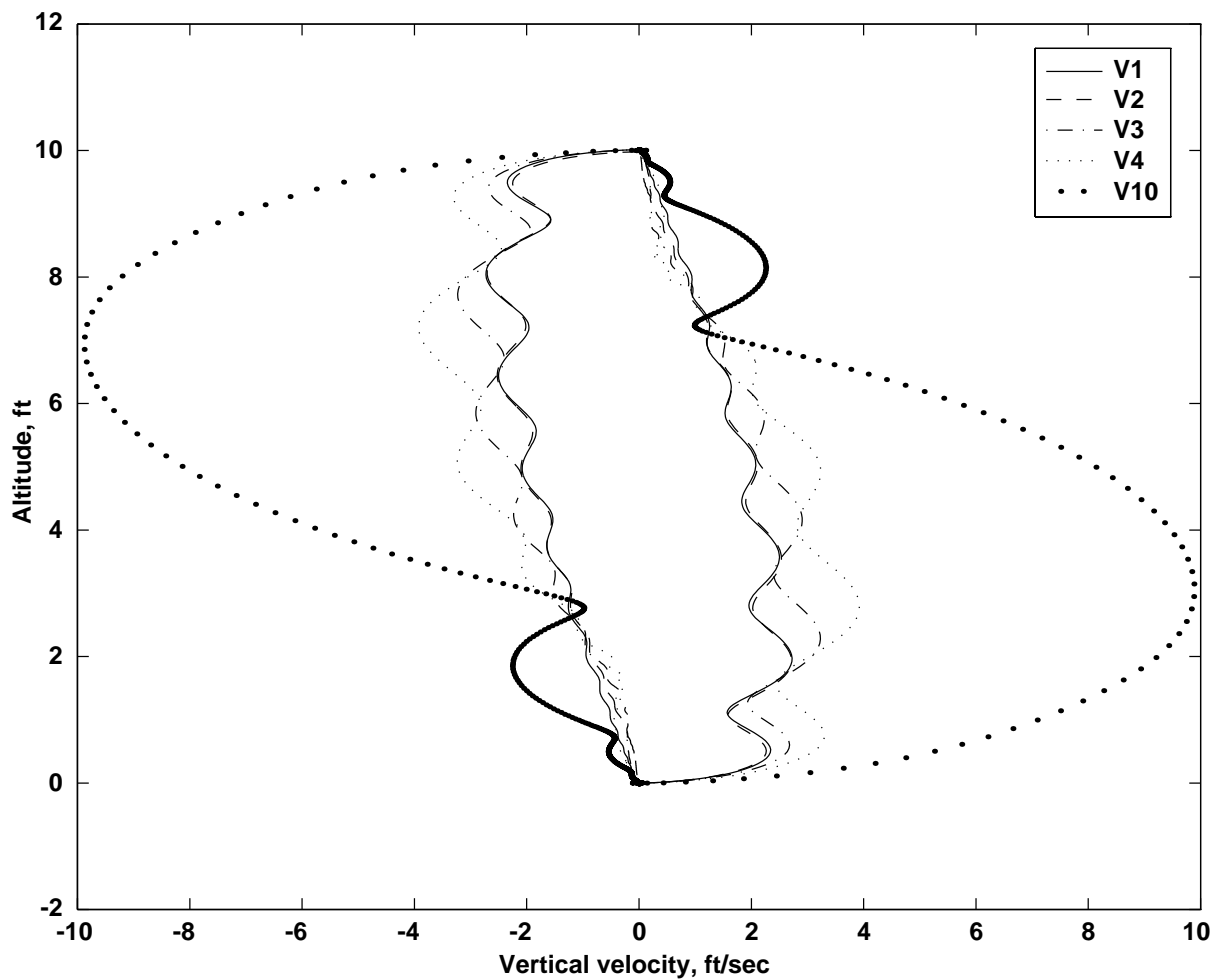


Figure B5. Predicted phase-plane responses.

Appendix C—Example of Repeated-Measures Analysis

A researcher wants to know if the differences among collected data are due to a manipulated experimental factor, or if they are due to random effects. If data are taken from a random sample of individuals, each of whom has experienced a different combination of the experimental factors, then experimental error may be attributed to two effects. The first effect is sampling error and the second effect is error resulting from differences among the individuals.

Repeated-measures allows the differences among individuals to be accounted for in the analysis. This is accomplished by having each individual experience each experimental manipulation. It is a technique often used when subjects are available for a long period of time, such as in a research institution. Details of repeated-measures theory may be found in Myers (ref. 54). Only a brief overview will be given here. An example of the data processing involved is given next.

The example uses the pilot compensation ratings for Task 1 in section 3 (15° yaw rotational capture). A plot of the data is given in figure 15. Table C1 contains the average compensation rating given by each pilot for all of the combinations of translational and rotational motion. The first column gives the pilot number, 1–6. The second column indicates if translational motion was present. A 1 means translational motion was present, and a zero means it was not. Column three indicates if rotational motion was present. Column four gives the average compensation rating, where the average is taken over the repeated runs performed by each pilot. Here the values correspond to 0 = minimal, 1 = moderate, 2 = considerable, and 3 = maximum tolerable.

The purpose of the statistical analysis is to determine if pilots provide better compensation ratings for particular motion configurations. Specifically, it can be determined if the ratings are influenced by the presence of translational motion, by the rotational motion, or by a combination of the two motions. Although figure 15 suggests that the translational motion is likely to be the dominant factor, the statistical analysis provides quantitative information on how often such variations are due to random effects. So, the analysis indicates how solid the inferences drawn from the data are.

Table C1. Average pilot compensation ratings for yaw experiment Task 1.

Pilot (i)	Translational on (j)	Rotational on (k)	Average rating (Y)
1	0	0	2.67
1	0	1	2.25
1	1	0	1.75
1	1	1	1.75
2	0	0	2.25
2	0	1	1.75
2	1	0	0.75
2	1	1	0.00
3	0	0	1.25
3	0	1	1.25
3	1	0	1.00
3	1	1	1.00
4	0	0	3.00
4	0	1	3.00
4	1	0	3.00
4	1	1	3.00
5	0	0	2.50
5	0	1	2.50
5	1	0	0.25
5	1	1	0.00
6	0	0	1.75
6	0	1	2.00
6	1	0	1.25
6	1	1	1.00

To determine whether the differences noted owing to translational motion are statistically significant, the ratio $MS_{\text{trans}} / MS_{\text{trans/pilot}}$ is formed. The numerator of this ratio, MS_{trans} is the between-groups mean square. The denominator of this ratio, $MS_{\text{trans/pilot}}$ is the population error variance. The higher this ratio, the more likely that the differences between the two translational configurations are due to the effect of translational motion and that they are not random results. The relations for these terms are:

$$F = \frac{MS_{\text{trans}}}{MS_{\text{trans/pilot}}} \quad (C1)$$

$$MS_{\text{trans}} = \frac{SS_{\text{trans}}}{(a - 1)} \quad (C2)$$

$$MS_{\text{trans/pilot}} = \frac{SS_{\text{trans/pilot}}}{(a-1)(n-1)} \quad (C3)$$

$$SS_{\text{trans/pilot}} = \frac{\sum_j \sum_i \left(\sum_k Y_{ijk} \right)^2}{b} - C - SS_{\text{trans}} - SS_{\text{pilot}} \quad (C4)$$

where

$$SS_{\text{trans}} = \frac{\sum_j \left(\sum_i \sum_k Y_{ijk} \right)^2}{nb} - C \quad (C5)$$

and for Task 1 in the Yaw experiment:

$$SS_{\text{pilot}} = \frac{\sum_i \left(\sum_j \sum_k Y_{ijk} \right)^2}{ab} - C \quad (C6)$$

$$C = \frac{\left(\sum_i \sum_j \sum_k Y_{ijk} \right)^2}{abn} \quad (C7)$$

$i = 1, \dots, 6 = \text{pilot}$

$j = 0, 1 = \text{translational configuration (off or on)}$

$k = 0, 1 = \text{rotational configuration (off or on)}$

$a = 2 = \text{number of lateral configurations}$

$b = 2 = \text{number of rotational configurations}$

$n = 6 = \text{number of pilots}$

Using the values from table C1, then the equations become

$$C = \frac{(40.92)^2}{(2)(2)(6)} = 69.77 \quad (C8)$$

$$SS_{\text{pilot}} = \frac{\left[\begin{aligned} &(8.42)^2 + (4.75)^2 + (4.50)^2 \\ &+ (12.00)^2 + (5.25)^2 + (6.00)^2 \end{aligned} \right]}{(2)(2)} - 69.77 = 10.55 \quad (C9)$$

$$SS_{\text{trans}} = \frac{(26.17)^2 + (14.75)^2}{(6)(2)} - 69.77 = 5.43 \quad (C10)$$

$$SS_{\text{trans/pilot}} = \frac{\left[\begin{aligned} &(4.92)^2 + (4.00)^2 + (2.50)^2 \\ &+ (6.00)^2 + (5.00)^2 + (3.75)^2 \end{aligned} \right]}{2} + \frac{\left[\begin{aligned} &(3.50)^2 + (0.75)^2 + (2.00)^2 \\ &+ (6.00)^2 + (0.25)^2 + (2.25)^2 \end{aligned} \right]}{2} - 69.77 - 5.43 - 10.55 = 3.98 \quad (C11)$$

$$MS_{\text{trans/pilot}} = \frac{3.98}{(1)(5)} = 0.796 \quad (C12)$$

$$MS_{\text{trans}} = \frac{5.43}{(1)} = 5.43 \quad (C13)$$

$$F = \frac{5.43}{0.796} = 6.82 \quad (C14)$$

Statistically, the F-ratio is the distribution of the ratio of two independently distributed chi-squares each divided by their degrees of freedom. The degrees of freedom are the number of independent observations that were summed in obtaining the chi-square distribution. For the above F-ratio example, the numerator and denominator have $(a-1=1)$ and $(n-1=5)$ degrees of freedom, respectively. The resulting F-ratio, for these degrees-of-freedom, is then be compared against tabulated critical regions to determine if it is large enough to be considered significant. If the F-ratio is large enough, then the effect of the experimental factor is said to be significant. Otherwise, the differences may be due to random error. In the example, an $F = 6.82$ means there are 4.7 chances in 100 that the differences would occur randomly. These low odds suggest that turning translational motion on and off is affecting the results.

Appendix D—Review of Cooper-Harper Handling Qualities Rating Scale

The term “handling qualities” is defined as “those qualities or characteristics of an aircraft that govern the ease and precision with which a pilot is able to perform the tasks required in support of an aircraft role” (ref. 53). The subjective scale that has become the worldwide standard for measuring handling qualities is the Cooper-Harper Handling Qualities Rating Scale (ref. 53), which is shown in figure D1.

After completing a flying task, the pilot assigns a numerical rating by proceeding through the decision tree on the left-hand side of the scale. The decision tree separates the handling qualities into four categories: (1) satisfactory (rating < 3.5), (2) unsatisfactory but tolerable ($3.5 < \text{rating} < 6.5$), (3) unacceptable ($6.5 < \text{rating} < 9.5$), and (4) uncontrollable ($9.5 < \text{rating}$). The first three categories are referred to as Level 1, Level 2, and Level 3 handling qualities, respectively.

The first question, “Is it controllable?” must be answered in the context of the task. If the pilot can control the aircraft in order to perform the task, even if it requires his undivided attention, then the aircraft is controllable. Otherwise, the aircraft is uncontrollable, and the assigned rating is a 10.

The second question, “Is adequate performance attainable with a tolerable pilot workload?” requires the experi-

menter to define performance standards. Engineers and pilots, at the beginning of an experiment, jointly decide on two performance standards: desired and adequate. An example would be for a pilot to fly a landing approach while maintaining airspeed to within ± 5 knots for desired performance and ± 10 knots for adequate performance.

Returning to the second question, the pilot now determines not only whether the adequate performance standard was met, but if the workload was also tolerable. If the answer to this question is yes, then the task can be performed with reasonable precision, even though it might take considerable mental and physical compensation on the part of the pilot.

If the pilot proceeds to the third question, “Is it satisfactory without improvement?” he now has to decide whether the vehicle is good enough as it is for its intended use or if he thinks it should be changed. The vehicle does not have to be perfect, just good enough.

When the pilot proceeds to the right-hand side of the scale, a numerical rating is assigned based on the descriptors of the aircraft characteristics and the demands on the pilot. This process is often a balance between the performance achieved and the compensation required by the pilot in order to achieve that performance.

The Cooper-Harper Handling Qualities Scale has been used successfully since 1969, and it is an excellent way to obtain high-quality subjective data from pilots. These data often correlate well with the objective data collected.

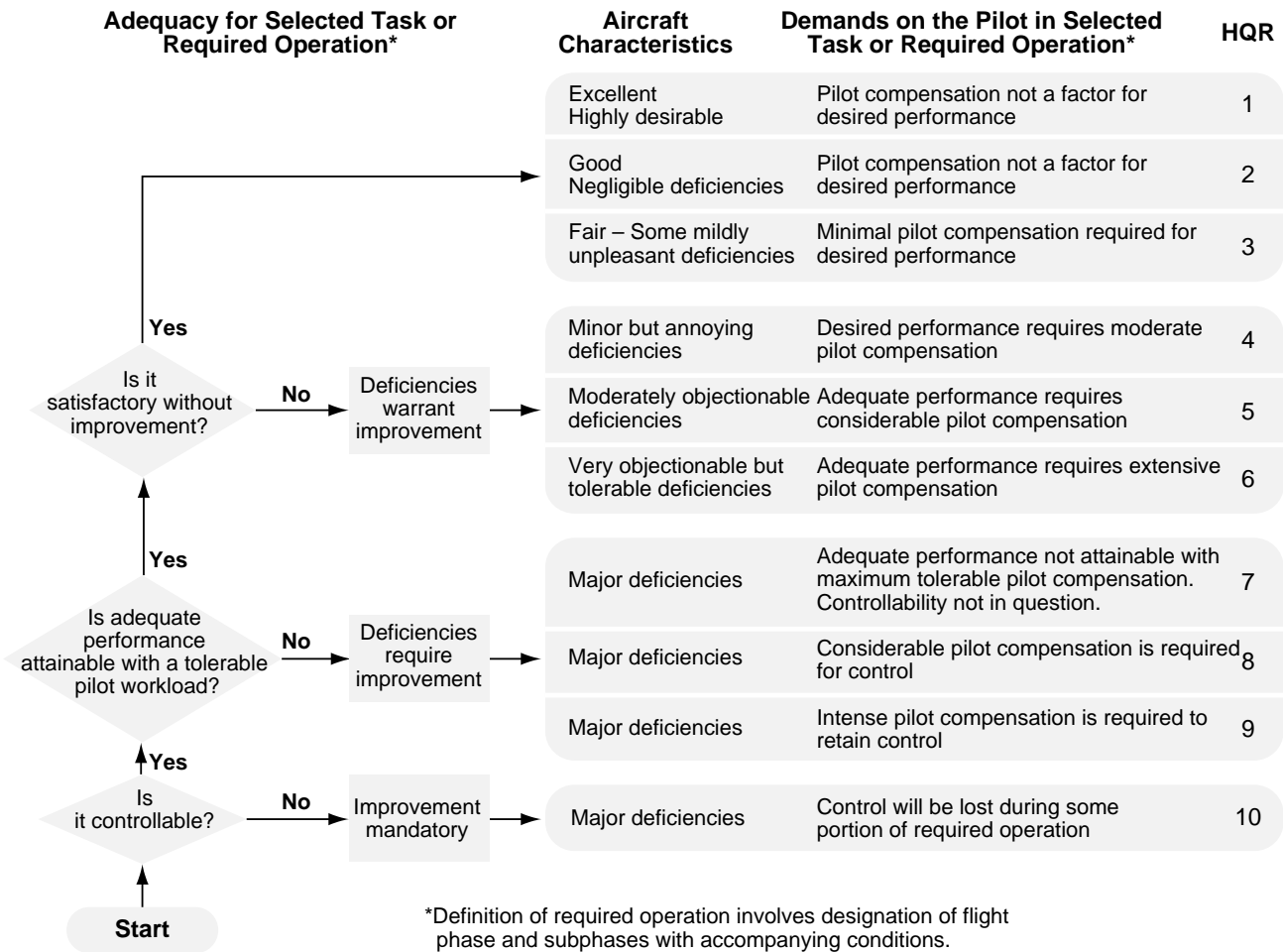


Figure D1. Cooper-Harper Handling Qualities Rating Scale.

References

1. Haward, D. M.: The Sanders Teacher. *Flight*, vol. 2, no. 50, Dec. 1910, pp. 1006–1007.
2. Baarspul, M.: A Review of Flight Simulation Techniques. *Progress in Aerospace Sciences*, vol. 27, 1990, pp. 1–120.
3. Airplane Simulator Qualification. FAA Advisory Circular AC 120-40B, U. S. Department of Transportation, Washington, D. C., July 1991.
4. Donohue, J. A.: Keepin' the Shiny Side Up. *Air Transport World*, vol. 32, no. 10, Oct. 1995, pp. 47–50.
5. Helicopter Simulator Qualification. FAA Advisory Circular AC-120-63, U. S. Department of Transportation, Washington, D. C., Oct. 1994.
6. Johnston, D. E.; and McRuer, D. T.: Investigation of Interactions between Limb-Manipulator Dynamics and Effective Vehicle Roll Control Characteristics. NASA CR-3983, 1986.
7. Watson, D. C.; and Schroeder, J. A.: Effects of Stick Dynamics on Helicopter Flying Qualities. AIAA Paper 90-3477, Proceedings of the AIAA Guidance, Navigation, and Control Conference, Portland, Oreg., 1990, pp. 1460–1479.
8. Boldovici, J. A.: Simulator Motion. U. S. Army Research Institute Technical Report 961, Alexandria, Va., Sept. 1992.
9. Cardullo, F. M.: An Assessment of the Importance of Motion Cueing Based on the Relationship Between Simulated Aircraft Dynamics and Pilot Performance: A Review of the Literature. Paper No. 91-2980, Proceedings of the AIAA Flight Simulation Technologies Conference, New Orleans, La., 1991, pp. 436–447.
10. Roscoe, S. N.: *Aviation Psychology*. The Iowa State University Press, Ames, Iowa, 1980.
11. Waters, B. K.; Grunzke, P. M.; Irish, P. A., III; and Fuller, J. H., Jr.: Preliminary Investigation of Motion, Visual, and g-Seat Effects in the Advanced Simulator for Undergraduate Pilot Training (ASUPT). Proceedings of the AIAA Visual and Motion Simulation Conference, 1976.
12. Gray, T. H.; and Fuller, R. R.: Effects of Simulator Training and Platform Motion on Air-to-Surface Weapons Delivery Training. AFHRL TR-77-29, July 1977.
13. Simulator Sickness Field Manual Mod. 3. U. S. Naval Training Systems Center, Orlando, Fla., 1988.
14. Hunter, S.; Gundry, A. J.; and Rolfe, J. M.: *Human Factors in Flight Simulation: Annotated Bibliography*. AGARD Report R-656, 1977.
15. Puig, J. A.; Harris, W. T.; and Ricard, G. L.: *Motion in Flight Simulation: An Annotated Bibliography*. NAVTRAEQUIPC-IH-298, Naval Training Equipment Center, Orlando, Fla., 1978.
16. Hall, J. R.: The Need for Platform Motion in Modern Piloted Flight Training Simulators. Technical Memorandum FM35, The Royal Aerospace Establishment, Bedford, U. K., Oct. 1989.
17. Showalter, T. W.; and Parris, B. L.: The Effects of Motion and g-Seat Cues on Pilot Simulator Performance of Three Piloting Tasks. NASA TP-1601, 1980.
18. Young, L. R.: Some Effects of Motion Cues on Manual Tracking. *AIAA J. Spacecraft and Rockets*, vol. 4, no. 10, 1967, pp. 1300–1303.
19. Hosman, R. J. A. W.; and van der Vaart, J. C.: Thresholds of Motion Perception and Parameters of Vestibular Models Obtained from Tests in a Motion Simulator: Effects of Vestibular and Visual Motion Performance on Task Performance. Memorandum M-372, Delft University of Technology, Delft, Netherlands, 1980.
20. McMillan, G. R.; Martin, E. A.; Flach, J. M.; and Riccio, G. E.: Advanced Dynamic Seat: An Alternative to Platform Motion. Proceedings of the 7th Interservice/Industry Training Equipment Conference, Nov. 1985, pp. 153–163.
21. Levison, W. H.; Lancraft, R. E.; and Junker, A. M.: Effects of Simulator Delays on Performance and Learning in a Roll Axis Tracking Task. AFFDL TR-3134, Wright-Patterson Air Force Base, Ohio, 1979, pp. 168–188.
22. Meiry, J. L.: The Vestibular System and Human Dynamic Space Orientation. NASA CR-628, 1966.
23. Shirley, R. S.; and Young, L. R.: Motion Cues in Man-Vehicle Control. *IEEE Trans. on Man-Machine Sys.*, vol. MMS-9, no. 4, 1968, pp. 121–128.
24. Bray, R. S.: Visual and Motion Cueing in Helicopter Simulation. NASA TM-86818, 1985.
25. Rolfe, J. M.; and Staples, K. J.: *Flight Simulation*. Cambridge University Press, Cambridge, 1986, p. 117.

26. Stapleford, R. L.; Peters, R. A.; and Alex, F. R.: Experiments and a Model for Pilot Dynamics with Visual and Motion Inputs. NASA CR-1325, 1969.
27. Bray, R. S.: Initial Operating Experience with an Aircraft Simulator Having Extensive Lateral Motion. NASA TM X-62155, May 1972.
28. Peters, R. A.: Dynamics of the Vestibular System and Their Relation to Motion Perception, Spatial Disorientation, and Illusions. NASA CR-1309, Apr. 1969.
29. Young, L. R.; Meiry, J. L.; Newman, J. S.; and Feather, J. E.: Research in Design and Development of a Functional Model of the Human Nonauditory Labyrinths. AMRL TR-68-102, Dayton, Ohio, 1969.
30. Gum, D. R.: Modeling of the Human Force and Motion-Sensing Mechanisms. AFHRL TR-72-54, Wright-Patterson Air Force Base, Ohio, June 1973.
31. Zacharias, G. L.: Motion Cue Models for Pilot-Vehicle Analysis. AMRL TR-78-2, Wright-Patterson Air Force Base, Ohio, Mar. 1978.
32. Van Egmond, A. A. J.; Groen, J. J.; and Jongkees, L. B. W.: The Mechanics of Semicircular Canal. *J. Physiol.*, vol. 110, 1949, pp. 1–17.
33. Jones, G. M.; Barry, W.; and Kowalsky, N.: Dynamics of Semicircular Canals Compared in Yaw, Pitch, and Roll. *Aerospace Medicine*, vol. 35, no. 10, 1964, pp. 984–989.
34. Young, L. R.; and Oman, C. M.: Model for Vestibular Adaptation to Horizontal Rotation. *Aerospace Medicine*, vol. 40, no. 10, 1969, pp. 1076–1080.
35. Levison, W. H.; and Junker, A. M.: A Model for the Pilot's Use of Motion Cues in Roll-Axis Tracking Task. Bolt, Beranek, and Newman Report No. 3528, June 1977.
36. Samji, A.; and Reid, L. D.: The Detection of Low Amplitude Yawing Motion Transients in a Flight Simulator. *IEEE Trans. Systems, Man, and Cybernetics*, vol. 22, no. 2, Mar./Apr. 1992, pp. 300–306.
37. McRuer, D. T.; and Krendel, E. S.: Mathematical Models of Human Pilot Behavior. AGARDograph No. 188, Jan. 1974.
38. Bergeron, H. P.: The Effects of Motion Cues on Compensatory Tasks. AIAA Paper 70-352, 1970.
39. van Gool, M. F. C.: Influence of Motion Washout Filters on Pilot Tracking Performance. Paper 19, AGARD-CP-249, 1978.
40. Cooper, D. E.; and Howlett, J. J.: Ground Based Helicopter Simulation. American Helicopter Society Symposium on Status of Testing and Model Techniques for V/STOL Aircraft, Essington, Pa., 1973.
41. Jex, H. R.; Magdaleno, R. E.; and Junker, A. M.: Roll Tracking Effects of g-Vector Tilt and Various Types of Motion Washout. NASA CP-2060, 1978, pp. 463–502.
42. Shirachi, D. K.; and Shirley, R. S.: Visual/Motion Cue Mismatch in a Coordinated Roll Maneuver. NASA CR-166259, Nov. 1981.
43. Jex, H. R.; Jewell, W. F.; Magdaleno, R. E.; and Junker, A. M.: Effects of Various Lateral-Beam Washouts on Pilot Tracking and Opinion in the Lamar Simulator. AFFDL-TR-79-3134, 1979, Dayton, Ohio, pp. 244–266.
44. Sinacori, J. B.: The Determination of Some Requirements for a Helicopter Flight Research Simulation Facility. NASA CR-152066, 1977.
45. Danek, G. L.: Vertical Motion Simulator Familiarization Guide. NASA TM-103923, 1993.
46. Tischler, M. B.; and Cauffman, M. G.: Frequency-Response Method for Rotorcraft System Identification: Flight Applications to BO-105 Coupled Rotor/Fuselage Dynamics. *J. Am. Helicop. Soc.*, vol. 37, no. 3, July 1992, pp. 3–17.
47. Mitchell, D. G.; and Hart, D. C.: Effects of Simulator Motion and Visual Characteristics on Rotorcraft Handling Qualities Evaluations. NASA CR-3220, 1993, pp. 341–359.
48. Schroeder, J. A.: Simulation Motion Effects on Single Axis Compensatory Tracking. Paper No. 93-3579, Proceedings of AIAA Flight Simulation Technologies Conference, Monterey, Calif., Aug 1993, pp. 202–213.
49. Schroeder, J. A.: Evaluation of Simulation Motion Fidelity Criteria in the Vertical and Directional Axes. *J. Am. Helicop. Soc.*, vol. 41, no. 2, Apr. 1996, pp. 44–57.
50. Handling Qualities Requirements for Military Rotorcraft. Aeronautical Design Standard 33D (ADS-33D), U. S. Army Aviation and Troop Command, St. Louis, Mo., July, 1994.

51. Schroeder, J. A.; Tischler, M. B.; Watson, D. C.; and Eshow, M. M.: Identification and Simulation Evaluation of a Combat Helicopter in Hover. *AIAA J. Guidance, Control, and Dynamics*, vol. 18, no. 1, 1995, pp. 31–38.
52. McFarland, R. E.: Transport Delay Compensation for Computer-Generated Imagery Systems. NASA TM-100084, 1988.
53. Cooper, G. E.; and Harper, R. P., Jr.: The Use of Pilot Rating in the Evaluation of Aircraft Handling Qualities. NASA TN D-5153, 1969.
54. Myers, J. L.: *Fundamentals of Experimental Design*. Allyn and Bacon, Inc., Boston, 1972, pp. 167–190.
55. Young, L. R.: Visually Induced Motion in Flight Simulation. Paper 16, AGARD CP-249, Brussels, 1978.
56. Zacharias, G. L.; and Young, L. R.: Influence of Combined Visual and Vestibular Cues on Human Perception and Control of Horizontal Rotation. *Experimental Brain Research*, vol. 41, no. 2, pp. 159–171.
57. Schroeder, J. A.; Morales, E.; and Merrick, V. K.: Simulation Evaluation of the Control System Command Monitoring Concept for the NASA V/STOL Research Aircraft (VSRA). AIAA Paper 87-2255, Proceedings of AIAA Guidance, Navigation and Control Conference, Monterey, Calif., Aug. 1987, pp. 133–154.
58. Heffley, R. K.; Jewell, W. F.; Lehman, J. M.; and VanWinkle, R. A.: A Compilation and Analysis of Helicopter Handling Qualities Data. Vol. 1: Data Compilation. NASA CR-3144, 1979.
59. Schroeder, J. A.; Tischler, M. B.; Watson, D. C.; and Eshow, M. M.: Identification and Simulation Evaluation of an AH-64 Helicopter Hover Math Model. Paper No. 91-2877, Proceedings of the AIAA Atmospheric Flight Mechanics Conference, New Orleans, La., 1991, pp. 264–297.
60. Bray, R. S.: A Study of Vertical Motion Requirements for Landing Simulation. *Human Factors*, vol. 15, no. 6, 1973, pp. 561–568.
61. Hess, R. A.; and Malsbury, T.: Closed-Loop Assessment of Flight Simulator Fidelity. *AIAA J. Guidance, Control, and Dynamics*, vol. 14, no. 1, 1991, pp. 191–197.
62. Snedecor, G. W.; and Cochran, W. G.: *Statistical Methods*, Sixth Ed., The Iowa State University Press. Ames, Iowa, 1967, p. 265.
63. Paulk, C. H., Jr.; Astill, D. L.; and Donley, S. T.: Simulation and Evaluation of the SH-2F Helicopter in a Shipboard Environment Using the Interchangeable Cab System. NASA TM-84387, 1983.
64. Ferguson, S. W.; Clement, W. F.; Cleveland, W. B.; and Key, D. L.: Assessment of Simulation Fidelity Using Measurements of Piloting Technique in Flight. Proceedings of the American Helicopter Society, May 1984, pp. 67–92.
65. Johnson, W. W.; and Schroeder, J. A.: Visual-Motion Cueing in the Control of Altitude. IEEE International Conference on Systems, Man, and Cybernetics, Vancouver, British Columbia, Oct. 1995, pp. 2676–2681.
66. Warren, R.: Optical Transformation during Movement: Review of the Optical Concomitants of Egomotion. Report No. AFOSR-TR-82-1028, Aviation Psychology Laboratory, Ohio State University, Columbus, Ohio, Oct. 1982.
67. Johnson, W. W.; and Awe, C. A.: The Selective Use of Functional Optical Variables in the Control of Forward Speed. NASA TM-108849, 1994.
68. Grant, P. R.; and Reid, L. D.: Motion Washout Filter Tuning: Rules and Requirements. *AIAA J. Aircraft*, vol. 34, no. 2, Mar.–Apr. 1997, pp. 145–151.
69. Grant, P. R.; and Reid, L. D.: PROTEST: An Expert System for Tuning Simulator Washout Filters. *AIAA J. Aircraft*, vol. 34, no. 2, Mar.–Apr. 1997, pp. 152–159.
70. Hess, R. A.: Model for Human Use of Motion Cues in Vehicular Control. *AIAA J. Guidance, Control, and Dynamics*, vol. 13, no. 3, 1990, pp. 476–482.
71. Hess, R. A.: Theory for Aircraft Handling Qualities Based upon a Structural Pilot Model. *AIAA J. Guidance, Control, and Dynamics*, vol. 12, no. 6, 1989, pp. 792–797.
72. Breuhaus, W. O.: Recent Experience with In-Flight Simulation., AGARD CP-17, pt. 2, Sept. 1966, pp. 577–620.
73. Heffley, R. K.; Clement, W. F.; et al.: Determination of Motion and Visual System Requirements for Flight Training Simulators. Technical Report 546, U. S. Army Research Institute for the Behavioral and Social Sciences, Fort Rucker, Ala., Aug. 1981.

REPORT DOCUMENTATION PAGE			Form Approved OMB No. 0704-0188	
Public reporting burden for this collection of information is estimated to average 1 hour per response, including the time for reviewing instructions, searching existing data sources, gathering and maintaining the data needed, and completing and reviewing the collection of information. Send comments regarding this burden estimate or any other aspect of this collection of information, including suggestions for reducing this burden, to Washington Headquarters Services, Directorate for Information Operations and Reports, 1215 Jefferson Davis Highway, Suite 1204, Arlington, VA 22202-4302, and to the Office of Management and Budget, Paperwork Reduction Project (0704-0188), Washington, DC 20503.				
1. AGENCY USE ONLY (Leave blank)		2. REPORT DATE July 1999		3. REPORT TYPE AND DATES COVERED Technical Publication
4. TITLE AND SUBTITLE Helicopter Flight Simulation Motion Platform Requirements			5. FUNDING NUMBERS 548-40-12	
6. AUTHOR(S) Jeffery Allyn Schroeder				
7. PERFORMING ORGANIZATION NAME(S) AND ADDRESS(ES) Ames Research Center Moffett Field, CA 94035-1000			8. PERFORMING ORGANIZATION REPORT NUMBER A-9900432	
9. SPONSORING/MONITORING AGENCY NAME(S) AND ADDRESS(ES) National Aeronautics and Space Administration Washington, DC 20546-0001			10. SPONSORING/MONITORING AGENCY REPORT NUMBER NASA/TP-1999-208766	
11. SUPPLEMENTARY NOTES Point of Contact: Jeffery Allyn Schroeder, Ames Research Center, MS 262-2, Moffett Field, CA 94035-1000 (650) 604-4037				
12a. DISTRIBUTION/AVAILABILITY STATEMENT Unclassified — Unlimited Subject Category 01 Availability: NASA CASI (301) 621-0390			12b. DISTRIBUTION CODE Distribution: Standard	
13. ABSTRACT (Maximum 200 words) To determine motion fidelity requirements, a series of piloted simulations was performed. Several key results were found. First, lateral and vertical translational platform cues had significant effects on fidelity. Their presence improved performance and reduced pilot workload. Second, yaw and roll rotational platform cues were not as important as the translational platform cues. In particular, the yaw rotational motion platform cue did not appear at all useful in improving performance or reducing workload. Third, when the lateral translational platform cue was combined with visual yaw rotational cues, pilots believed the platform was rotating when it was not. Thus, simulator systems can be made more efficient by proper combination of platform and visual cues. Fourth, motion fidelity specifications were revised that now provide simulator users with a better prediction of motion fidelity based upon the frequency responses of their motion control laws. Fifth, vertical platform motion affected pilot estimates of steady-state altitude during altitude repositionings. Finally, the combined results led to a general method for configuring helicopter motion systems and for developing simulator tasks that more likely represent actual flight. The overall results can serve as a guide to future simulator designers and to today's operators.				
14. SUBJECT TERMS Flight simulation, Helicopters, Motion platforms			15. NUMBER OF PAGES 84	
			16. PRICE CODE A05	
17. SECURITY CLASSIFICATION OF REPORT Unclassified	18. SECURITY CLASSIFICATION OF THIS PAGE Unclassified	19. SECURITY CLASSIFICATION OF ABSTRACT	20. LIMITATION OF ABSTRACT	